NTNU – Trondheim
Norwegian University of
Science and Technology

Calorimetric measurements with CO2 capture solvents

Heat capacity, Cp, measurements for loaded and unloaded alkanolamine solutions using CPA202 Reaction Calorimeter

Paul Magne Amundsen

Chemical Engineering and Biotechnology
Submission date: June 2015
Supervisor: Hallvard Fjøsne Svendsen, IKP
Co-supervisor: Inna Kim, SINTEF
Hanna Knuutila, IKP

Norwegian University of Science and Technology
Department of Chemical Engineering

Abstract

Most chemical and physical processes are accompanied by heat effects, which may contain significant information concerning the mechanisms of the processes. Quantitative knowledge of the thermodynamic properties of CO_2 capture solvents is important for the design and operation of CO_2 capture and solvent regeneration processes. In the present work a particular laboratory equipment for measurement of heat, the CPA202 Reaction Calorimeter from ChemiSens, is used to measure the specific heat capacity of alkanolamines as a function of temperature and solvent composition. The capture solvents studied are Monoethanolamine (MEA), N-Methyldiethanolamine (MDEA) and their loaded (α=0,2 and α=0,4) and unloaded 30 wt% aqueous solutions. In order to observe the temperature effect, specific heat capacities was obtained at 308.15 K, 318.15 K, 328.15 K and 338.15 K. The CPA202 Reaction Calorimeter's reactor vessel, flowmeters, dosing syringes and heat flow measurements was calibrated. As part of the process of developing an experimental procedure for future C_P experiments, measures have been made to reduce the effect of intrinsic error sources for the apparatus. The experimental procedure developed was based on procedures recommended by the manufacturer of the apparatus, and validation by heat capacity experiment with ethyl alcohol show an accuracy of 98,53 % compared to existing literature data.

Keywords: *Reaction calorimeter, calibration, specific heat capacity, Monoethanolamine, N-methyldiethanolamine, loaded 30 wt% solution*

Acknowledgements

I would like to give special thanks to my main supervisor Professor Hallvard Fjøsne Svendsen for all of his input and support along the way, and for allowing me to work independently and in the manor I am most comfortable with. I would also like to thank my co-supervisor Inna Kim, research scientist as SINTEF, for all the support she has given. It has been many late nights at the laboratory, and Inna's dedication to her scientific work has been inspiring as she is always the first to show up and last to leave.

It has been challenging to achieve high accuracy for the heat capacity experiments with the CPA202. It might be that I have had too high expectations, and although both Hallvard and Inna have reassured me along the way that the measurement accuracy was good enough, I am glad that I never listened to them.

The manufacturer of the calorimeter, ChemiSens, have been very helpful during this study, and I would like to acknowledge Holger Nilsson especially for his support.

Last, but not least, I would like to give special thanks to my lovely partner Tonje Pettersen for her impeccable patience this semester. Most of my time has gone to the work on my master thesis and my business startup, and I am forever grateful for her support.

TABLE OF CONTENTS

List of figures

List of tables

Nomenclature

A	Heat transfer area (m^2)
h_T	Heat transfer coefficient on the reactor side ($W/(m^2K)$)
λ	Specific heat conductivity of constructing material in reactor bottom ($W\ m^{-1}\ K^{-1}$)
d	Distance between temperature measurement points (m)
ΔT	Temperature step of scanning experiment
Cp	Specific heat capacity of reactor content mass
s	Molecular struction correction factor
ρ_x	Standard density for component x [g/l]
Cp_x	Specific heat capacity for component x [cal/(g*°C)]
T	Temperature [K]
P_x	Pressure for system x [Pa]
V_x	Volume for system x [m^3]
n	Mol
R	Gas constant [J/(k*mol)]
r	Radius [m]
h	Height/length [m]
T_R	Reactor temperature [K]
T_J	Jacket temperature (Thermostat bath/heat sink temperature) [K]
q_W	Heat effect [$W\ m^{-2}$]
j	Current density [$A\ m^{-2}$]
α	Thermoelectric potential gradient [$V\ K^{-1}$]
T_w	Absolute surface temperature (Peltier element) [K]
ΔH_{vap}	Enthalpy of evaporation [J]
Δh_{vap}	Molar enthalpy of evaporation [J/mol]
V_R	Reactor volume [cm^3]
V_{Liq}	Liquid reaction mass volume [cm^3]
T_{Avg}	Average temperature in scanning interval [°C]
P_{vap}	Vapor pressure of pure compound [Pa]
m_{liq}	Mass of liquid reaction mass

Abbreviations

SS	Stainless Steel
GCF	Gas Correction Factor
GFR	Measured Gas Flow Rate
MV	Measured Volume pumped from piston pump
SV	Stated Volume pumped from piston pump by ChemiCall V2 software
WWH	Wetter Wall Height
DSC	Differential Scanning Calorimetry
DTA	Differential Thermal Analysis
MEA	Monoethanolamine
DEA	Diethanolamine
FS	Full Scale (Accuracy as percentage of)
RDG	Percentage error relative to the reading

1 Introduction

Heat effects accompany almost all chemical processes and physical transitions. Calorimeters are best suited to study these heat effects and is therefore the most universal method to investigate corresponding processes [1]. Reaction calorimetry have been employed in various capacities over the last 30 years, and as a scientific tool it is designed to measure the rate of heat evolution during physical or chemical changes [2].

The dominant process for separation of acid gases such as H_2S and CO_2 from natural gas streams are absorption by aqueous alkanoalamine solutions. In order to prevent corrosion and to increase the heating value, CO_2 present in the natural gas needs to be removed [3, 4]. Amine based technologies have also the important application of CO_2 separation from flue gases at process plants, which is part of the steadily progressing carbon dioxide sequestration efforts including capture and underground storage. Chemical absorption of CO_2 is generally recognized as the most efficient post-combustion separation technology, as it is easily installed in existing process plants. CO_2 absorption in amine solutions has been extensively studied the last decades, and it is claimed that this solution could play an important role in solving the problem of greenhouse gas emissions. Among others, both Monoethanolamine (MEA) and N-methyldiethanolamine (MDEA) have been proven to be of commercial interest for gas purification [3].

Literature heat capacity data is scarce for both loaded and unloaded 30 wt% solutions of mentioned alkanolamines. In this study the specific heat capacity for MEA and MDEA aqueous solutions at a weight concentration of 30%, and with CO_2 loading of 0,2 and 0,4, is presented. Part of the motivation for these heat capacity experiments was to evaluate the capabilities of the CPA202 Reaction Calorimeter and obtain heat capacities accurate enough to observe the temperature effect. The study has the following three main objectives:

1. Calibrate and asses the capabilities of the CPA202 Reaction Calorimeter
2. Develop an experimental procedure for future heat capacity experiments with the CPA202 reaction Calorimeter
3. Obtain accurate specific heat capacities for MEA and MDEA, 30 wt% aqueous solutions of MEA and MDEA, and loaded 30 wt% solutions of MEA and MDEA.

The report is structured in accordance with the main objectives. The basis for this study, and the CPA202 Reaction calorimeter, is first presented. Then the results from the calibration work is presented an discussed, and the apparatus is assessed and validated. In this section the possible error sources for heat capacity experiments with the apparatus is described and measures for error reduction is presented. An experimental procedure was developed throughout this study, and is presented and verified with the use of ethyl alcohol. An calculation example is given for use in future heat capacity experiments. The final section is dedicated to the results from the heat capacity experiments performed according to the developed procedure. At the end of the report, conclusions regarding each objective is presented.

2 Basis

In the following chapters, the underlying theory for this thesis is presented. The background for calorimetric studies and its relationship with heat capacity experiments is discussed. The underlying method of the measurements performed with the CPA202 Reaction Calorimeter is presented, as well as the chemicals and solutions used in the heat capacity part of this study.

2.1 Calorimetry

Calorimetry is one of the oldest technologies know to science, dating back to the 18th century [5]. Its broad applicability stems from one central theme, virtually every process liberates or consumes some finite amount of heat and thusly calorimetry is the study of the heat flow that accompanies physical and/or chemical changes [2]. There has evolved several trends within calorimetry such as DSC, DTA, Bomb/Solution/Reaction Calorimetry, ARC, and several others [2, 6-8], and the following experimental work is part of Reaction Calorimetry which is defined as the measurement of energy evolution/consumption attendant to a changing/reacting system which permit all pertinent rate processes to be measured [2]. The measurement of heat is performed in order to determine thermodynamic properties such as internal energy changes, and to do this with accuracy the thermal equilibrium process must be slowed down enough for the thermometer to be able to measure temperature change. This can only be achieved if the immediate surroundings are sufficiently insulated against. Implicit to the concept of calorimetry is that both thermodynamics and kinetics contribute to the observed measurement, where thermodynamics emerge as integrated enthalpies of physical/chemical change and kinetics as rates of heat evolution [2, 9].

The apparatus commonly used to measure this heat flow is a calorimeter, and its fundamental constituents is a medium to transfer heat into or out of, a thermometer to measure temperature change and a way of insulating the system. There are two basic types of calorimeters, namely constant volume and constant pressure calorimeters, which are both run under either isothermal, isoperibolic or adiabatic conditions. Many variations of calorimeters within the basic constituents, have been reported. The CPA 202 Reaction Calorimeter utilized in this thesis is a multipurpose, isothermal and pseudo adiabatic, constant volume reaction calorimeter, but under the experimental conditions of this thesis it functions as a two-phase calorimeter. The term isothermal calorimeter implies that the measurement of the rate of change of the integral heat evolution Q as a function of time t are performed at a almost constant temperature.

$$q = \frac{dQ}{dt} \qquad (2.1-1)$$

When the calorimeter is utilized at temperatures below the boiling point of the liquid content, the pressure can be assumed constant. At these temperatures the heat capacity measured is close to isobaric specific heat capacity, even though it is measured under saturated circumstances, as explained further in chapter 5. In order to measure heat capacities with a high level of accuracy, there should not be any unmeasured heat gained or lost from the calorimeter. As described by Osborne et al. [10], this ideal is often approached by one or more of the three following means;

1. The calorimeter is perfectly insulated from its surroundings
2. The temperature of the surroundings are kept approximately at the temperature of the calorimeter
3. All heat transferred to or from the calorimeter are accounted for

In the CPA202 Reaction Calorimeter from ChemiSens, all of these three means are utilized. Calorimeters come in several different sizes, all with different advantages and disadvantages. Within DSC and DTA microcalorimeter design are often used, where q is measured under nonisothermal conditions in sample volumes smaller than 20 µl [9]. The CPA202 apparatus is thoroughly described in chapter 3. Table 3.1-1 show some of the differences between the calorimeter used in this study and typical characteristics for DSC and conventional reaction calorimeters, as listed by Nilsson, Hess, 2008 [1].

Table 2.1-1 Comparison between different calorimeters

Characteristics	DSC	Conventional RC	CPA202
Size	Milligrams	1-2 L	10-180 ml
Standard experiment	Scanning	Isoperibolic	Isothermal
Calibration	Occasionally	Frequently	Not required
Speed of test	Fast	Slow	Fast
Scale-up potential	Very limited	High	High
Dosing, sensors, ect	No	Yes	Yes
Main application	Solids	Liquids	Liquids

2.2 Heat capacity

Heat capacity describes the ability of any material to retain heat energy, and is measured through the quantity of heat needed to raise the temperature of one gram of the material by one degree Celsius. This measure is termed specific heat capacity and is represented by the symbol C. A direct consequence of higher specific heat capacity is less temperature rise when a given heat energy is absorbed. But heat capacity describes not only how much heat may be absorbed, but also the ability of the material to deliver heat to an cooler substance. As the specific heat capacity decreases, the ability to deliver heat to a cooler material increases.

The thermodynamic properties described by thermodynamic state functions can only be related to the heat measured, or to each other, as the volume or pressure are kept constant. The circumstances under which the specific heat capacity has been measured, namely isochoric, isobaric or saturation, is denoted as a subscript represented by the symbols C_v, C_P and C_{Sat}. The isochoric heat capacity is rarely determined experimentally for liquids and is primarily of theoretical interest, while both isobaric and saturation heat capacity data is reported in the literature. The SI unit for specific heat capacity is J/(g*K), while in literature it is also commonly given as cal/(g*K). The isobaric and saturation heat capacity is defined as follows [11]:

$$C_P = T\left(\frac{\partial S}{\partial T}\right)_P = \left(\frac{\partial H}{\partial T}\right)_P \quad (2.2-1)$$

$$C_{Sat} = T\left(\frac{\partial S}{\partial T}\right)_{Sat} \quad (2.2-2)$$

Where sat denotes that pressure changes with temperature along the vapor-liquid curve. The relationship between isobaric and saturation heat capacity is derived from the entropy differential expression, and the equation connecting these heat capacities, at the same temperature and vapor pressures, are [11]:

$$C_{Sat} = C_P - T\left(\frac{\partial V}{\partial T}\right)_P \left(\frac{\partial p}{\partial T}\right)_{Sat} \quad (2.2-3)$$

The second term on the right hand side only becomes important at temperatures above boiling point temperature, and below this the difference between C_p and C_{Sat} is substantially smaller than (<0,1%) the uncertainty in precise heat capacity measurements [11]. The experimental heat capacities found in this

study are saturation heat capacities, but as the temperature is kept below boiling point the difference between isobaric and saturation heat capacity is assumed negligible.

Isochoric and isobaric specific heat capacity is related by the following relations

$$C_P - C_V = \frac{\alpha^2}{\beta_T} \quad (2.2-4$$

$$\frac{C_P}{C_V} = \frac{\beta_T}{\beta_S} \quad (2.2-5)$$

Where α is the thermal expansion coefficient, β_T is the isothermal compressibility and β_S is the isentropic compressibility. For liquids the isothermal and isentropic compressibility is virtually the same, and there is thus no difference between C_P and C_V. In this study the heat capacity is measured for liquids and the obtained heat capacities is denoted C_P du to the mentioned compressibility. In addition, the effects of the gas phase is reduced through measures described in chapter 5.6, and the contribution from the heat capacity of the gas phase is negligible compared to the overall contribution from the liquid phase.

Excess molar heat describes the difference between heat capacity estimated for a solution based on the heat capacities for its pure constituents, and heat capacity measured for the actual solution. In this study excess molar heat is not calculated due to inconsistent data for the pure alkanoamine constituents. Excess molar heat capacity C_P^E for a mixture is defined by Lide and Kehiaian as follows in equation (2.2-6) [12]:

$$C_P^E = C_P - \sum_j x_j C_{P,j} \quad (2.2-6)$$

Where $C_{P,j}$ is the molar heat capacity of the pure component *j*.

2.3 Measurements and method

The actual heat flow, denoted True Heat Flow, is obtained by subtracting the heat flow through the base flange from the heat flow through the reactor base [13]. This can be expressed as [14]:

$$THF = \frac{\lambda}{d} A(T_2 - T_1) \quad (2.3-1)$$

Where the measured heat flow is denoted THF(W), λ (W m^{-1} K^{-1}) is the specific heat conductivity of the constructing material, A (m^2) is the heat transfer area and d (m) is the distance between measurement points. The equation illustrates that the measurements are independent from changes in experimental conditions.

During fast changes in the rate of reaction, i.e. in transition regions, significant amount of heat is accumulated in inert parts such as reactor base and inserts, and the reacting mass. This is accounted for in the total power [1];

$$Total\ power = THF + \sum Cp_{mass+inert} \frac{dT}{dt} \quad (2.3-2)$$

Total Power is the sum of all power generating processes inside the reactor, while True Heat Flow is a pure sensor signal without any dynamic corrections. In steady state conditions the True Heat Flow is equal to the Total Power. In order to calculate the total power the accumulated heat in reactor parts and reactor content must be considered. This is complicated further by added heat from mixing enthalpies, heat from reactions, heat flow from stirring and dosing, and heat flow through the lid and reactor glass

walls. The heat flow through the insulated Pyrex glass walls and through the reactor lid is, according to ChemiSens, below instrumental resolution of 0,01 W [1]. In this study the use of differential methodology allows for neglecting of heat flow from most sources as they are small compared to heat flow through bottom flange and reactor base, but an correction must be made to account for the effect of different wetted wall height and its affect on unmonitored heat flow through Pyrex glass walls. This correction if presented in chapter 5.

The heat flow sensors are situated in strategic locations in the reactor, namely in the bottom metal flange and the reactor base. In ordinary heat flow reaction calorimeters the temperature measurements are of the reaction temperature, T_r, and the jacket temperature, T_j [14]. Thusly the temperature difference between the content and the surroundings are monitored. Changes in experimental conditions such as liquid level and viscosities may unfortunately affect the heat flow to the surroundings, and consequently a new calibration for each experiment must be done [1]. In the CPA202 the temperature measurements are done at two points in the reactor base and bottom metal flange. Thus, changes in heat transfer coefficient will not affect the measurements and the baseline is known through the experiment [14].

2.4 Chemicals

The chemicals employed in the following work are listed in Table 2.4-1, and are used as received without further treatment. Distilled deionized water was used in all experiments. The aqueous solutions used in this study was made in-house by weight measurement on bench scales with accuracy of ±0,01 g or better. Pure alkanolamine was added to a beaker while placed on mentioned scale. Distilled deionized water was then added until 30 wt% solution was achieved. Solutions with carbon dioxide loading was made based on previously made aqueous solutions. The solution was placed on mentioned scale while carbon dioxide gas was bubbled through the solution from the bottom of the beaker. This procedure was stopped when 0,2 or 0,4 loading was achieved. The solutions used in this study, and the amount of its respective constituents, are listed in Table 2.4-2.

Table 2.4-1 Chemicals used in study

Component	CAS number	Supplier (purity)
Monoethanolamine (MEA)	141-43-5	Sigma Aldrich (≥99%)
N-methyldiethanolamine (MDEA)	105-59-9	Sigma Aldrich (≥99%)
Ethyl alcohol absolute	64-17-54	Prolab (Assay 99,85%)
Carbon dioxide	124-38-9	(99,995%)
Distilled deionized water	7732-18-5	-

Table 2.4-2 Batch solutions used in this study

	Weighed amount [g]		
Solution	Amine	Water	CO_2
30 wt% MEA (1)	120,72	279,38	-
30 wt% MEA (2)	120,21	280,12	-
30 wt% MEA (1) 0,2 loading	96,33	223,79	13,86
30 wt% MEA (2) 0,4 loading	120,51	279,81	34,84
30 wt% MDEA	150,28	396,02	-
30 wt% MDEA 0,2 loading	90,74	211,73	6,70
30 wt% MDEA 0,4 loading	150,29	349,12	22,04

3 CPA202 Reaction Calorimeter System

Reaction calorimeters are often employed for liquid phase reactions, and the apparatus used in this study is the commercially available CPA202 Reaction Calorimeter system from ChemiSens. In the following chapter the apparatus is described. The theory behind how the apparatus performs its measurements is described in further detail in chapter 2, 4 and 5.

3.1 About CPA202

The apparatus contain a small-scale reactor, suited for both chemical and physical processes. The main output signal from the reaction calorimeter is the heat flow associated with physical or chemical processes, but it is capable of measuring the following according to the CPA202 hardware manual [13]; thermal power, pressure, pH, stirrer speed, stirrer power and gas flow. A torque transducer measures the stirrer speed and the stirrer power applied to the liquid [1]. These parameters can be monitored in real time using ChemiCall V2 software from ChemiSens. The apparatus consists of three major parts; the CPA202 thermostating unit and reactor, the VRC202 dosing controller, and the CPA202 system control unit, all of which are placed in a fume hood for safety [13]. The overall equipment is shown in Figure 3.1-1.

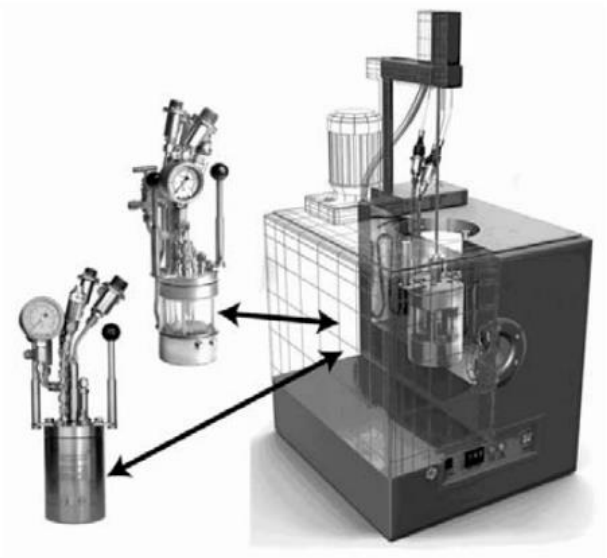

Figure 3.1-1 High pressure reactor (left), Pyrex glass reactor for regular pressure (behind), and thermostating unit with stirrer motor and observation window (ringht) [1]

The reactors

The CPA202 system package consists of two reactors, one in stainless steel for high pressure experiments up to 200 bar and one with transparent Pyrex glass walls capable of withstanding pressures up to 20 bar. The reactors are both 250 mL stirred tank reactors and can operate in temperatures from -50 ^{o}C to 200 ^{o}C, depending on the choice of external cooling system. . The reactor has a working volume of 40-180 ml, with an upper limit in order to ensure that the liquid content is not in contact with the upper metal flange or the lid, as these do not contain heat flow transducers [13]. The effect of such liquid contact is explained in chapter 5.1.1.6. The reactors contain a sealed magnetic stirrer to ensure leak-free operation. Ports in the lid and bottom allow sampling and charging from both liquid and gas phase, and can be used for supplementary equipment. It has heat flow transducers in the bottom and bottom steel flanges, which monitor the heat flow between the reactor content and the surrounding liquid bath acting

as a heat sink. The Pyrex glass walls are made of double glass jackets to minimize heat flow through passive insulation. In the experiments performed for this thesis, only the Pyrex glass reactor is utilized. A schematic of the Pyrex glass wall reactor is shown in Figure 3.1-2.

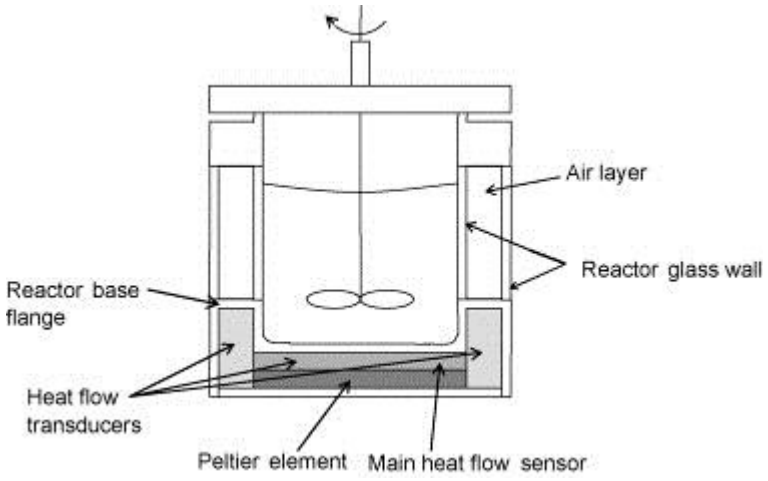

Figure 3.1-2 Schematic of the CPA202 reactor [14]

The heat flow registered as True Heat Flow in the CPA202 system is only dependent on the heat exchange through the bottom, which also contain an Peltier element. This involves subtracting the heat flow through the bottom metal flange and neglecting heat flow due to imperfect insulation, such as through the Pyrex glass walls. This is explained in further detail in chapter 4. There is thusly an assumption that the reactor is insulated perfectly, contributed to by the active insulation effect from the thermostat-controlled bath. The heat flow transducers in the reactor base measure the temperature at two points, T_1 and T_2, and the heat flow measurements are therefore not affected by changes in the heat transfer coefficient, h_T. The heat transfer area, A, is constant. In addition to the mentioned heat trancducers, the reactor is equipped with a Pt-100 temperature sensor, which measures the reactor content temperature. This sensor determines the absolute temperature of the system, from which other temperatures are related.

When the electric current through the Peltier element in the reactor base is varied, the heat flux through the wall can be controlled. Both T_R, T_J and the Peltier current is mesasured, but the Peltier element is not involved in temperature measurements, but is used for heating or cooling the reactor. Depending on the direction of which a current is passed through the Peltier element, one side lowers its temperature and absorbs heat while the other side increases its temperature and delivers heat [1]. A negative heat effect, q_{Wc}, is evolved at the cold side and a positive heat effect, q_{Wh}, is evolved at the hot side with a given current density, j (A m^{-2}), through the element:

$$q_{W_c} = -\alpha T_{W_c} j \ \ (Wm^{-2}) \qquad (3.1-1)$$

$$q_{W_h} = \alpha T_{W_h} j \ \ (Wm^{-2}) \qquad (3.1-2)$$

Where α is the thermoelectric potential gradient (V K^{-1}), and T_{W_c} and T_{W_h} (K) are the absolute surface temperatures [9]. The heat transducers are located between the Peltier element and the reactor bottom, as shown in Figure 3.1-3 below.

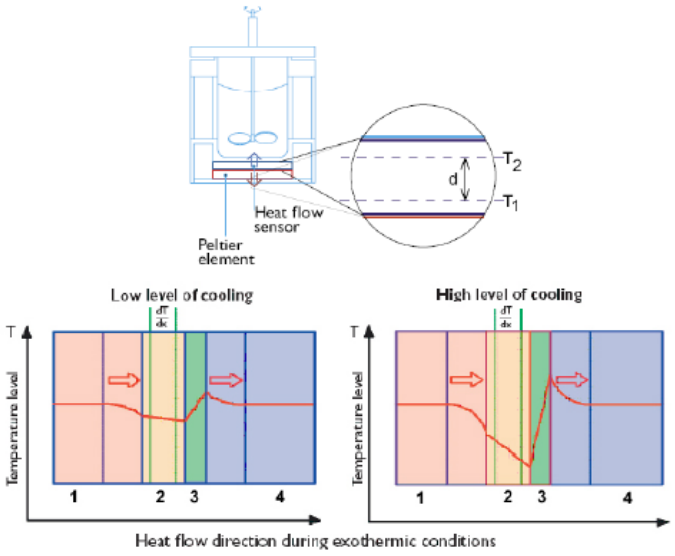

Figure 3.1-3 Heat flow trancducer placement, (1) T_r, (2) Trancduser, (3) Peltier element, and (4) T_J [13]

The reactor is also fitted with a general purpose electrical validation heater. The operator can give the heater a desired power value between 1 and 6 W, and using a default value for the resistance the corresponding current is calculated and supplied to the validation heater. From the voltage drop across the heating coil the generated power is determined, and the supplied current is automatically adjusted until power output corresponds with set value. The validation heater also contain a temperature sensor to prevent back conductivity of generated heat through the heater enclosure to the reactor base wall [13].

Thermostating unit

The reactor is immersed in a thermostating unit with an internal liquid volume of approximately 13 liters, which supply a stable environment and an efficient safety layer [1]. For experiments up to 95 °C water is used, while for higher temperatures diethylene glycol is used. The reactor not exposed to circulating thermostat liquid through a jacket, but is submersed completely. The liquid bath represent a large heat capacity and acts as a thermal reference for the reactor [1]. The transportation of heat from the reactor content to the bath is through the Peltier element, not through a active heat pump as is common in many calorimeters. The thermostat-controlled bath is kept at a temperature 0,2 °C higher than the reactor in order to provide active insulation, which is explained further in chapter 5.

4 Calibration of CPA202

The CPA202 system hardware represent new equipment for the Environmental Engineering and Reactor Technology group and in accordance with common practice, the equipment must be calibrated locally in order to assure accurate experimental values and to be able to assess equipment capabilities. Experience from SINTEF show that fluctuations in parameters that are commonly perceived as constant, such as room temperature, may affect measurement accuracy, and calibration procedures should therefore be performed regularly and as part of start-up procedures for experimental work.

As described in the hardware manual, the thermal measuring system of the CPA202 is only dependent on the properties the constructing material and the sensitivity of the sensors. This also means that chemical or physical properties of the reactor content, such as heat transfer, do not affect the calibration data [13]. The heat flow measurements was calibrated and controlled over the entire temperature range at delivery by ChemiSens, which also states that the calibration data are valid for a long time period [13]. It is nevertheless necessary to calibrate external equipment such as pump and flowmeters, and the internal reactor volume, in order to minimize measurement error for heat capacity and reaction heat studies. This is described in the following subchapters. The heat flow measurement accuracy have also been examined for the same purpose.

4.1 MSC202 dosing syringe calibration

The CPA202 utilizes two MSC202 precision drive units for Motorized Syringe Control (MSC), both with capacities of approximately 50 mL. The dosing units are connected to the CPA202 thermostating unit through stainless steel pipes and to the VCR202 dosing controller through signal-lines MSC1 and MSC2. The dosing units have a maximum flow capacity of 5 $\frac{mL}{min}$ out and 10 $\frac{mL}{min}$ in. The calibration of the dosing units, hereby referred to as Pump1 and Pump2, have been done on the basis of finding the correlation between added volumetric amount stated by ChemiCall V2 software (through VRC202 dosing controller) and the actual amount manually weighed on a XXXX weight scale. The MSC202 is shown in Figure 4.1-1.

Figure 4.1-1 MSC202 precision drive unit for Motorized Syringe Control

Procedure

Water was placed in a temperature-monitored reservoir at room temperature from which Pump1 are fed. The dosing unit was fed through a 30 cm long stainless steel tube, and water was initially forced through the unit in order to remove any air trapped in the dosing unit system. The dosing unit was then manually put into revers mode in order to fill the MSC chamber. The unit was then placed in automatic mode in

order to be controlled through the ChemiCall V2 software. Through the software, Pump1 is set to pump at 2.5 or 5 ml/min for 1 or 2 minutes into a 20 ml beaker repeatedly until the piston chamber is empty and must be manually refilled. The water pumped into the beaker is weighed after each pumping session, and the temperature is measured. The beaker is dried and weighed before each session. This procedure was repeated for Pump1 until 16 pumping sessions were made, then the pump was changed to Pump2 and the procedure was started again.

Results

The ChemiCall V2 software are using the register pumping speed and pumping time to estimate the volume added to the reactor. ChemiSens does not state in their manuals if this is based on literature data on water, but it is natural to assume this. By the use of the weighed amount and temperature of the water from each pumping session in combination with literature density data, the exact volume pumped was calculated and compared to the stated volume in ChemiCall V2 software. The water density for the measured temperature was found through the following expression (4.1-1), which is valid in the range 263-373 K [15]:

$$\rho(T) = 0{,}9165 + \left(0{,}08339 * e^{2{,}0682058215} - 0{,}004738 * (T - 273)\right) * e^{-\frac{5{,}6095*100{,}65425}{T}} \quad (4.1-1)$$

The calibration data for Pump1 are based on 17 measurements, from which 2 are considered outliers and removed from the dataset. Calibration of Pump1 show an overall average deviation from stated volumetric amount of -1.78% according to (4.1-2). When Pump1 was set to pump 10 ml the software registered 10,080 ml, while the weighing resulted in an average of 9,916 ml meaning that the software and MSC dosing unit system was 98,38 % accurate according to (4.1-3). When the unit was set to pump 5 ml the software registered 5,04 ml, while the weighing resulted in an average of 4,94 ml meaning that the software and MSC dosing unit system was 98,1 % accurate according to (4.1-3). The data set have a standard deviation of 0.23 % (0,014 mL) from average measured volume according to (4.1-4). The difference between stated volume and actual volume is shown in Figure 4.1-2.

$$Overall\ average\ deviation = \frac{\frac{\sum MV_n}{n} - \frac{\sum SV_n}{n}}{\frac{\sum SV_n}{n}} (4.1-2)$$

$$System\ accuracy_{10ml\ or\ 5ml} = \frac{\frac{\sum MV_n}{n}}{SV} \quad (4.1-3)$$

$$Standard\ deviation\ from\ mean\ value = \frac{\sqrt{\frac{\sum(MV_n - \frac{\sum MV_n}{n})^2}{n}}}{\frac{\sum MV_n}{n}} \quad (4.1-4)$$

Where n are the number of pumping sessions, MV are the measured volume from each session, SV are the stated volume from ChemiCall V2 for each session.

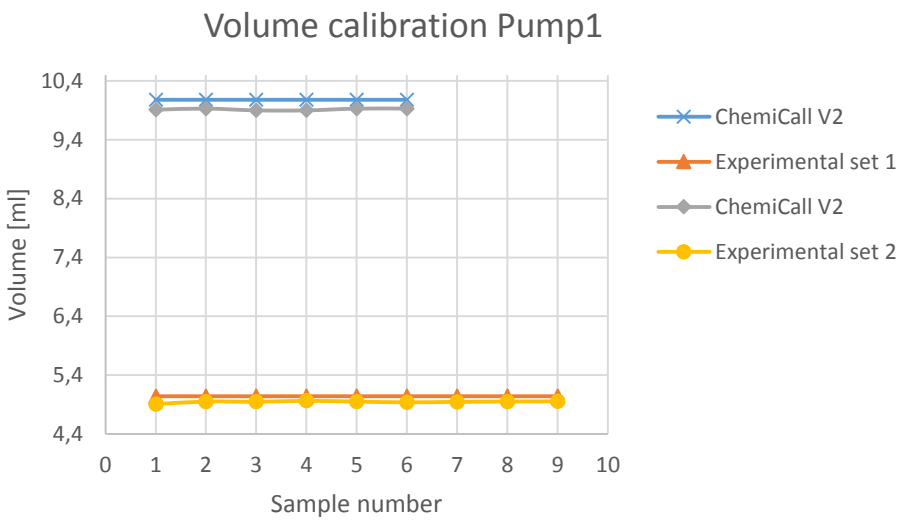

Figure 4.1-2 Difference in stated and measured volume for Pump1

The calibration data for Pump2 are based on 15 measurements, from which 1 are considered outlier and removed from the dataset. Calibration of Pump2 show an overall average deviation from stated volumetric amount of -2,39 % according to (4.1-2). When Pump2 was set to pump 10 ml the software registered 10,083 ml, while the weighing resulted in an average of 9,918 ml meaning that the software and MSC dosing unit system was 98,37 % accurate according to (4.1-3). When the unit was set to pump 5 ml the software registered 5,083 ml, while the weighing resulted in an average of 4,928 ml meaning that the software and MSC dosing unit system was 96,9 % accurate according to (4.1-3). The data set have a standard deviation of 0.39 % (0,027 mL) from average measured volume according to (4.1-4). The difference between stated volume and actual volume is shown in Figure 4.1-3.

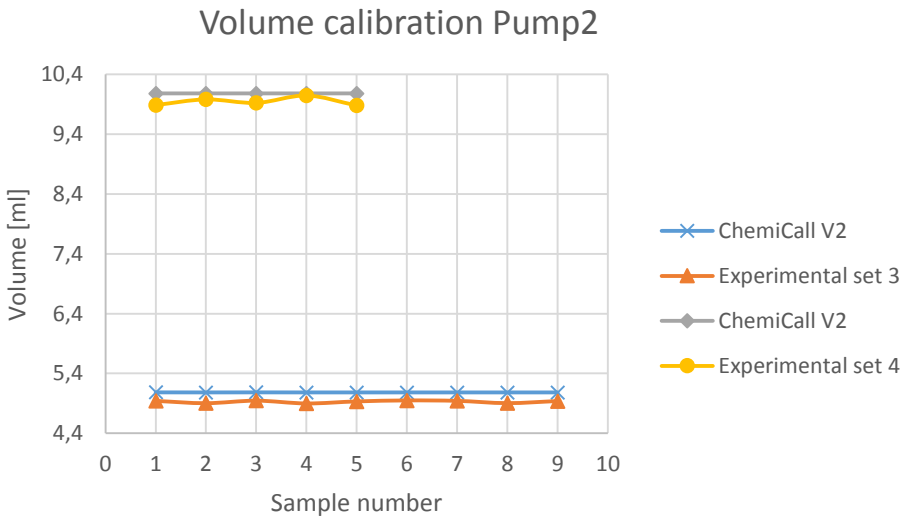

Figure 4.1-3 Difference in stated and measured volume for Pump2

Discussion

No significant correlation is found between flow rate and accuracy, or amount and accuracy. The overall standard deviation in the datasets for Pump1 and Pump 2 is 0,31 % (0,0205 ml). Low standard deviation in each data set show high consistency in pump performance as expected from piston pumps. The overall difference between stated volume and actual volume for both dosing units is -2,085 %, which means that the stated amount fed into the reactor is, on average, 0,14 ml more than the exact amount. Since the standard deviation in the data set is low, it is more correct to assume that the actual amount fed into the reactor is 0,14 ml $\pm 0{,}0205$ ml less than stated in the ChemiCall V2 software. One of the challenges that the system faces is that the last droplet of water from the feeding tube may, or may not, fall into the reactor. It is nevertheless part of the reactor content, but may contribute to energy loss through evaporation at a later stage since that is a slow process. It may be assumed that vibrations in the reactor are enough to make the last droplet fall into the liquid phase.

4.2 Flowmeter calibration

The CPA202 thermostating unit has two flowmeters, one on each side, used for controlling gas feed dosing. Calibration efforts of these flowmeters has been made in order to obtain a correlation between flowmeter voltage (capacity) and CO_2 flow. The actual flow from the flowmeters, hereby referred to as Linout_A and Linout_B are measured with the flow calibrator Bronkhorst HI-TEC E-7102-10-12-F1 for gas flows between 1-5000 ml/min. The calibrator have two range settings, above or below 200 ml/min, with different measurement resolutions. The lower setting was used for gas flow up to 200 ml/min, and the higher setting was used for higher flow rates. The flow calibration device is, as default, calibrated for the measurement of flow rate for nitrogen gas (N_2) because it has, in room temperature, characteristics close to ideal gas. Since the gas measured in this study is CO_2, a correction factor (denoted GCF) is needed. The gas correction factor for carbon dioxide is 0,74 according to equation (4.2-1) [16]:

$$Actual\ flow\ rate\ of\ gas = Flow\ rate\ of\ nitrogen * Correction\ factor$$

$$GCF(N_2) = 1$$

$$GCF(CO_2) = \frac{0{,}3106 * s}{\rho_{CO_2} Cp_{CO_2}} \quad (4.2-1)$$

Where:

$GCF(CO_2)$ is the gas correction factor for carbon dioxide

0,3106 is (standard density of nitrogen) * (specific heat of nitrogen)

s is the molecular structure correction factor, which is 0,941 for triatomic gasses and 1,000 for diatomic gasses

ρ_{CO_2} is the standard density of carbon dioxide (1,977 g/l)

Cp_{CO_2} is the specific heat of carbon dioxide (0,1956 cal/(g*°C))

Procedure

Carbon dioxide gas flow rate was measured with flowmeter calibration device for every 5% interval (0.5 V) of increased flow capacity for the external flow meter up to maximum capacity of 100% (10 V). The measurements was done three times for each flowmeter, with constant inlet pressure from gas reservoir at approximately 6 bar. Additional four measurement rounds were made for varying inlet pressure between 4 and 8 bar. The relationship between flow rate and capacity was found by data fitting through linear trend line approach.

Results

The calibration data at constant pressure (6 bar) for Linout_A is based on 45 measurements in 3 sessions, from which none are considered outliers. The data set for Linout_A has a standard deviation of 0.34% (0.94 ml/min) from the average value, as calculated from equation (4.1-3). The dataset reviled a linear correlation between flowmeter capacity and CO_2 flow rate as shown in Figure 4.2-1. From this a linear trendline was developed based on the average flow rate values for each capacity interval, and the linear relationship is described in equation (4.2-2) and shown in Figure 4.2-2. The equation is valid at an inlet pressure of 6 bar.

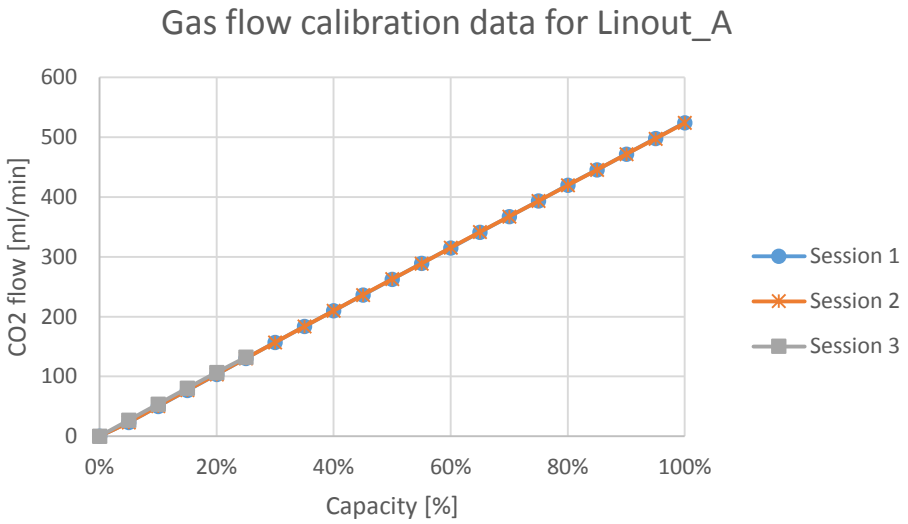

Figure 4.2-1 Measured CO_2 flow vs flowmeter capacity for Linout_A

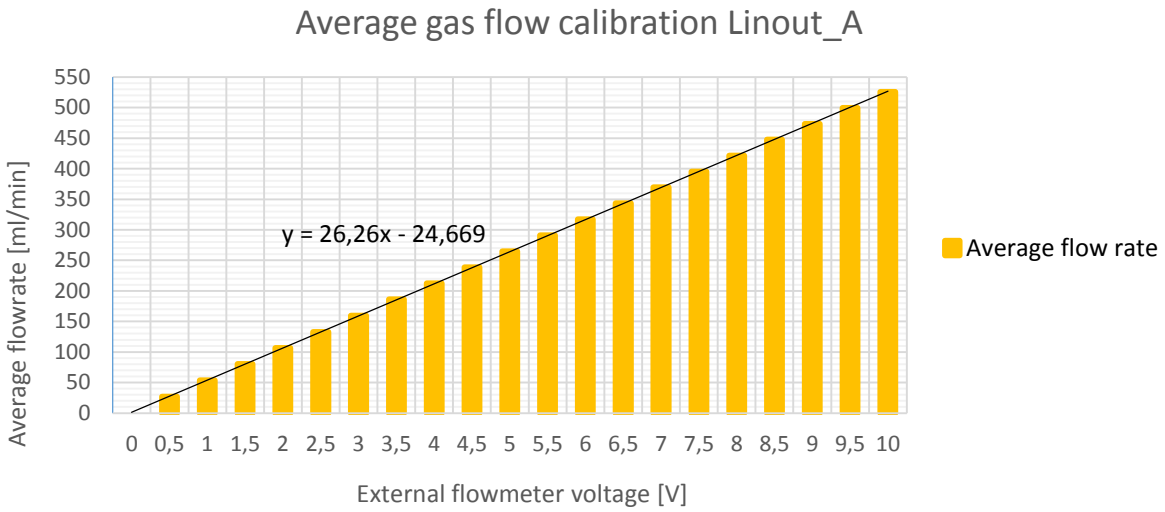

Figure 4.2-2 Linear trendline based on average gas flow values for Linout_A

$$CO_2\ flow\ rate\left[\frac{mL}{min}\right] = 26.26 * X\ [V] - 24.669\ \ (4.2-2)$$

The calibration data at constant pressure (6 bar) for Linout_B is based on 45 measurements in 3 sessions. The data set has a standard deviation of 0.44% (1,21 ml/min) from the average value, as calculated from equation (4.1-3). The data set also reviled a linear correlation between flowmeter capacity and CO_2 flow rate as shown in Figure 4.2-3. From this a linear trendline was developed based on the average flow rate values for each capacity interval, and the linear relationship is described in equation (4.2-3) and shown in Figure 4.2-4. The equation is also only valid at an inlet pressure of 6 bar.

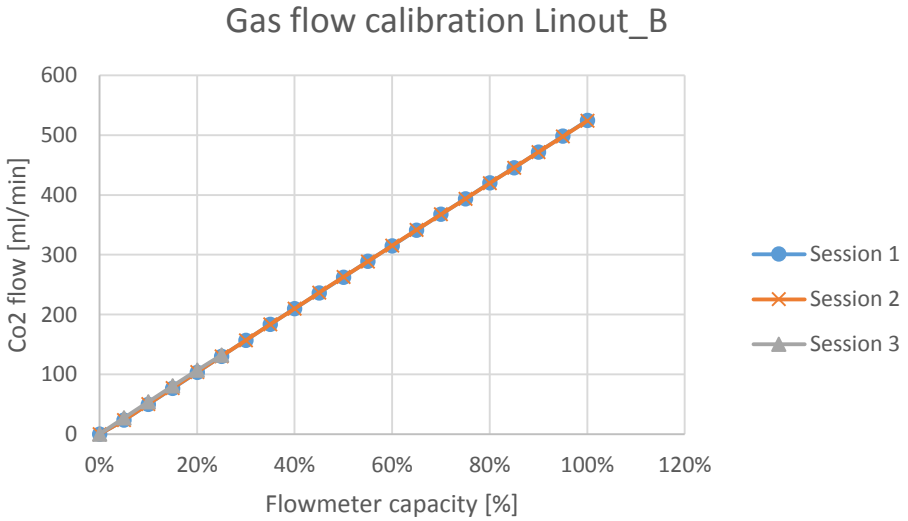

Figure 4.2-3 Measured CO_2 flow vs flowmeter capacity for Linout_B

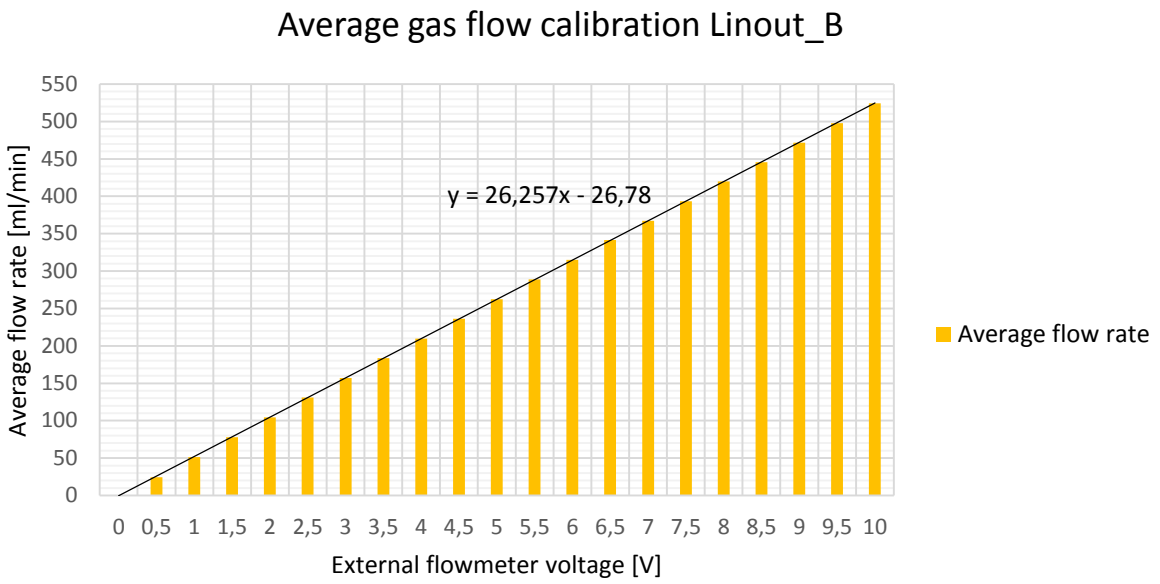

Figure 4.2-4 Linear trendline based on average gas flow values for Linout_B

$$CO_2\ flow\ rate\left[\frac{mL}{min}\right] = 26.257 * X[V] - 26.78 \quad (4.2-3)$$

Varying inlet pressure may have a significant influence on the actual gas flow rate through the flowmeters, and Linout_B was therefore additionally calibrated for varying inlet pressure. The procedure was the same as for the calibration at 6 bar inlet pressure, and the inlet pressures utilized was 8, 7 and 4 bar. The calibration for varying inlet pressure is based on 30 measurements in 3 different sessions, each at a new inlet pressure. The measured gas flow rates are shown in Figure 4.2-5, and the data from each session revels a linear relationship with flowmeter voltage. The sessions with inlet pressures of 7 and 8 bar show both a consistent negative deviation from the measurement data at 6 bar, with a mean standard deviation from 6 bar measurements of -0,872 % for the former and -1,007 % for the latter. The session with inlet pressure at 4 bar show an positive deviation from measurements at 6 bar, with a mean standard deviation of 1,308 %. The standard deviations was calculated by the expression (4.2-4).

$$Average\ standard\ deviation\ [\%] = \frac{\left(\frac{\sqrt{\sum(GFR_n - GFR_{6\ bar,n})^2}}{GFR_{6\ bar,n}}\right)}{n} \quad (4.2-4)$$

Where GFR_n is the measured gas flow rate at 8,7 or 4 bar, $GFR_{6\ bar}$ is the measured gas flow rate for 6 bar (average values from all 3 sessions for Linout_B), n is the steps in flowmeter voltage (1 to 10)

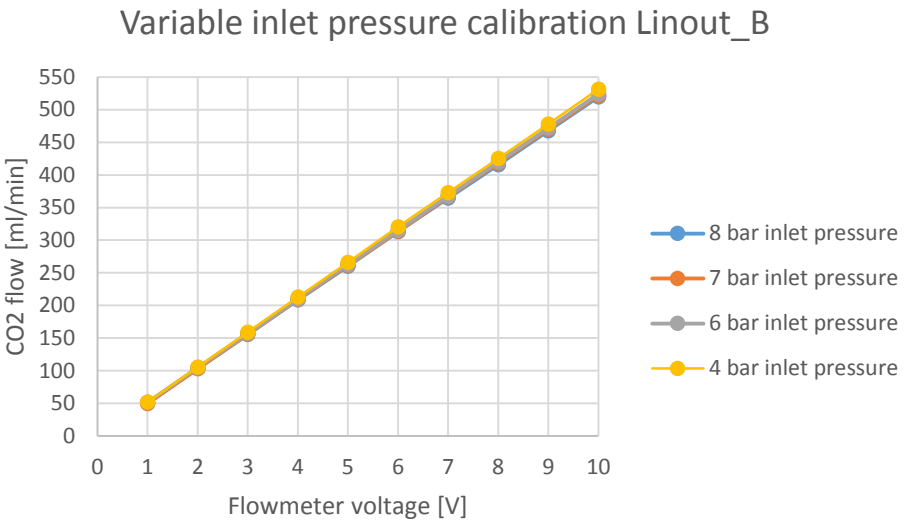

Figure 4.2-5 Gas flow rate vs flowmeter voltage for 8,7,6 and 4 bar inlet pressure

The measured flow rates at 8, 7 and 4 bar inlet pressure had, at each flowmeter voltage, the standard deviations from the average measured flow rates for 6 bar inlet pressure as shown in Figure 4.2-6. The figure shows that the standard deviation stabilizes when flowmeter voltage is set over 3 V. The standard deviation was calculated according to expression (4.2-5).

$$Standard\ deviation\ at\ n\ voltage\ [\%] = \frac{\sqrt{\frac{\sum(GFR_n - GFR_{6\ bar,n})^2}{n}}}{GFR_{6\ bar,n}} \quad (4.2-5)$$

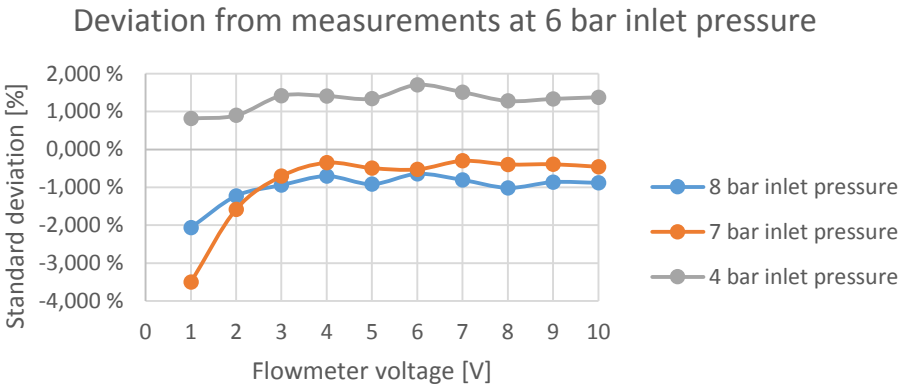

Figure 4.2-6 Standard deviation from the average flow rate values at 6 bar for Linout_B

Discussion

A significant decrease in the standard deviation from mean value, which describes the measurement data spread, was found for increasing capacity for both Linout_A and Linout_B at 6 bar. For Linout_A, flow rate data at 5% capacity (0,5 V) had a standard deviation of 2.62%, while flow rate data at 95% capacity (9,5 V) had a standard deviation of 0.017%. The same correlation between standard deviation and capacity was also present for Linout_B, implying that experiments gas should be fed into the reactor at higher capacity (voltage). This correlation is shown in Figure 4.2-7, and from this one can see above a flowmeter setting of 3 volts the decrease in data spread decreases. From this one can deduce that

experiments should be performed with flowmeters set to 3 volts or higher to increase measurement accuracy. Flow rate measurements for varying inlet pressures show the following correlations; increased flow rate for reduced inlet pressure and reduced flow rate for increased inlet pressure. The deviations from measured flow rates at 6 bar inlet pressure seem to be systematic, and a change of inlet pressure by $\pm$ 2 bar results in a average change of measured flow rate by $\pm$ 1,15 % accordingly.

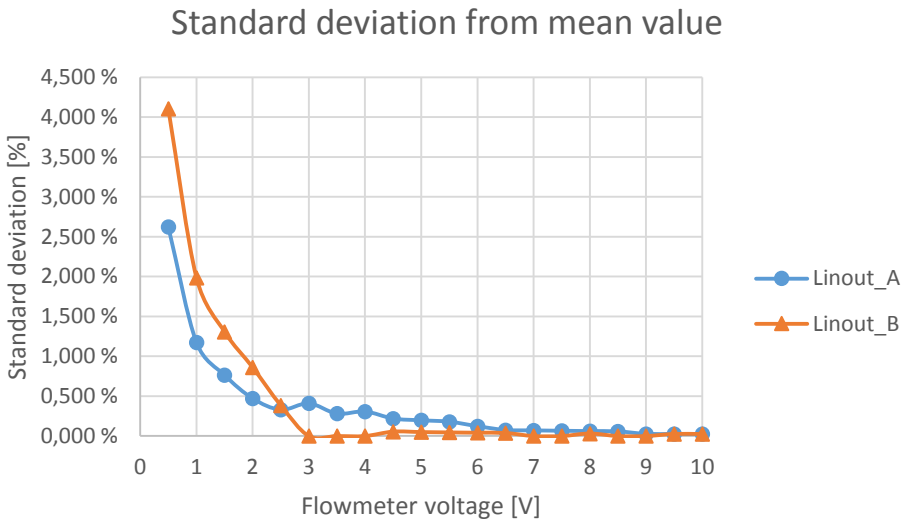

Figure 4.2-7 Standard deviation from average value from all 3 sessions at each flowmeter voltage

4.3 Reactor volume calibration

The CPA202 reactor holds about 250 ml and ChemiSens recommend to not fill the reactor with more than 180 mL of liquid due to risk of contact with upper lid, upper steel flange, and tubing and sensor equipment in upper lid [13]. The manual states that the volume of the reactor content do not affect the calibration, but the relationship between total reactor volume and reactor content volume affect the mol of material present in the gas phase. The change of mole in gas phase during temperature scanning experiments may affect the results due to the heat of vaporization, and the volume must therefore be calibrated in order to accurately calculate this effect. The calibration of the reactor volume was achieved through the use of a known reference volume and a pressure calibration device. The calibration device utilized was the pressure calibrator BEAMEX MC5, with a uncertenty of ± (0,025% RGD + 0,015% FS). Nitrogen gas was used in the calibration procedure because of close proximity to ideal gas law behavior.

Procedure

Before the calibration of the reactor volume can commence, a reference volume must be measured. A 1000 ml stainless steel gas cylinder was weighed while dry and then weighed again while filled with distilled water. The cylinder tank has valves attached in each end. The distilled water was filled in a slow manor to reduce air bubbles and to ensure a completely filled cylinder, including valves at each end. The distilled water was allowed to run through the cylinder and valves for 5 minutes in order to further reduce trapped air in the system. The temperature of the water was measured, and the procedure was repeated six times. The volume of the cylinder tank was found by using density calculated from equation (4.1-1) [15].

The SS-cylinder was connected to the reactor through a stainless steel pipe going through the bottom metal flange, to a nitrogen gas outlet in the wall and to the high resolution gas pressure calibrator. A vacuum pump was connected to the reactor vessel through a valve in the reactor lid, and the system was evacuated. After achieving a pressure of less than 0,03 bar in the system, the valve to the vacuum pump was closed. The SS-cylinder was subsequently filled with nitrogen gas to a pressure above 5 bar. The pressure was allowed to stabilize as the nitrogen gas reached room temperature. The total system, comprising of three subsystem, is described in Table 4.3-1 and shown Figure 4.3-1. The SS-cylinder with valves constitutes subsystem 1, and because this subsystem is a known volume reference and the gas pressure is known, the mol of nitrogen gas is subsequently known. From this starting point, all subsystem volumes can be found through the pressure difference to the previous subsystem.

Subsystem 1 was filled with nitrogen gas and the pressure was noted. Then the valve from the SS-cylinder to the stainless steel piping, which lead to the valve at the inlet tube of the reactor, was opened. Subsystem 2 was subsequently filled with nitrogen gas and the pressure was then noted. Then the valve at the inlet tube to the reactor vessel was opened. Subsystem 3 was allowed to fill with nitrogen gas and the pressure was noted. After this the entire system was subsequently evacuated through the use of the vacuum pump. This procedure was repeated 8 times. The inlet tube length and diameter was measured, and its volume found.

Table 4.3-1 System description

System	***Description***
Subsystem 1	SS-cylinder with valves
Subsystem 2	System1 + steel tubing between cylinder and inlet tube for reactor
Subsystem 3	System2 + reactor, inlet tube

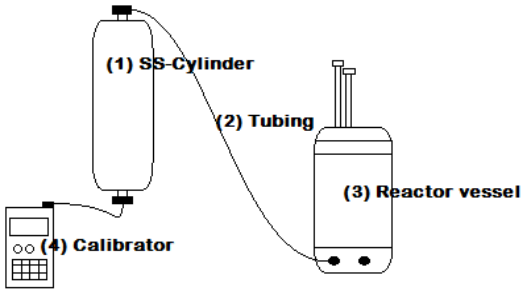

Figure 4.3-1 Constituents of calibration setup

Results

The calibration of the reference volume is based on 6 measurements, from which none are considered outliers. The dataset has a standard deviation from the average measured volume of 0.0034% (0.03 cm^2). The measured volumes are calculated based on the measured weight, temperature and temperature dependent density data found in literature [15], and the results are shown in Figure 4.3-2. The average volume for the SS-cylinder with valves was 1002.73 ± 0.03 cm^3.

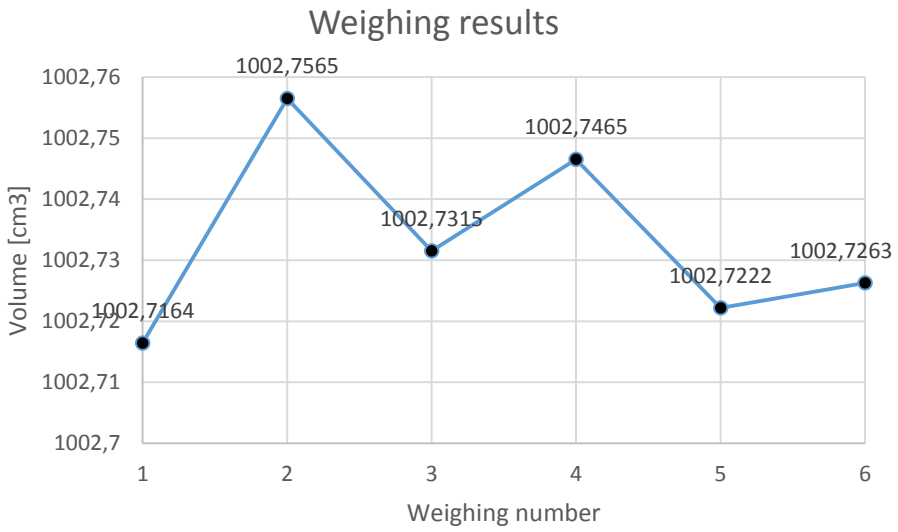

Figure 4.3-2 Volume measured for the SS-cylinder (reference volume)

The reference volume constitutes subsystem 1. By opening the valve and measure the pressure of subsystem 2, its volume can be calculated from ideal gas law. The mol of nitrogen in the system is known and assumed constant, the temperature is known and assumed constant, and the gas constant is constant. Therefore the only variables are volume and pressure. When knowing the pressure of subsystem 2, its volume can be found according to equation (4.3-1).

$$P_1V_1 = nRT = P_2V_2 \quad (4.3-1)$$

The calibration of the reference volume is based on 8 measurements, from which 1 is considered a outlier. The volume of subsystem 2 was found to be 1004,26 $\pm$0,09 cm^3.In the same fashion, the volume of subsystem 3 was found to be 1263,6 $\pm$0,20 cm^3. The volume of the inlet tube was calculated by equation (4.3-2) using measured length and diameter, and found to be 0,593 cm^3. By subtracting the volumes of subsystem 2 and inlet tube from subsystem 3, the reactor volume was found. The calibration of the reactor volume had a standard deviation from average value of 0.054% (0.14 cm^2) according to equation (4.4), and thus resulted in an average volume of 258.86 ± 0.14 cm^3. The results for reactor volume is shown in Figure 4.3-3.

$$V_{cyclinder} = \pi * r^2 * h \quad (4.3-2)$$

Where r is the radius of the tube and h is the length of the tube.

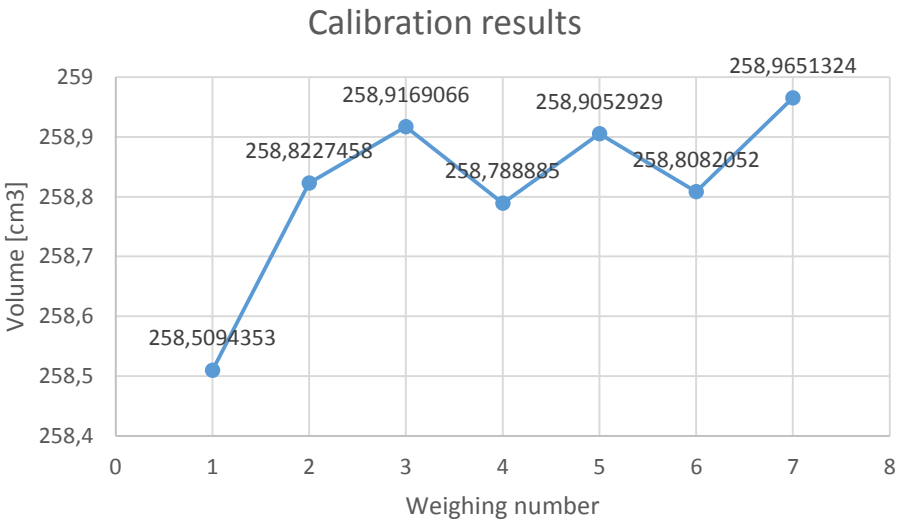

Figure 4.3-3 Results for calibration of reactor volume

Discussion

The calibrated reactor volume is 3,5% higher than the reactor volume as stated in the manual (250 cm^3). This is assumed to be because of openings in the lid for tubes, pressure gage, pressure release and other equipment. The reactor was kept in the thermostat bath, which was set to room temperature. The room temperature during the experiment was measured to 20,9 °C. The gas was allowed to reach room temperature in all subsystems, which gave a stable pressure signal and a low standard deviation from average. A stable signal from each subsystem indicate that there was no leakages present. After filling the system with nitrogen gas, it was allowed to settle and reach room temperature.

4.4 Heat flow calibration confirmation

The heat flow sensors of the CPA202 is calibration free, and only need to be pre-calibrated once at the factory. Therefor it is important to validate the heat flow signal output in order to assure accurate readings. The CPA202 reactor have, as mentioned earlier, heat flow transducers in the reactor base flange and reactor bottom, but only the base is used as heat exchange area against the surrounding bath [13]. The heat flow used in this study is the heat flow denoted Total Power, as described in chapter 2.3 with equation (2.3-2). The use of this dynamically corrected output is recommended by Nilsson in his dymanic test of the device [17]. The Total Power measurement is based on True Heat Flow, which is the measured heat flow through the reactor base, with the heat flow through the base flange subtracted from this. The latter is a consequence of the small offset temperature between the surrounding thermostat bath and the reactor content. The reactor is fitted with a general purpose electrical calibration heater, and it can heat the content with a known effect (maximum 6W). The error of this heater is unknown. The calibration of the heat flow transducers was performed in order to confirm that the Total Power measurements are accurate.

Procedure

The reactor was set at isothermal setting in order to maintain a preset temperature. Via ChemiCall V2 software, the validation heater was turned on at 6 watts and the Total Power and True Heat Flow was subsequently measured. After the validation heater was turned on the system was allowed to stabilize its temperature. This procedure was repeated 13 times, from which 7 under preset temperature of 50 °C and 350 RPM stirrer speed and 6 under preset temperature of 40 °C and 300 RPM stirrer speed. The amount of heat extracted from the reactor should the equal to the heat added by the validation heater. Between each measurement, the liquid content was increased with 7,5 ml (for preset temperature of 50 °C) and 10 ml (for preset temperature of 40 °C). By adding liquid, the validation of measured heat flow is assured over a large range of reactor filling levels.

Results

The heat flow measurements are based on 13 measurements, from which none are considers outliers. The values was found by using ChemiCall V2 software functionality, and thusly integrating both validation heater signal, Total Power and True Heat Flow. This procedure is shown in Figure 4.4-3. The integrated in Joules found are presented in Figure 4.4-1. The figure shows a close relationship between actual heat input from the validation heater and the heat flow integral of both Total Power (TP) and True Heat Flow (THF). The average standard deviation between the integral of the added heat from the Validation Heater and the integral of the heat flow necessary to maintain temperature was 1,25 % for TP and 1,21 % for TH, as calculated from equation (4.4-1). The standard deviations between measured heat flow and validation heater input for each session is shown in Figure 4.4-2.

$$Average\ deviation\ between\ HF\ and\ VH = \frac{\sum \frac{HF_n - VH_n}{HF_n}}{n} \qquad (4.4-1)$$

Where HF_n is the heat flow integral for session n, VH_n is the added heat integral for session n, and n is the total number of sessions.

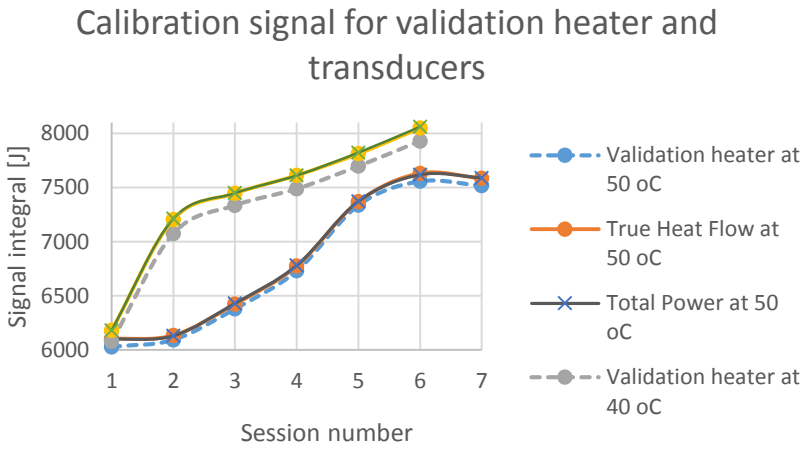

Figure 4.4-1 Integrated signal for validation heater and True Heat Flow transducers

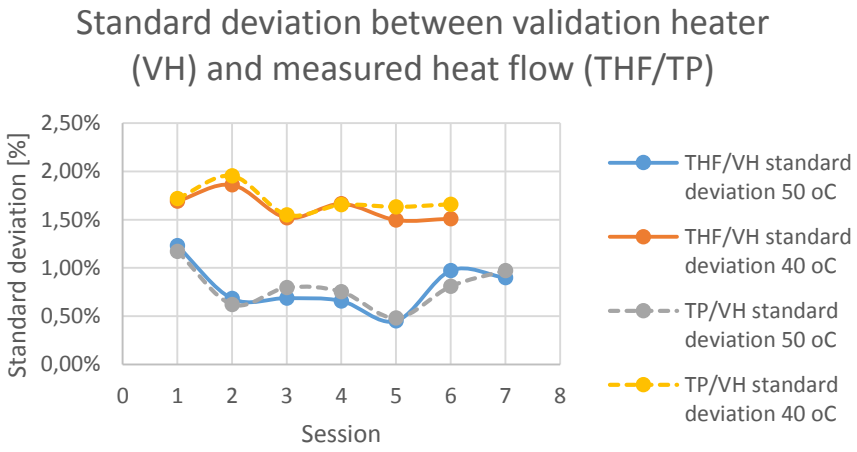

Figure 4.4-2 Deviation between True heat Flow and validation heater effect for each session

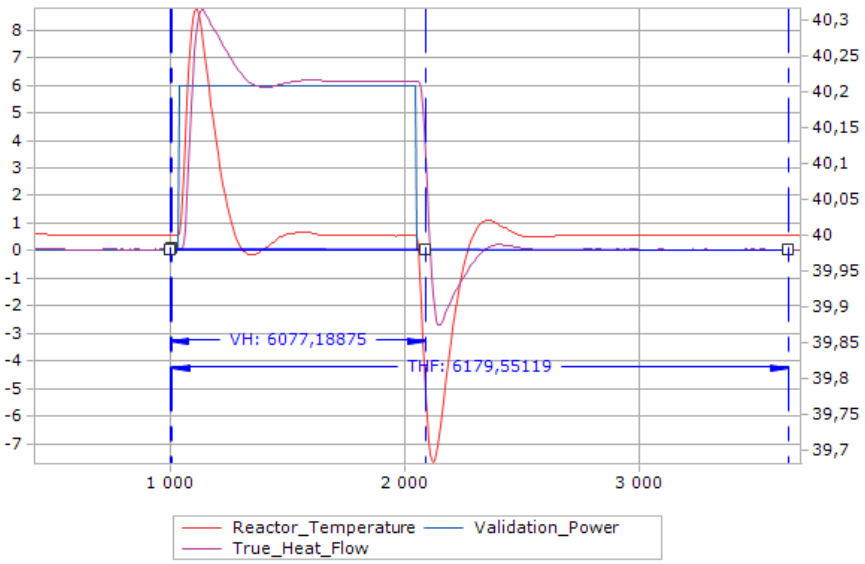

Figure 4.4-3 True Heat Flow calibration with the use of validation heater with temperature set to 40 °C

Discussion

The average difference between measured heat flow with and without dynamic correction was 5,7 J, which is 0,08% of the average heat input from the validation heater. The accuracy measured heat flow was shown to be 98,79 % for the True Heat Flow measurement, and 98,75 % for the dynamically corrected Total Power measurement. A heat flow calibration test performed by Nilsson and Hess [1] show a accuracy of 99,66 %. It is unknown if the uncertainty is connected to the heat flow transducers, the validation heater or the experimental procedure. In this experiment no corrections were used in order to account for the unmonitored heat flow through the Pyrex glass walls of the reactor. The high accuracy found by Nilsson and Hess involve optimization of the experimental conditions. This test show a greater accuracy for the sessions at higher temperature and stirring speed. Tuning of such parameters could improve accuracy.

5 System validation and other considerations

There are several parameters that may affect the experimental results, and must therefore be further investigated. As explained in chapter 5.1, there are known error sources which must be minimized and corrected for in order to achieve accurate experimental results for heat capacity and absorption heat studies. In addition to these, parameters such as unmonitored heat loss/gain and phase transitions effects must be accounted for. These are all important parameter for the experimental procedures utilized during this study, and will be thoroughly collaborated on during the following subchapters.

5.1 Common error sources

As mentioned, there are known error sources that can affect measurement accuracy during heat capacity experiments. Some of these error sources, such as filling level, baseline, logging and integration of heat flow, can also affect absorption heat experiments. The following error sources are, according to ChemiSens, critical during determination of heat capacity [18]:

Scanning rate	Too high scanning rate may cause a delay in the heating of upper flange and unmonitored armature. This phenomenon will cause internal reflux and result in additional unknown heat losses.
Filling level	Filling level must be considered in combination with stirring rate, and the liquid level must not reach upper flange.
Baseline	The baseline must have reached a true stable level before a scanning session is commenced.
Logging	The shortest logging interval must be used to improve integration accuracy
Integration of True Heat Flow	Customized baseline must be used. To find a correct baseline level it is recommended to use a first order filter.
Reflux and condensation	All surfaces and cavities exposed to vapor phase must have a temperature higher than the liquid temperature. If not, condensation may occur and when the cold surface reaches up with the liquid temperature the condensed liquid will evaporate. This is a slow process and will contribute to an exothermic power.
Heating of inserts	Inserts in major contact with lid must be avoided. Heating of inserts through the liquid is assumed.
Isothermal or isoberibolic mode	Correct operation mode must be chosen for the experiment.

5.2 Accounting for phase transition effects

The exact volume of the reactor have been shown to be 258,86 cm^3, while the maximum liquid content of the reactor must never exceed 180 ml. This volume difference, depending on the content volume, results in a significant volume for the vapor phase. The amount of mol of the reactor content in vapor phase will change because of differences in vapor pressure, due to the temperature change during temperature scanning experiments. Phase transition during such temperature scanning experiments may cause wrong heat flow measurements.

The experimental method for differential temperature scanning experiments works best for content differences more than 50 ml. This volume difference will affect the size of the phase transition contribution to the measured heat flow, and this contribution will be different for each of the two temperature scanning sessions.

Calculations

Phase transition involves subtraction or addition of energy to the reactor content, and will result in condensation of vapor or evaporation of liquid. This effect is taken into consideration by the use of ideal gas law, vapor pressure for average temperature in temperature scanning interval, heat of vaporization for the reactor content and specific heat capacity for the reactor content. The following equation (5.2-1) show how evaporation or condensation energy is estimated:

$$\Delta H_{vap} = \left(P_{vap} * \frac{V_R - V_{Liq}}{R * T_{Avg}} \right) * \Delta h_{vap} \quad (5.2-1)$$

Where ΔH_{vap} is the energy consumed or released in evaporation or condensation, P_{vap} is the vapor pressure of solution for the average temperature in the temperature scanning interval, V_R is the total volume of the reactor, V_{Liq} is the volume of the liquid sample (also referred to as reaction mass), R is the gas constant, T_{Avg} is the average temperature in the scanning interval and Δh_{vap} is the molar heat of evaporation from literature.

Results

The energy calculated is subtracted or added to the measured heat flow depending on the temperature scanning direction. Table 5.2-1 show data from two downwards temperature scanning experiments with water, with calculated energy contribution from condensation. This energy is measured by the heat flow transducers as it must be taken out of the reactor to reduce the temperature of the content. The energy must therefore be subtracted from the heat flow measurements, as it is not describing the temperature reduction in the reactor content. The average heat of vaporization contribution amounts to 0,31 % of the average measured Total Power for the scanning session of 104,847 g H_2O, which had an standard deviation from average value of 0,31 % calculated from equation (5.2-1). For the scanning session of 160,168 g H_2O the average contribution is 0,13 %, while the measurement data had a standard deviation from average value of 0,13 %. In both cases, the contribution from this phase transition effect is equal to the standard deviation in the data set. This indicates that the phase transition effect has a significant contribution that must be taken into consideration. If the measurements was performed with True Heat Flow, the measured heat flow value would be larger which would reduce the impact of the phase transition effect by some degree, but I would still not be negligible.

$$Standard\ deviation\ [\%] = \frac{\sqrt{\frac{\sum\left(M_{TP,n} - Av_{TP}\right)^2}{n}}}{Av_{TP}} \quad (5.2-2)$$

Where $M_{TP,n}$ is the measured Total Power for each session, Av_{TP} is the average Total Power measured, and n is the number of sessions.

Table 5.2-1 Average Total Power measurements from upwards temperature scanning session of 104,847 g and 160,168 g of H_2O with calculated energy contribution from condensation

Avg. Temp [ºC]	TP [J]	SD [%]	ΔH_{vap} [J]	ΔH_{vap}/ TP [%]
		104,847 g H_2O		
65	5053,86	0,24 %	24,73	0,49 %
55	4976,97	0,35 %	17,25	0,35 %
45	4966,04	0,31 %	11,67	0,24 %
35	5019,91	0,34 %	7,64	0,15 %
		160,168 g H_2O		
65	7754,55	0,02 %	15,58	0,20 %
55	7665,94	0,13 %	10,92	0,14 %
45	7663,87	0,20 %	7,42	0,10 %
35	7730,16	0,15 %	4,88	0,06 %

5.3 Wetted wall height

The CPA202 reactor performs its temperature measurements through heat flow transducers, but have none in its Pyrex glass walls. The Pyrex glass walls are not, and cannot be assumed to be, perfectly isolated. Therefore, there will be some heat exchange between the reactor content and the inner Pyrex glass wall, between the inner and outer Pyrex glass wall, and between the outer Pyrex glass wall and the surrounding thermostating bath. Due to the reactors small size, small differences in reactor content will greatly affect the amount in contact with the inner glass wall. The differences in reactor content amount thusly affect what is known as the wetted glass area, which in turn may have a significant effect on the systems heat flow measurement accuracy due to the mentioned unmonitored heat loss or gain.

ChemiSens recommend to use a correction for this effect, which includes both the heat capacity for the Pyrex glass walls and the lost energy to the thermostat bath. Based on the general geometry of the reactor and height of bottom flange, ChemiSens calculate the wetted wall height in cm and use a correction of 15 J/cm. This represent, as mentioned, both the heat absorbed by the Pyrex glass material and the unmonitored heat flow through the walls. The ChemiSens estimations assume a perfect cylindrical shape, while in reality the inserts will affect the inner geometry of the reactor. Because of this, there is a need for a more accurate wetted wall height estimation based on what inserts are used, how the inserts displace the reactor content and at what height this displacement occur.

Procedure

The maximum filling level for the CPA202 regular Pyrex glass wall reactor is 180 ml. As explained earlier, this is because of the risk of liquid entering the sensor equipment in the lid and the avoidance of liquid contact with the upper metal flange and lid. The reactor was taken apart and each insert and reactor part was measured to assure high accuracy of wetted wall height calculations. The inserts measured was baffles and the stirrer with paddles and torque transducer. In the reactor vessel, both height and diameter

of the glass wall and bottom metal flange was measured. In addition to measurements, the reactor was repeatedly filled with water up to the point where the Pyrex glass wall begins, and weighed. No inserts reach below the bottom edge of the inner glass wall, and will therefore not affect the bottom flange volume.

Results

The volume of the bottom metal flange is estimated by ChemiSens to be 41 ml, while measurements, and filling with water and weighing, show that it was closer to 42 ml. Thusly, the reactor content volume must be more than 42 ml in order to be in contact with the inner Pyrex glass wall.

The calculation of wetted wall height is based on the volume of the liquid content in the reactor and the density of the liquid content. Temperature dependent density is assumed, and temperature will therefore affect the content volume. For water, equation (4.4-1) is used to find the density. The average temperature in each temperature scan interval is used for density and volume calculations. The displacement of the baffles, which was found to be 3,2 cm^3, are evenly distributed across the height of the volume defined by the Pyrex glass wall, and its volume is therefore subtracted from the reactor glass wall volume. The volume of the cylinder defined by the inner Pyrex glass wall was therefore found to be 197,18 cm^3. The stirrer with torque transducer changes in thickness along the height of the Pyrex glass wall (84,0 mm), and its displacing volume is divided into three parts as shown in Figure 5.3-1. The cylinder volume defined by the inner Pyrex glass wall is therefore also divided into three sections; Section 1 is from 0 - 1,1 cm along the height of the glass wall, Section 2 is from 1,1 – 3,25 cm, and Section 3 is from 3,25 – 8,4 cm (top of glass wall). The displaced volume caused by the stirrer is calculated into the reactor section volume one and two through a decrease in diameter. Volumes found in the reactor are given in Table 5.3-1.

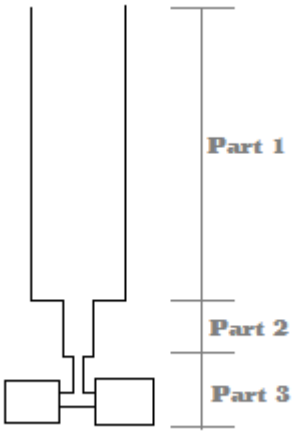

Figure 5.3-1 Stirrer divided into 3 parts

The combined volumes of the bottom metal flange and Section 1 is 86,44 cm^3. Since the minimum filling level is 100 cm^3, the liquid surface will always preside in Section 2 or 3. Thusly there is only need for two calculations of wetted wall height; WWH_1 and WWH_2. The former is described in equation (5.3-1) and the latter in equation (5.3-2):

$$WWH_1(< 120{,}9\ ml) = \frac{Vol_{Content} - Vol_{Bottom\ flange} - Vol_{Section\ 1}}{\pi * r_{Section\ 2} + h_{Section\ 2}} \quad (5.3-1)$$

$$WWH_2(> 120{,}9\ ml) = \frac{Vol_{Content} - Vol_{Bottom\ flange} - Vol_{Section\ 1+2}}{\pi * r_{Section\ 3} + h_{Section\ 3}} \quad (5.3-2)$$

Where $Vol_{content}$ is the volume of the liquid content, $Vol_{Bottom\ flange}$ is the volume of the bottom metal flange, $Vol_{Section\ 1}$ is the volume of Section 1, $r_{Section\ 2}$ is the radius of Section 2 (2,79 cm), $r_{Section\ 3}$ is the radius of section 3 (2,71 cm), and h is the height of Section 2 or 3. Estimates for wetted wall height for reactor content volumes below 120,9 ml are calculated using WWH_1, while for volumes over 120,9 ml WWH_2 must be used.

Table 5.3-1 Volumes measured in CPA202 reactor

Constituent	**Volume [cm^3]**
Original cylinder volume, inner Pyrex glass wall	200,36
Bottom metal flange	42,0
Baffle volume, total	3,19
Stirrer part 3, paddles	0,60
Stirrer part 2	0,35
Stirrer part 1	7,98
Cylinder volume section 1 (0-1,1 cm)	26,44
Cylinder volume section 2 (1,1-3,25 cm)	52,50
Cylinder volume section 3 (3,25 – 8,2 cm)	118,63

Discussion

The stirrer speed used will affect the wetted wall height as the liquid will be lifted upwards along the glass wall due to centripetal forces. Because of this effect, low stirrer speeds are recommended while performing temperature scanning [13, 18]. Turbulent flow are not needed for water, alcohol, pure amine or amine solution experiments, and the stirrer speed will therefore be kept at 100 rpm which provide sufficient mixing considering the paddle size against the small reaction mass volume.

5.4 System correction: Pyrex glass wall heat capacity and other heat losses

As discussed in the previous subchapter, it is necessary to use a correction for the unmonitored effects taking place in the system, such as unmonitored heat loss and Pyrex glass wall heat capacity. ChemiSens use 15 J/cm as a correction, which is multiplied with the difference in wetted wall height between two temperature scanning sessions. This constant correction is based on assumed heat capacities for the reactor vessel and inserts, and is not temperature dependent. In temperature scanning experiments performed with the CPA202 reaction calorimeter, a temperature dependent heat capacity for the reactor vessel and inserts, often referred to as the reactor constant, was discovered as shown in Figure 5.4-1. This reactor constant includes all heat flow connected to reactor and insert heat capacity and unknown heat losses. The measured True Heat Flow per Kelvin was used, and when data fitting to Osborne heat capacity values [10] the reactor heat capacity was found through equation (5.4-1). Figure 5.4-1 also show that the heat capacity for the reactor vessel and inserts is not only dependant on temperature, but also on filling level (amount of liquid in vessel).

$$\frac{\int Total\ power\ dT - \Delta H_{vap}}{\Delta T} - HC_{Reactor+inserts,\Delta T} = m_{liquid} * C_{p,Osborne} \quad (5.3-1)$$

Where $HC_{Reactor + inserts, \Delta T}$ is the calculated heat capacity for the reactor vessel and inserts [J/K] based on Osborne heat capacity, $Cp_{Osborne}$ ia the specific heat capacity from Osborne [J/(K*g)], ΔH_{vap} is the heat of evaporation, m_{H20} is the mass used in the temperature scanning session, and $\frac{\int Total\ power\ dT}{\Delta T}$ is the measured heat capacity for the total system of reactor vessel and liquid content [J/K]. $HC_{Reactor + inserts, \Delta T}$ was found through use of the "goal seek" excel function, an automated trial and error approach .

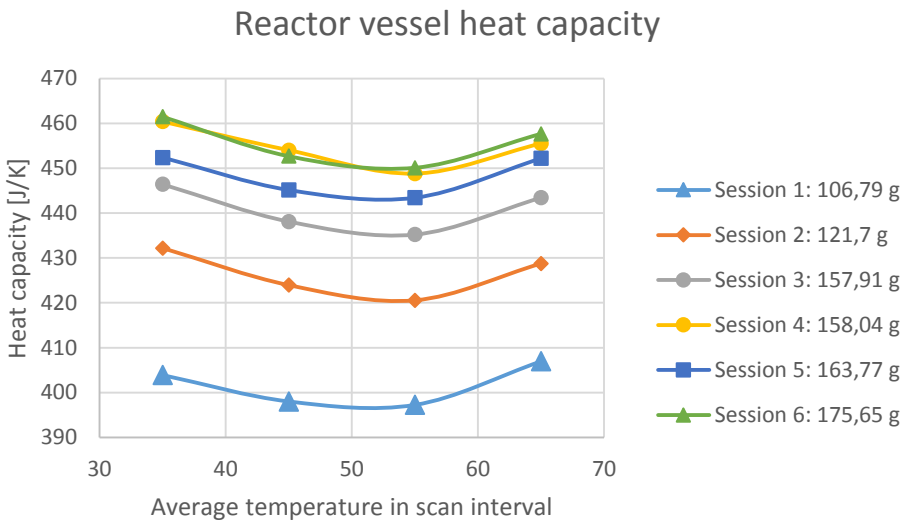

Figure 5.4-1 Heat capacity based on data fitting to Osborne experimental data for specific heat capacity for water

In Figure 5.4-2 a comparison is given between True Heat Flow and Total Power. As seen in the figure, the dynamic correction used in Total Power does not change the temperature dependency. From both figures it is apparent that the use of a constant correction factor will not be sufficient, and will not achieve a good enough accuracy for future heat capacity experiments.

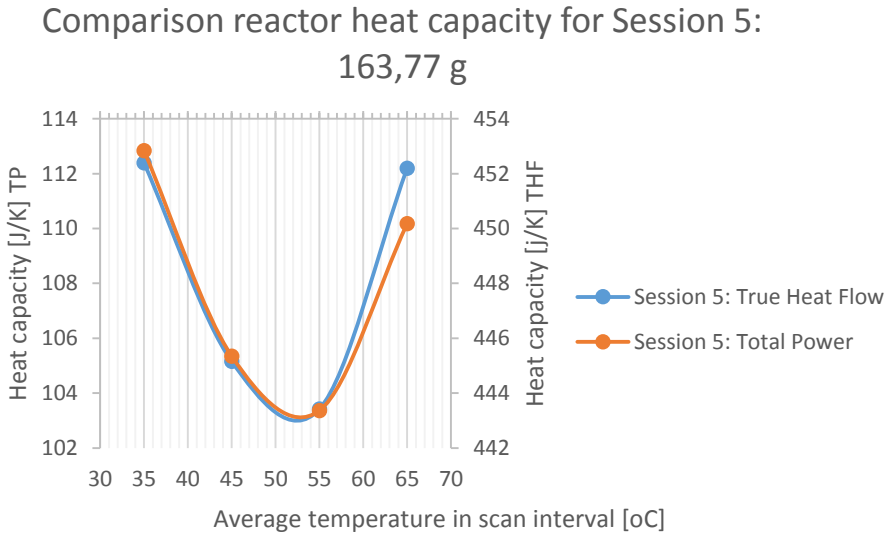

Figure 5.4-2 Comparison of calculated reactor heat capacity with True Heat Flow and Total Power for session 5

The correction factors used in this study is calculated with equation (5.4-1) based on 16 temperature scanning measurements on water at two fillings levels, 104,847 g and 160,168 g respectively. No outliers was observed. The temperature dependent density for water was found with equation (4.1-1), and used to obtain the average volume of the liquid water in each 10 ^{o}C temperature scan interval. From this, the wetted wall height was calculated using equation (5.3-1) and (5.3-2). The vapor pressure for the solution was calculated using Raoult's law, and vapor pressure for pure water [19]. With this, the phase transition effect was calculated using equation (5.2-1).

From equation (5.4-1) a total of 16 reactor heat capacities was obtained, two for each temperature scan interval at each filling level. The average reactor heat capacity was obtained for each temperature interval at each filling levels, resulting in 8 obtained values as listed with the corresponding wetted wall height in Table 5.4-1. Wetted wall height was then plotted against obtained $HC_{reactor+inserts}$ for both filling levels and all 4 temperature intervals as shown in Figure 5.4-3. A linear regression line was then obtained using excel trendline function, and from the obtained regression equations listed in Table 5.4-2, all correction factors used in this study was calculated. The input variable WWH for the correction factor was then the actual wetted wall height for each individual experiment.

Table 5.4-1 Obtained reactor constants for temperature scanning experiment with water based on literature data from Osborne

	WWH [cm]	$HC_{Reactor+inserts}$ **[J/K]**
		104,847 g
70-60 °C	2,676	64,005
60-50 °C	2,653	57,558
50-40 °C	2,633	57,327
40-30 °C	2,616	63,244
		160,168 g
70-60 °C	5,091	103,398
60-50 °C	5,054	95,705
50-40 °C	5,021	96,404
40-30 °C	4,994	103,491

Figure 5.4-3 Plot of WWH against $HC_{reactort+inserts}$ to obtain a linear regression correlation

Table 5.4-2 Obtained linear regression equation from which all correction factors are calculated

Temp. interval [°C]	Linear regression equation
70-60	$\boldsymbol{HC_{Reactor+inserts}} = 16{,}312 * \mathrm{WWH} + 20{,}347$
60-50	$\boldsymbol{HC_{Reactor+inserts}} = 15{,}891 * \mathrm{WWH} + 15{,}395$
50-40	$\boldsymbol{HC_{Reactor+inserts}} = 16{,}363 * \mathrm{WWH} + 14{,}241$
40-30	$\boldsymbol{HC_{Reactor+inserts}} = 16{,}926 * \mathrm{WWH} + 18{,}959$

Due to time constrictions for this study, the correction factors are only based on two filling levels. It is recommended that the correction factors are based on 3 or more filling levels between 105 and 165 ml for future heat capacity experiments. It is also recommended to use a higher number of measurements for each filling level in order to achieve averages that are more accurate.

5.5 Scanning speed considerations

According to ChemiSens, when performing temperature scanning experiments the scanning speed should be no more than 0,5 °C/min. To avoid internal temperature reflux effects, and to maintain maximum system control, the temperature of the thermostating bath is always kept in close proximity to the reactor content temperature [1, 13]. The thermostating bath is on average kept 0,2 degrees above the reactor content temperature regardless of thermal operating mode. This results in a small constant heat flow into the reactor content through the reactor vessel, which is measured in the base metal flange and subtracted from the True Heat Flow. If the thermostat bath is below reactor content temperature, condensation is the gas phase could become a significant error source. When the temperature of the thermostating bath is kept higher than the reactor content temperature, condensation if minimized because the reactor vessel temperature is kept above content temperature. To maintain the close temperature proximity, a low scanning speed is needed. If the scanning speed is too high, the delayed temperature of the upper metal parts of the reactor might cause internal heat reflux [13].

Procedure

50 scanning experiments in the temperature interval between 60 and 70 °C was performed with three different scanning speeds; 0,5 °C/min, 0,3 °C/min and 0,2 °C/min. The scanning was performed under isothermal operating mode, and in both upwards and downwards direction. All scanning experiments was performed on 138,027 g of distilled deionized water. True Heat Flow is used to see the full effect of scanning speed without dynamic correction. The goal of the experiment was to investigate the scanning speeds effect on measurement accuracy.

Results

From the 50 measurements, none was considered outliers. The measurement data is shown in Table 5.5-1. There was discovered a correlation between lower scanning speed and higher data point density, meaning that the standard deviation from average measured value was lower, as shown in Figure 5.5-1. The standard deviation of the dataset was shown to decreased with decreasing scanning speed, calculated from equation (5.2-2). The reduction in standard deviation was largest between 0,5 °C/min and 0,3 °C/min, which resulted in an average reduction of 40 %. There was no significant reduction between 0,3 °C/min and 0,2 °C/min, as the difference between 0,3 °C/min and 0,2 °C/min are significantly lower than the standard deviation in the data set.

Table 5.5-1 Measurement data for scanning speed experiment

	Scan speed [°C/min]	Avg THF/K [J/K]	ΔT [°C]	Standard deviation [J/K]	Standard deviation [%]	Deviation reduction [%]
Session 1	0,5	1013,13297	10,0002	6,59617278	0,6511 %	
						36,20 %
	0,3	1014,7048	9,9999	4,20806203	0,4147 %	
Session 2	0,5	1003,31981	10,0001	4,12457144	0,4111 %	
						44,36 %
	0,3	1005,62774	10,0002	2,29508597	0,2282 %	
						-0,10 %
	0,2	1008,61716	10,0004	2,29738447	0,2278 %	

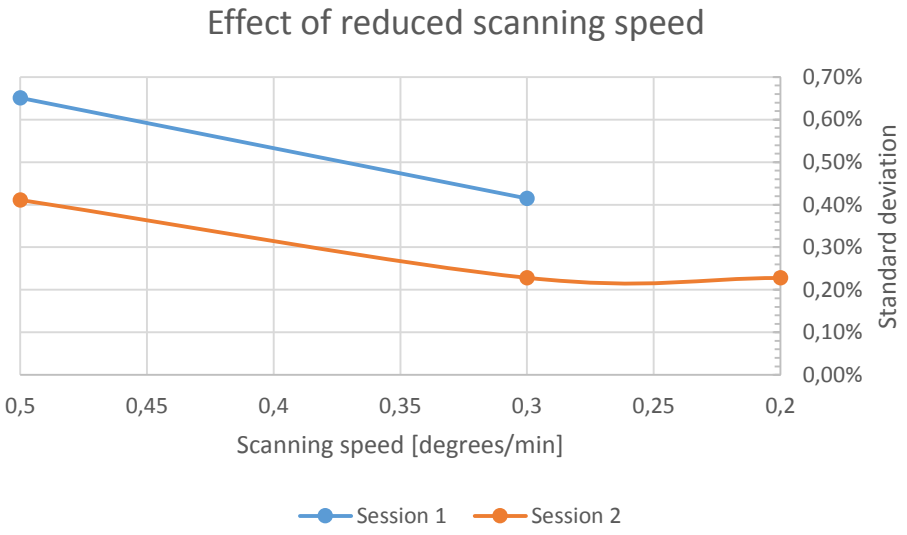

Figure 5.5-1 Reduction in standard deviation from average measured value between different scanning speeds

When scanning speed is reduced, the signal size is also reduced, and this increases the uncertainty of the signal integration. In Figure 5.5-2 the signal size of 4 consecutive True Heat Flow measurements at 0,5 ºC/min, 0,3 ºC/min and 0,2 ºC/min respectively. The figure shows that a scanning speed of 0,2 ºC/min yield a signal strength of 3,5 W, compared to 8,5 W at 0,5 ºC/min and 5 W at 0,3 ºC/min. From this figure it is apparent that the signal strength is significantly reduced between 0,5 ºC/min and 0,2 ºC/min.

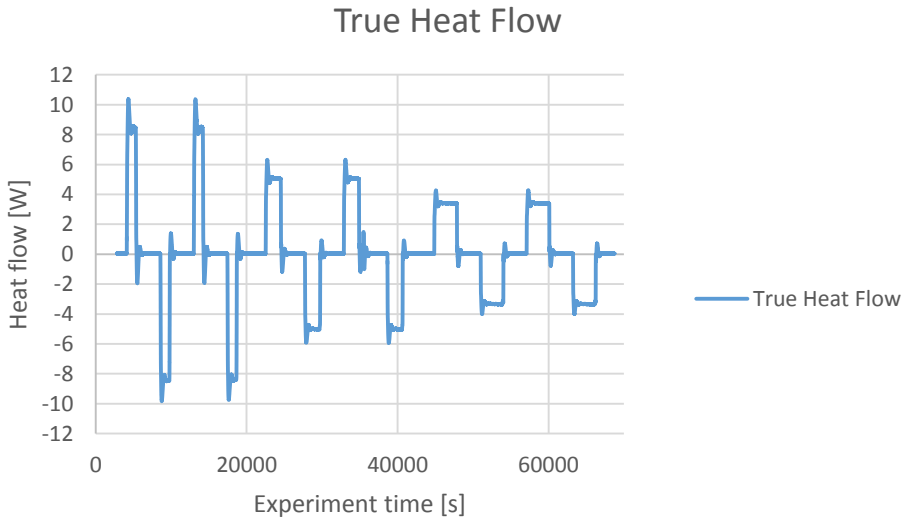

Figure 5.5-2 4 consecutive temperature scanning sessions at 0,5 ºC/min, 0,3 ºC/min and 0,2 ºC/min respectively

Discussion

The experiments show that a scanning speed lower than 0,3 ºC/min will not necessarily result in higher measurement accuracy. There is a tradeoff when considering scanning speed between signal strength and experimental accuracy. If the signal strength is to low, the accuracy of the experimental values decreases due to higher uncertainty during the integration of the signal. If the signal strength is unnecessary high (because of high scanning speed), the accuracy of the experimental values decreases

due to heat reflux. The signal strengths achieved at 0,3 °C/min and 0,2 °C/min is considered to be too low, and for this study a scanning speed of 0,4 °C/min is used.

5.6 Scanning directionality and thermal operating mode considerations

Scanning directionality must be taken into consideration when performing temperature scanning experiments. The optimal directionality is connected to the utilized thermal operating mode and to the internal workings of the reactor. The CPA202 operating system ChemiCall V2 can use several thermal modes, and the most suited for this study are the isothermal and isoperiobolic operating modes.

Isoperibolic operating mode

The isoperibolic mode measures the temperature in the bottom of the reactor, which contains both a Peltier element and heat flow trancducer, and the system tries to maintain this temperature at a set level. Use of this thermal mode may result in a temperature change lag within the reactor content as the reactor content temperature changes slower than the bottom temperature. When scanning upwards ChemiSens advices to use isoperibolic operation mode. This assures that condensation on the lid is minimized because the reactor content temperature is delayed compared to the temperature of the vessel itself.

Isothermal operating mode

The isothermal mode measures the temperature in the reactor content, and when scanning downwards in the temperature interval, isothermal mode is recommended by ChemiSens [18]. This is because of the risk of internal heat reflux that may affect the results of the experiment. If isoperibolic mode is used, the reactor content temperature may lag behind the base plate temperature. The isothermal mode relates the temperature ramp of the scanning procedure to the temperature of the reactor content, also referred to as the reaction mass. When the temperature of reactor and content is changed, the inner part of the bottom metal flange will be heated by the reactor content and the outer part will be heated by the thermostating bath. Only the internal part will contribute to the True Heat Flow, but the relationship between what is heated from the inside or not is not constant.

Scanning direction

When considering upwards or downwards scanning direction, the recommended differential temperature scanning experiment method from ChemiSens was used. The specific heat capacity of water was calculated using this method, and the effect of scanning directionality checked. Scanning direction has been studied with the use of water because of very accurate heat capacity data available. The experimental data from Osborne have been used for comparison [10] to specific heat capacity found with temperature scanning experiments. From two temperature scanning sessions for 121,702 g H_2O and 158,041 g H_2O respectively, a specific heat capacity for water was found by the use of differential temperature scanning method. These values are shown in Table 5.6-1. Both scanning sessions were performed at 0,4 °C/min in both upwards and downwards direction. The results show that the average difference between Osborne heat capacity data and heat capacity found in the experiment was 1,69 % for heat capacity based only on upwards scanning data. For downwards scanning data the average difference was 1,34 %.

Downwards scanning consistently result in a higher measured True Heat Flow than upwards scanning, but there is no significant correlation between scanning direction and consistency in measurement data (standard deviation from average). There is a slight correlation between scanning direction and accuracy

(closer to Osborne data), as heat capacity based on downwards scanning achieve more accurate results when compared to Osborne data. From these experiments it was shown that downwards scanning is the preferred scanning direction, in combination with isothermal operating mode.

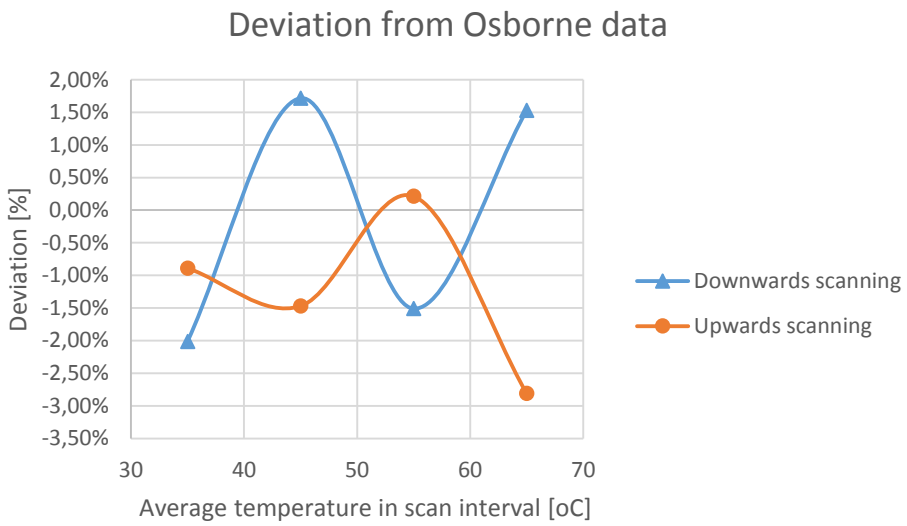

Figure 5.6-1 Deviation in percentage from Osborne experimental data

Table 5.6-1 Specific heat capacity for water based on upward, downwards or both scanning directions

Average temperature [°C]	Downward scanning [J/(K*g)]	Upward scanning [J/(K*g)]	Osborne data [J/(K*g)]
65	4,25	4,06	4,18614
55	4,12	4,19	4,18164
45	4,25	4,11	4,17854
35	4,09	4,14	4,17739

5.7 Reactor filling level and stable baselines

Determination of heat capacity with the CPA 202 Reaction Calorimeter requires that the heat capacity of the reactor parts are taken into consideration. This is because the heat capacity of the rector vessel is large compared to the reactor content, and to improve the accuracy the reactor content amounts should not be too small [18]. As mentioned earlier, the CPA202 glass wall reactor cannot be used with liquid contents above 180 ml. This is to avoid liquid contact with the upper metal flange and lid. Because of the small size of the reactor, which results in in a small reactor content compared to the reactor vessel itself, ChemiSens recommends to use as much reaction mass as possible. When performing differential temperature scanning experiments, ChemiSens also recommend that the difference in amount (ΔLiquid mass) should exceed 50 ml for best result.

In differential temperature scanning experiments on water performed during this study, no significant increase or decrease in experimental accuracy (obtained C_p compared to Osborne data) was shown when different ΔLiquid mass between 35 ml and 60ml was used. There was however shown a strong correlation between reaction mass amount (liquid mass) and experimental data standard deviation, as shown in Table 5.7-1. For amounts less then 105 ml, a significant increase in standard deviation occur. The larger amounts used, the smaller the standard deviation. This effect was shown up to 170 ml, from

which the standard deviation started to increase. This is related to the proximity to the upper metal flange and lid.

The measurement data shown in Table 5.7-1 is based on 84 measurements from which 7 are considered outliers. The temperature scanning experiments have been performed under equal conditions, and the standard deviation from average value within each temperature interval for each respective filling level is calculated according to equation 4.2-5. Based on these results, the heat capacity measurements performed for alkanolamine solutions in this study have been of liquid amounts of more than 105 ml and less than 170 ml.

Table 5.7-1 Standard deviations for temperature scanning experiments on distilled deionized water

Temp interval [°C]	**Standard deviation [%]**						
	100,12 g	**100,69 g**	**106,79 g**	**125,04 g**	**151,34 g**	**159,99 g**	**175,65 g**
70-60	0,18 %	0,76 %	0,08 %	0,15 %	0,07 %	0,09 %	0,01 %
60-50	0,13 %	0,12 %	0,19 %	0,09 %	0,08 %	0,12 %	0,13 %
50-40	0,10 %	0,10 %	0,12 %	0,04 %	0,13 %	0,12 %	0,29 %
40-30	0,15 %	0,08 %	0,10 %	0,03 %	0,04 %	0,04 %	0,05 %
Avg SD	0,14 %	0,26 %	0,12 %	0,08 %	0,08 %	0,09 %	0,12 %

If a temperature scan is to achieve high accuracy, a stable baseline for reactor temperature and heat flow is needed. ChemiSens recommends an average signal stability variation for heat flow of $\Delta W = 0,02$ W over a minimum of 200 seconds [20]. The "condition set" command in ChemiCall V2 ProFind automation program was set to obtain a maximum average signal variation of ±0,03 W for the measured heat flow and ±0,003 °C for measured reactor temperature over a period of 600 seconds. This "condition set" command was used before and after temperature scan in order to allow for accurate integration. Throughout this study it has been observed that the CPA202 Reaction Calorimeter needs more than 2000 seconds to achieve this level of signal stability, and therefore the standard "condition set" command used during the alkanolamine heat capacity experiments was to achieve the mentioned signal average signal variation over 600 seconds within 900 seconds of recording. In this way the "condition set" command will run twice, and the second run will be guaranteed to achieve the set values.

6 Experimental procedure

When determining heat capacity using the CPA202, ChemiSens recommends two experimental procedures; temperature scanning experiment and addition of liquid. In addition ChemiSens strongly recommend to use as large amount of reaction mass as possible to improve the precision as different inert parts in the reactor is relatively large compared to the heat capacity of the reaction mass [18].

In the following chapters heat capacity experimental procedures recommended by ChemiSens for the CPA202 Reaction Calorimeter is discussed, and a developed procedure for heat capacity experiments is presented. The developed procedure for future heat capacity experiments is based on the recommendations from ChemiSens, and the conditions used are based on the calibration and validation work presented in chapter 4 and 5.

6.1 ChemiSens recommendation: Addition of liquid

Addition of liquid is often considered the simplest technique for determining the heat capacity. While the reactor operates at isothermal operating mode and under a preset temperature, a known amount of the same liquid is added to the reactor. The heat capacity is then calculated based on the measured heat flow necessary for heating up the reaction mass to the preset temperature [18]. This addition can be done batch-wise using the MSC202 dosing syringe or continuously by using a pump. The temperature for the added liquid must be known, and it is recommended that it is close to ambient temperature. ChemiSens recommend the use of the special reactor cover with large openings for this technique. A common error source is variable wetted wall areas due to splashes from the added liquid. The added liquid must be measured at the inlet of the reactor, and ChemiSens recommends using a special armature for correct measurements. The calculation method for batch-wise addition is given by equation 6.1-1 and for continuous addition by equation 6.1-2 [18].

$$C_P = \frac{\int TrueHeatFlow * dt}{Added\_mass * \Delta T} \qquad (6.1-1)$$

$$C_P = \frac{\int TrueHeatFlow * dt}{\int Added_{mass} * \Delta T * dt} \qquad (6.1-2)$$

Where ΔT refers to the temperature difference between the liquid in the reactor and the added liquid, $\int TrueHeatFlow * dt$ is the integral of the measured true Heat Flow.

Discussion

Preliminary heat capacity measurements of water was performed using this method in order to assess its accuracy. The method used was batch-wise addition, and 23 measurements at 40 and 50 ºC was performed from which 7 was considered to be outliers. The achieved heat capacities from these measurements had an average deviation from Osborne of 16,7%, and no systematic temperature effect on measured heat capacity was observed. The reactor setup used in this study was without the recommended special armature, and the temperature of the liquid added was assumed to be at ambient temperature. It was quickly apparent that this approach would not render accurate heat capacity measurements without special armature with which temperature of added liquid could be accurately measured.

6.2 ChemiSens recommendation: Temperature scanning experiment

The basic technique is to run a scanning experiment between two preset temperatures, and then repeat the experiment with a decreased or increased amount in the reactor. The evaluation is based on integral values and thusly the average value for the temperature range is obtained. From this the heat capacity versus the temperature can be obtained. By running the experiment with two different amounts the inserts and inert parts of the reactor is compensated for [18]:

$$\frac{\int True\ heat\ Flow\ dt}{\Delta T} = C_{p_{reactor\ content}} + C_{p_{Inserts}} + C_{p_{Inert\ parts}} \qquad (6.2-1)$$

It is essential that the experimental circumstances are the same for both runs. The system must be in perfect thermal equilibrium and the start- and endpoints for the integration must be sufficiently far from the transient regions or the integral values will be erroneous [18]. The specific heat capacity is calculated through the following equation:

$$\frac{\int True\ heat\ Flow_{(Mass+\Delta Mass)}\ dt}{\Delta T} - \frac{\int True\ heat\ Flow_{(Mass)}\ dt}{\Delta T} = \Delta Mass * Cp \qquad (6.2-2)$$

Where Mass is the original mass of the content and ΔMass is the additional mass from the second run. ΔT is the temperature step, $\int True\ heat\ Flow\ dt$ is the integral of the measured True Heat Flow, and Cp is the specific heat capacity of the reactor content [18].

6.3 ChemiSens recommendation: NTNU Template

At delivery of the CPA202 Reaction Calorimeter, an experimental method for heat capacity measurements was presented by ChemiSens in an Excel template file in order to demonstrate the capabilities of the apparatus. The following conditions was recommended:

- Maximum stirring rate of 100 RPM with turbine or propeller. Recommended to achieve minimum vortex.
- Scanning rate of 0,5 °C/min over a 10 °C temperature interval
- Downwards scanning
- Minimum 100 ml liquid reaction mass

A known amount of liquid is cooled down and the measured heat flow is integrated. The heat capacity of the reactor and inserts is subtracted from the measured heat capacity, and then divided by the reaction mass in order to obtain the specific heat capacity if the reaction mass. The Cp is calculated as shown I equation 6.3-1.

$$m_{liq} * C_P = \frac{\int True\ heat\ flow\ dt}{\Delta T} - HC_{reactor} \qquad (6.3-1)$$

$$HC_{Reactor}\left[\frac{J}{K}\right] = 220 + Inserts + Wetted\ glas\ area + correction\big(0{,}5 * (T-30)\big) \qquad (6.3-2)$$

$$Wetted\ glas\ area\ = \frac{V_{liq} - V_{Reactor\ base}}{23{,}7} \qquad (6.3-3)$$

Where *correction* is the correction factor of 15 J/cm, *Inserts* is the estimated heat capacities for the used inserts [J/K], and T is the average temperature in the scan interval [°C].

In Table 5.3-1 the results of this method, as listed by ChemiSens in the NTNU template, are shown. As can be seen from the table, the method yield specific heat capacities for water at a accuracy of 97,27 % compared to Osborne data. There is no observable systematic temperature effect present due to the high

uncertainty. This approach was tested and the obtained values was quickly rejected as the obtained heat capacities had even higher inaccuracy than in the template. This method did not achieve high enough accuracy to be able to show the temperature effect on the specific heat capacity of water. The problem is thought to be connected to the use of static reactor heat capacity estimates, and an inaccurate correction factor.

Table 6.3-1 Results from Cp measurements in NTNU Template

Mass [g]	Volume [ml]	Int(THF) [J/K]	Temp-int [ºC]	Av.Temp [ºC]	Wetted wall heigh [cm]	HC_Reactor [J/K]	Cp [J/g,K]	Error [%]
100	100	720,2	50 to 40	45	2,5	293,8	4,26	2,0
100	100	725	70 to 60	65	2,5	303,8	4,21	0,8
100	100	735	80 to 70	75	2,5	308,8	4,26	2,0
100	100	797	50 to 40	45	2,5	365,3	4,32	3,3
100	100	797	40 to 30	35	2,5	359,3	4,38	4,7
150	150	1040	50 to 40	45	4,6	397,0	4,29	2,6
150	150	1041	40 to 30	35	4,6	391,0	4,33	3,7

6.4 Experimental procedure for heat capacity measurements

The following experimental procedure is developed through trial and error in order to achieve specific heat capacities accurate enough to describe the temperature effect. The experimental procedure developed can be seen as a combination of the NTNU template procedure and the temperature scanning experiment procedure, both developed by ChemiSens. The procedure uses two different filling levels in order to reduce to impact wetted wall area and reactor heat capacity has on the measurement. It takes phase transition effects into consideration, and has a more dynamic calculation of the heat capacity for reactor vessel and inserts, which also accounts for unknown heat losses. This procedure calculates specific heat capacity for low and high filling level, but it is recommended to take the average between these to achieve the most accurate C_p. If there is no time constrictions, more than 2 filling levels are recommended.

The recommended conditions for the system are the following:

- Stirrer speed at 100 RPM. If sample liquid has high viscosity, a small increase in stirrer speed is recommended.
- Condition set: an average $\Delta W = 0{,}03$ for heat flow and $\Delta T = 0{,}003$ for reactor temperature during 600 seconds from a 900 second collection.
- Filling level between 105 ml and 165 ml. It is recommended that the difference in filling levels exceed 50 ml, although the proposed method is not sensitive to this.
- It is recommended to use similar filling levels to what was used when obtaining the correction factors. The liquid used for obtaining correction factors should be similar in viscosity, and other physical properties, to the sample liquid.
- A temperature interval of $\Delta T=10$ ºC was used with success. In literature however, it is often recommended to use shorter intervals to avoid obtaining average heat capacities over too long temperature ranges.
- A scanning rate of 0,4 ºC/min was used successfully. Scanning rate below 0,3 ºC/min and above 0,5 ºC/min is not recommended.
- Downwards scanning under isothermal operating mode.

- Total Power is recommended due to its dynamic correction which yield higher accuracy in transition regions.
- Reactor mass volume must be calculated, or otherwise obtained, with temperature dependency for accurate wetted wall height calculation

It is of high importance that the experimental conditions used, also for obtaining correction factors, are the same for all heat capacity experiments as the apparatus is sensitive to changes. The heat capacity is calculated using equation (6.4-1) and correction factors for each temperature interval listed in table 6.4-1:

$$\frac{\int Total\ power\ dt - \Delta H_{vap}}{\Delta T} - HC_{Reactor+inserts,\Delta T} = m_{liquid} * C_p \quad (6.4-1)$$

Where m_{liquid} is the mass of solution, $HC_{Reactor+inserts,\Delta T}$ is the correction factor for the spesific temperature interval, and $\int Total\ power\ dt$ is the integral of the measured Total Power. The input *X* in the correction factor $HC_{Reactor+inserts,\Delta T}$ is the wetted wall height, WWH, calculated by equation (6.4-2) and (6.4-3):

Table 6.4-1 Correction factors for 4 temperature intervals between 70 and 30 °C

Temp. interval [°C]	Linear regression equation
70-60	$\boldsymbol{HC_{Reactor+inserts}} = 16{,}312 * \mathrm{WWH} + 20{,}347$
60-50	$\boldsymbol{HC_{Reactor+inserts}} = 15{,}891 * \mathrm{WWH} + 15{,}395$
50-40	$\boldsymbol{HC_{Reactor+inserts}} = 16{,}363 * \mathrm{WWH} + 14{,}241$
40-30	$\boldsymbol{HC_{Reactor+inserts}} = 16{,}926 * \mathrm{WWH} + 18{,}959$

The $HC_{Reactor+inserts}$ is obtained as described in chapter 5.4, and accounts for the heat capacities of the reactor vessel and inserts, as well as the unmonitored heat losses through the Pyrex glass walls. When this is obtained with a reference sample such as water, two filling levels are used.

$$WWH_1(< 120{,}9\ ml) = \frac{Vol_{Content} - Vol_{Bottom\ flange} - Vol_{Section\ 1}}{\pi * r_{Section\ 2} + h_{Section\ 2}} \quad (6.4-2)$$

$$WWH_2(> 120{,}9\ ml) = \frac{Vol_{Content} - Vol_{Bottom\ flange} - Vol_{Section\ 1+2}}{\pi * r_{Section\ 3} + h_{Section\ 3}} \quad (6.4-3)$$

Where $Vol_{content}$ is the volume of the liquid content, $Vol_{Bottom\ flange}$ is the volume of the bottom metal flange (42 ml), $Vol_{Section\ 1}$ is the volume of Section 1, $r_{Section\ 2}$ is the radius of Section 2 (2,79 cm), $r_{Section\ 3}$ is the radius of section 3 (2,71 cm), and h is the height of Section 2 or 3. Estimates for wetted wall height for reactor content volumes below 120,9 ml are calculated using WWH_1, while for volumes over 120,9 ml WWH_2 must be used.

$$\Delta H_{vap} = \left(P_{vap} * \frac{V_R - V_{Liq}}{R * T_{Avg}}\right) * \Delta h_{vap} \quad (6.4-4)$$

Where ΔH_{vap} is the energy consumed or released in evaporation or condensation, P_{vap} is the vapor pressure of solution for the average temperature in the temperature scanning interval, V_R is the total volume of the reactor, V_{Liq} is the volume of the liquid sample (also referred to as reaction mass), R is the gas constant, T_{Avg} is the average temperature in the scanning interval and Δh_{vap} is the molar heat of evaporation from literature.

The experimental procedure should be seen as a work in progress, as there is room for improvement in order to increase accuracy by accounting for more unknown effects. Future users is recommended to continue the work with accounting for:

- *Heat of absorption:* As the molecules in vapor phase is reabsorbed into the liquid under equilibrium conditions or due to condensation, a small heat effect from the heat of absorption can be assumed to affect the heat flow measured. It is recommended that this is taken into consideration.

6.5 Experimental procedure: Calculation example and correction factor validation with ethyl alcohol

Heat capacity experiment according to the procedure described in chapter 6.4 was performed on ethanol with a purity of 99,85%. The dataset is comprised of 16 measurements, consisting of 2 temperature scans for each temperature interval at both filling levels. None of the obtained measurements was considered outliers. In Table 6.5-1 the average values at each filling level is listed.

Table 6.5-1 Average values from heat capacity experiment for ethyl alcohol

		82,849 g	
T [oC]	**TP [J]**	**T_1 [ºC]**	**T_2 [ºC]**
70-60	3099,76596	70,00025	60,00014
60-50	2913,19728	60,000115	50,000465
50-40	2791,40087	50,000465	40,000195
40 30	2748,55511	40,000195	29,999995

		126,600 g	
T [oC]	**TP [J]**	**T_1 [ºC]**	**T_2 [ºC]**
70-60	4726,33581	69,999605	59,999915
60-50	4495,6995	60,000015	50,00011
50-40	4315,56319	50,00011	40,00013
40 30	4216,15143	40,00013	29,999585

Calculating the phase transition effect

When determining the specific heat capacity for ethanol, the phase transition effects must be taken into consideration in accordance with chapter 5.2. In order to calculate the vapor pressure for ethanol the Antione equation (6.5-1) was used with parameters from Kretschmer et al. [21] shown in Table 6.5-2. The density of ethanol at the average temperature in each temperature interval is calculated with equation (6.5-2) from Ortega [22]. From this the volume of the liquid at each average temperature is calculated as shown in Table 6.5-3. The volume of the reactor is V_R = 258,86 ml. Equation 6.4-4 is used to calculate the heat of condensation, which must be subtracted from the measured Total Power. The calculated energies released in condensation is listed in Table 6.5-3.

$$log_{10}(P) = A - \frac{B}{T + C} \qquad (6.5-1)$$

Where A, B and C are fitted parameters, and T is the temperature in K.

Table 6.5-2 Parameters for Antione equation for ethanol vapor pressure [21]

Temperature [K]	A	B	C
273,15 – 351,70	5,37229	1670,409	-40,191

$$\rho = A * e^{B*T} \qquad (6.5-2)$$

Where the fitted parameter A is 0,8108 g/cm^3, fitted parameter B is -1,23*10^3 1/^{o}C and T is the temperature in ^{o}C.

Table 6.5-3 Liquid volume for each temperature interval, ethanol

T [^{o}C]	82,849 g V_{Liq} [ml]	126,600 g V_{Liq} [ml]
70-60	112,12	171,33
60-50	110,48	168,82
50-40	108,88	166,38
40 30	107,33	164,01

Table 6.5-4 Calculated energy consumed by condensation in each temperature interval, ethanol

T [^{o}C]	82,849 g ΔH_{vap} [J]	126,600 g ΔH_{vap} [J]
70-60	51,30	30,68
60-50	36,58	22,25
50-40	25,34	15,66
40 30	16,99	10,66

From equation (6.4-2) and (6.4-3), with the volumes found in Table 5.3-1, the wetted wall height of the liquid was calculated for each temperature interval and both filling levels. The obtained wetted wall heights is listed in Table 6.5-5.

Table 6.5-5 Wetted wall height for each temperature intervals, ethanol

T [^{o}C]	82,849 g WWH [cm]	126,600 g WWH [cm]
70-60	2,89	5,44
60-50	2,82	5,21
50-40	2,76	5,11
40 30	2,69	5,01

Calculating the heat capacity for liquid and reactor system

Based on the obtained values so far, the heat capacity of the entire system can be calculated according to the first part on the LH of equation (6.4-1), namely the following equation (6.5-3) where ΔT = T_1 – T_2 for every temperature interval. The calculated heat capacities is listed in Table 6.5-6.

$$\frac{\int Total\ power\ dt - \Delta H_{vap}}{\Delta T} = \frac{TP}{K}[\frac{J}{K}] \quad (6.5-3)$$

Table 6.5-6 Calculated heat capacities for the total system (liquid+reactor vessel+inserts+heatloss), ethanol

	82,849 g	**126,600 g**
T [ºC]	**TP/K [J/K]**	**TP/K [J/K]**
70-60	304,84	469,58
60-50	287,67	447,34
50-40	276,59	429,99
40 30	273,15	420,52

Calculating the reactor constant

From the calculated wetted wall heights, WWH, listed in Table 6.5-5 the correction factors for each temperature interval can be obtained. The correction factor is, as discussed earlier, often referred to as the reactor constant and include the heat capacity for the reactor vessel and inserts in addition to the unmonitored heat flow between reactor and thermostat bath. The correction factors are calculated with the equations listed in Table 6.4-1, and the resulting $HC_{Reactor+inserts}$ for each temperature interval is listed in Table 6.5-7.

Table 6.5-7 Calculated reactor constants for each temperature interval, ethanol

	82,849 g	**126,600 g**
T [ºC]	$\boldsymbol{HC_{Reactor+inserts}}$ **[J/K]**	$\boldsymbol{HC_{Reactor+inserts}}$ **[J/K]**
70-60	67,46	109,04
60-50	60,23	98,19
50-40	59,33	97,86
40 30	64,62	104,00

Calculating the specific heat capacity of ethanol and comparing it to literature data

All variables of equation (6.4-1) are now obtained, and the specific heat capacity of ethanol at the average temperature in each temperature interval can be calculated. For low filling level $m_{liquid} =$ 82,849 g, and for high filling level $m_{liquid} =$ 126,600 g. The obtained specific heat capacities is listed in Table 6.5-8.

Table 6.5-8 Specific heat capacity for low and high filling level, ethanol

T [°C]	82,849 g C_p [kJ/(kg*K)]	126,600 g C_p [kJ/(kg*K)]
70-60	2,87	2,85
60-50	2,75	2,76
50-40	2,62	2,62
40 30	2,52	2,50

In order to assess the accuracy of the procedure and correction factors, a comparison against literature data is needed. The average value between the obtained specific heat capacities for each temperature interval is used for best accuracy. The equation (6.5-4) of thermodynamic property, heat capacity, for ethanol is found obtained by Sun et al. [23] using least-squares method based on experimental data found in literature. In Table 6.5-9 the obtained specific heat capacities for ethanol is compared to literature data from Sun et al. The procedure achieved an average accuracy of 98,53%.

$$C_P = 2111{,}617 - 2{,}016296 * T - 3{,}858685 * 10^{-3} * T^2 + 4{,}78882 * 10^{-5} * T^3 \quad (6.5-4)$$

Where Cp is presented in J/(kg*K), and T is in K.

Table 6.5-9 Specific heat capacity for ethanol compared to literature data

	Cp, [kJ/(kg*K)]		
Temp [C°]	**Sun et al., 1988 [23]**	**This study**	**Deviation from Sun et al.**
35	2,52	2,51	1,66 %
45	2,62	2,62	0,12 %
55	2,73	2,75	2,49 %
65	2,84	2,86	1,63 %

7 Heat capacity measurement results

The correction factors used in this study is based on heat capacity measurements of water as described in chapter 5. The correction factors adjust the measured specific heat capacity for water to be equal to the heat capacities found in the study of Osborne et al. [10]. These corrections was tested on Ethyl alcohol, and gave an average deviation between heat capacity from Sun et al. data and measured heat capacity of 0,9525 %. The following chapters include results from heat capacity experiments for MEA and MDEA and their loaded and unloaded 30 wt% aqueous solutions.

7.1 Ethanolamine (MEA), ≥99%

There is significant differences found between different data sources for measured heat capacities of MEA, as shown in Table 7.1-1. It is apparent that the heat capacity found by Lide [24] is too high, and the heat capacity found by Riccick et al. [25] is too small, when compared to the overall heat capacity data available [26]. The consistency of the measurement data between Lee [27] and Chiu et al. [26] indicates that the values found in this study are too high, although the inconsistency and high deviations in the literature in general make it difficult to reach a conclusion about the accuracy of the measured heat capacity. It is noticed that the heat capacity measured by Pagé et al. [28] seems to be consistent with the measurement in this study. Some of the heat capacities of pure ethanolamine found in the literature is given in Table 7.1-1. A visual comparison between heat capacity found in this study and in literature are given in Figure 7.1-1.

Table 7.1-1 Measured heat capacties and literature data for Ethanolamine (MEA), ≥99%

		Cp, [kJ/(kg*K)]						
Temp [Cº]	**Estimated values**	**Riddick et al., 1986 [25]**	**Lee, 1994 [27]**	**Lide, 1994 [24]**	**Chiu et al., 1999 [26]**	**Hepler et al. 1997 [29]**	**Pagé et al., 1993 [28]**	**This study**
20	2,656[a]							
25	2,670[b]			3,201		2,727	2,833	
30	2,715[c]	2,082	2,720		2,74			
35	2,738[c]		2,760		2,76			2,84
40	2,760[c]		2,801		2,78			
45	2,783[c]		2,841		2,81			2,91
50	2,904[b]		2,882		2,83	2,768		
55	2,828[c]		2,923		2,86			2,98
60	2,850[c]		2,963		2,88			
65	2,873[c]		3,004		2,91			3,01
70	2,895[c]		3,044		2,93			
75	2,918[c]		3,085		2,95	2,917		
80	2,940[c]		3,125		2,98			

[a] Chueh and Swanson, 1973 [30], [b] Missenard, 1965 [31], [c] Hepler, 1997 [29]

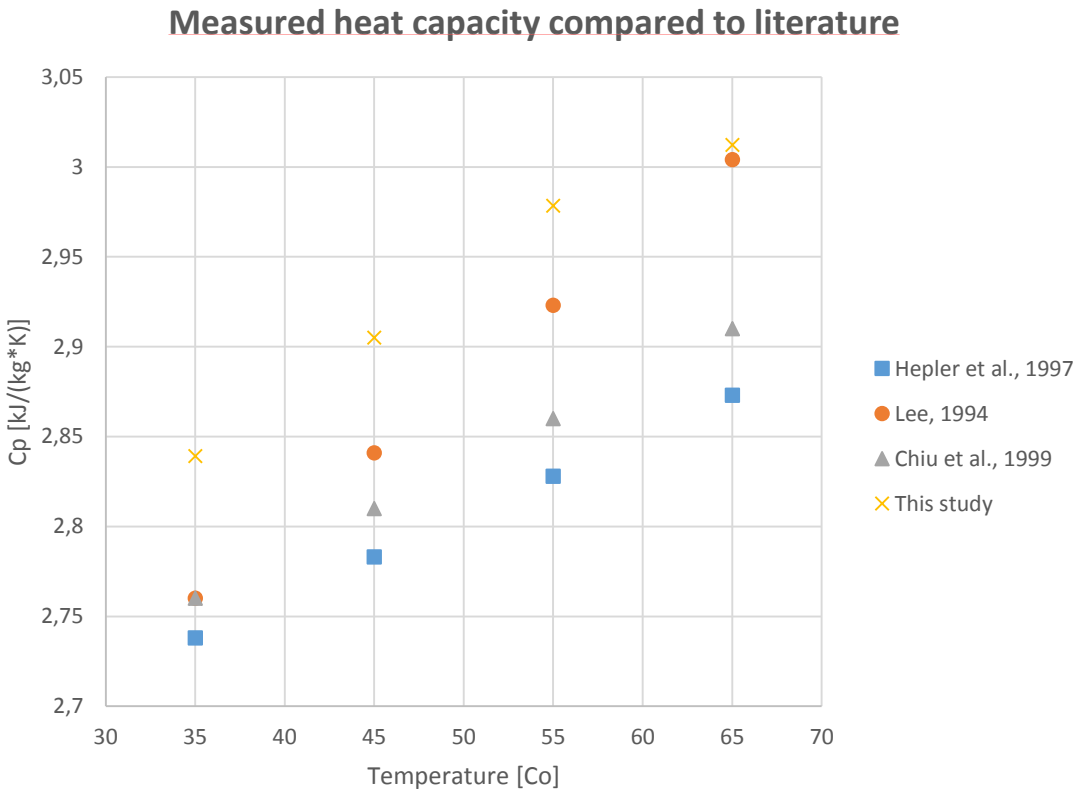

Figure 7.1-1 Measured heat capacity for MEA compared to literature

The measured heat capacity is based on 40 measurements, from which one is considered an outlier. The scanning sessions was performed according to mentioned experimental procedure in chapter 6. Two different amounts of MEA was used, 103,946 g and 155,447 g, and 5 scanning sessions was performed on each amount consisting of 4 measurements in each temperature interval. The results of the calculated heat capacities in each temperature interval, at the average temperature in each interval, are shown in Figure 7.1-1. The temperature dependent density was found using the prediction equation developed by Cheng et al. [32]:

$$\rho_{MEA} = 1023.75 - 0.5575T - 0.00187T^2 \qquad (7.1-1)$$

Where T is the temperature in degrees Celsius. The accuracy of the calculated density was validated against experimental data from Mandal et al. [33]. The importance of accurate temperature dependent density is connected to the influence wetted wall height have on the measured heat capacity, as described in chapter 5.2. The average deviation of the measurements in each temperature interval, as calculated by equation (7.1-3), is listed in Table 7.1-2. The overall average deviation of the measured heat capacities is 0,54 %. The low average deviation indicates that the deviation from literature data is systematic. The calculated heat capacity for each of the 39 utilized measurements are shown in Figure 7.1-2. The temperature dependent vaporization enthalpies and vapor pressures used when calculating heat capacity according to the method described in chapter 6, was found by Kapteina et al. [34]. The vapor pressure for MEA was calculated using Antoine equation (7.1-2) with parameters from Matthews et al. [35]. The output of the Antoine equation with parameters from Matterws is vapor pressure in Pa and the input temperature, T, is in ^{o}C. The latent heat of vaporization for MEA used in this study was found by National Center for Biotechnology Information [36] to be 51111 J/mol.

$$ln(P) = A - \frac{B}{T - C} \qquad (7.1-2)$$

$$SD[\%] = \frac{\sqrt{\frac{\sum(Cp_n - Cp_{average})^2}{n}}}{Cp_{average}} \qquad (7.1-3)$$

Where Cp_n is the heat capacity calculated for each measurement, n is the number of measurements and $Cp_{average}$ is the average Cp found for each temperature interval.

Table 7.1-2 Heat capacity standard deviation from average value

Temperature interval [ºC]	Standard deviation [%]
70-60	0,35
60-50	0,61
50-40	0,81
40-30	0,40

The obtained heat capacity for each average temperature is the average for the obtained heat capacity at low and high filling level as described in chapter 6. For pure MEA there is no significant difference between heat capacities found at each filling level. The heat capacities and the standard deviation for each scanning interval, is given in Table 7.1-3.

Table 7.1-3 Comparison between Cp found at low and high filling level

	Low filling level (103,946 g)		High filling level (160,564 g)	
Temp [ºC]	Measured Cp [kJ/(kg*K)]	Standard deviation [%]	Measured Cp [kJ/(kg*K)]	Standard deviation [%]
35	2,83	0,29	2,85	0,23
45	2,88	0,40	2,93	0,36
55	2,97	0,39	2,99	0,30
65	3,01	0,35	3,01	0,34

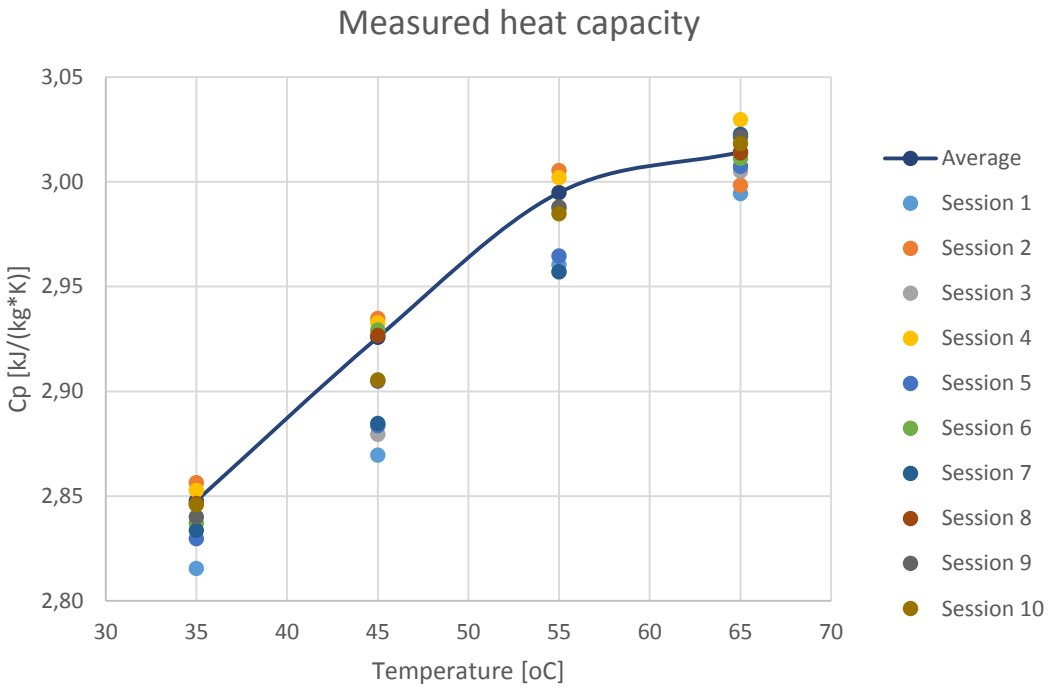

Figure 7.1-2 Heat Capacity measurements by CPA202 reaction Calorimeter for pure MEA

7.2 30 wt% MEA aqueous solution

Literature data for Ethanolamine solution heat capacity are scarce, and for 30 wt% aqueous solution only Weiland et al. [37] and Abdulkadir et al. [38] was found to have experimental results as shown in Table 7.2-1. As with pure MEA, the literature data show significant differences for equal concentration of MEA. While measured heat capacity for pure MEA was shown to probably be too high, the measured heat capacity for 30 wt% MEA solution coincides quite well with existing literature data as shown in Table 7.2-1. In Figure 7.2-1 the measured heat capacity is compared with experimental data from Chiu et al. [39]. The measurements from Chiu et al. show that heat capacity for MEA solutions increases as the MEA concentration decreases, and as seen in the figure the measured heat capacities in this study fits well within this trend. This is further indicated in Figure 7.2-2 where measured heat capacity is compared with experimental data from Abdulkadir et al. [38].

The measurement method and apparatus is sensitive to differences in physical properties such as heat conductivity and viscosity as discussed in chapter 6, which may be the reason why the heat capacities for pure MEA was found to be too high. Since the standard deviation in the measurement data is low in each case, one hypothesis may be that the differences in physical properties between MEA and water, from which the correction factors was calculated, contributes to a systemic error in the calculation, measurement method or apparatus.

Table 7.2-1 Measured heat capacity and literature data for 30 wt% MEA solution

	Cp, [kJ/(kg*K)]					
Temp [C°]	**Weiland et al., 1997 [37]**	**Pagé et al., 1993 [28]**	**Hillard, 2008 [40]**	**Abdulkadir et al., 2014 [38]**	**Chiu et al., 1999 [39]**	**This study**
	30 wt %	*24,5wt%*	*3,5 M 23,4 wt%*	*5 M*	*x_1= 0,2*	*x_1= 0,112 30 wt% 4,97 M*
20						
25	3,734	3,8493				
30				3,92	3,52	
35				3,93	3,55	3,89
40		3,9075	3,9059	3,94	3,58	
45			3,9227	3,94	3,60	3,93
50			3,9384	3,95	3,63	
55			3,9552	3,96	3,66	3,96
60			3,9700	3,97	3,68	
65			3,9810	3,99	3,71	3,98
70			3,9918	4,01	3,74	
75			4,0034	4,02	3,76	
80			4,0165	4,03	3,79	

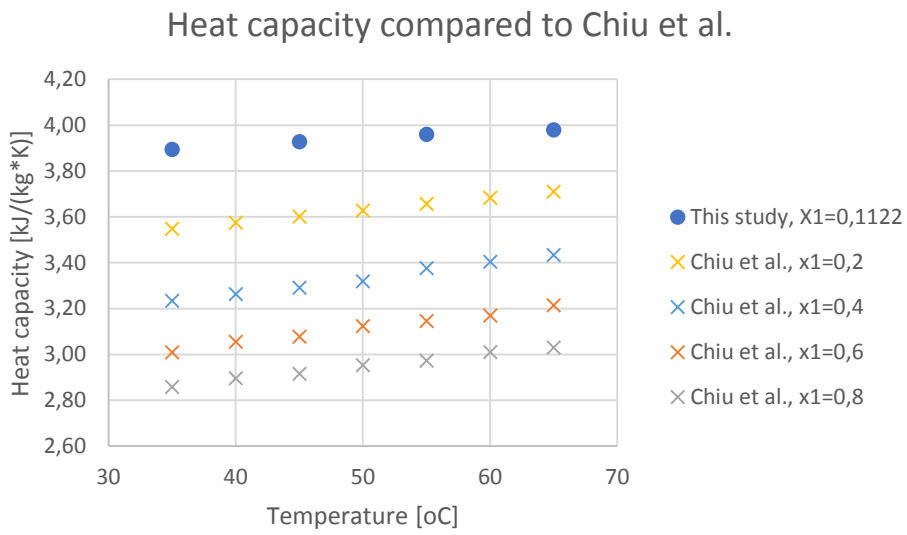

Figure 7.2-1 Comparison between Cp found experimentally in this study and experimental values from Chiu et al. [39]

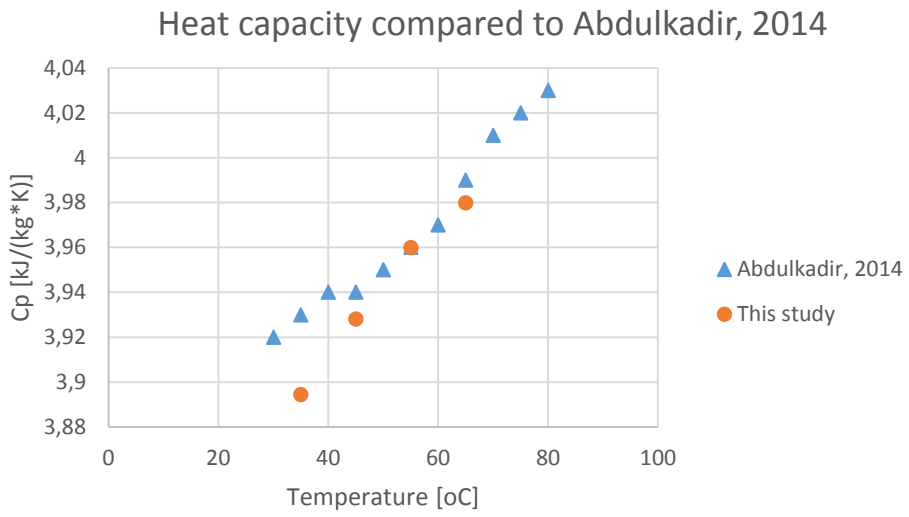

Figure 7.2-2 Comparison between Cp found experimentally in this study and experimental values from Abdulkadir [38]

The measured heat capacity is based on 40 measurements, from which no outliers are found. The scanning sessions was performed according to mentioned experimental procedure in chapter 6. Two different amounts of MEA was used, 108,419 g and 160,564 g, and 5 scanning sessions was performed on each amount consisting of 4 measurements in each temperature interval. The individual Cp measurements can be seen in Figure 7.2-3. The overall standard deviation in the measurement data, as calculated by equation (7.1-3), was found to be 0,41 %. The standard deviations within each temperature interval is listed in Table 7.2-2.

The density of 30 wt % MDEA solution was found using the model equation developed by Cheng et al. [32]:

$$\rho = (1-C)\rho_{H_2O} + C\rho_{MEA} + C(1-C)\left(5.8430 - 0.3139T + 510.6409\frac{C}{T^{0,46}}\right) \quad (7.2-1)$$

$$\rho_{H_2O} = 1002.3 - 0.1321T - 0.00308T^2 \quad (7.2-2)$$

Where T is the temperature [°C], C is the solution weight fraction [dimensionless] and ρ is the density [kg/m^3]. The accuracy of the calculated densities was validated against experimental data from Mandal et al. [33] and Amundsen [41], which is given in Table 7.2-2. The vaporization enthalpy for 30 wt% MEA usied in the Cp calculations was obtained by multiplying vaporization enthalpy for water [19] and MEA [34] with the respective molar fraction.

Vapor pressures for 30 wt% MEA solution was calculated with Antoine equation (7.1-2) based on parameters found from Wu et al. [42] based on experimental data from Xu et al. [43]. The parameters are valid in the temperature interval used in this study, and for the concentration used. The parameters used are listed in Table 7.4-4. With these parameters, vapor pressure is given in Pa, an input temperature is in K.

Table 7.2-2 Antoine equation parameters from Wu et al. [42] for 30 wt% MEA

A	B	C
24,199	4524,1	-19,281

Table 7.2-3 Densities for 30 wt% MEA solution from Mandal et al. and Amundsen

Density for 30 wt% MEA solution ρ [g/cm^3]							
25 ºC	**30 ºC**	**35 ºC**	**40 ºC**	**45 ºC**	**50 ºC**	**60 ºC [41]**	**70 ºC**
1,012	1,009	1,005	1,003	1,001	0,998	0,993	0,976

Table 7.2-4 Heat capacity standard deviation from average value

Temperature interval [ºC]	Standard deviation [%]
70-60	0,37
60-50	0,35
50-40	0,42
40-30	0,49

When comparing the calculated heat capacities obtained upon low and high filling level it is noticed that the measurements performed on the higher filling level, with 160,564 g, achieved a lower overall standard deviation from average value of 0,16 % in comparison with 0,36 % for lower filling level. The heat capacities and standard deviations found for low and high filling level is shown in Table 7.2-4. There is no significant differences between the heat capacities obtained at low and high filling levels, and subsequently both filling levels are used to obtain the heat capacities in the manor described in chapter 6.

Table 7.2-5 Comparison between Cp found at low and high filling level

	Low filling level (108,419 g)		High filling level (160,564 g)	
Temp [ºC]	**Measured Cp [kJ/(kg*K)]**	**Standard deviation [%]**	**Measured Cp [kJ/(kg*K)]**	**Standard deviation [%]**
35	3,91	0,32	3,88	0,19
45	3,94	0,24	3,91	0,14
55	3,96	0,43	3,96	0,17
65	3,98	0,48	3,98	0,14

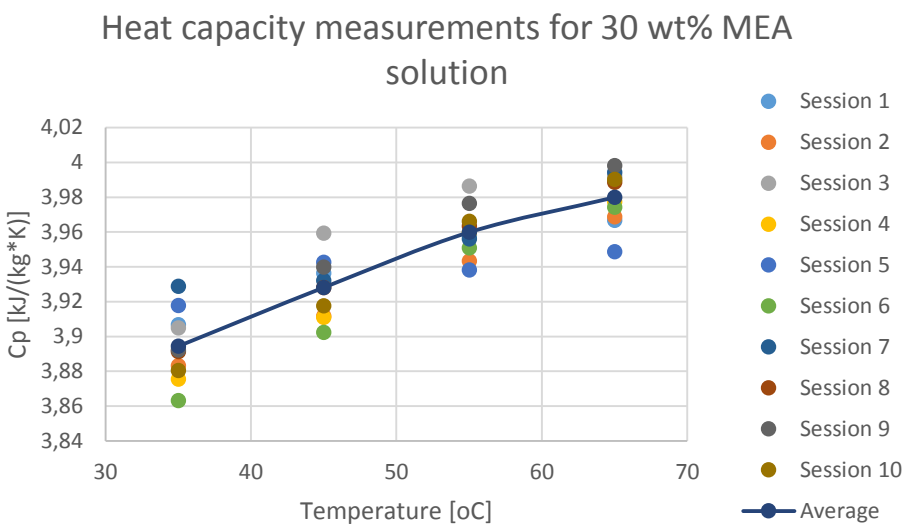

Figure 7.2-3 Heat capcity measurements by CPA202 Raction Calorimeter for 30 wt% MEA solution

7.3 CO_2 loaded MEA aqueous solution

For the heat capacity experiments with CO_2-loaded solutions, two 30 wt% aqueous MEA solutions have been preloaded at a loading of 0,2 and 0,4 respectively. The liquid density of CO_2-loaded aqueous MEA solutions has been found experimentally by Han et al. [44], and is listed in Table 7.2-1 for 30 wt% MEA aqueous solution with CO_2 loading of 0,21 and 0,44 [44]. These densities are used for the heat capacity calculations in this study. For comparison, Amundsen found that the density of 30 wt% MEA with CO_2-loading of 0,2 and 0,4 at 25 °C was 1054 kg/m^3 and 1095 kg/m^3 respectively [41]. The densities found by Han et al. also coincides with experimental data from Weiland et al. [45]. Density for 0,2 and 0,4 loading is calculated using interpolation and assuming linear relationship between density and loading found in Han et al. The density for the average temperature within each temperature scan interval is calculated assuming a linear relationship between the densities for each temperature shown in Table 7.3-1, using interpolation.

Table 7.3-1 Densities for CO2 loaded 30 wt% MEA solution

Temp. [C°]	**α = 0,21 [kg/m^3]**	**α = 0,44 [kg/m^3]**
25	1033,3	1096,4
40	1025,3	1089,1
50	1019,6	1083,8
60	1013,8	1078,2
70	1007,6	1072,3

The latent heat of vaporization for carbon dioxide used in the calculation of the phase change effect is 16,4 kJ/mol and was found by Stepheson et al. [46]. The vapor pressure for the loaded solutions was found experimentally by Jou et al. [47]. These values was validated against partial pressure data for loaded solution in 30 wt% MEA solution by Ma'munn et al. [48].

7.3.1 0,2 CO_2 loading

The scarcity of heat capacity data, as mentioned earlier, is even more apparent when it comes to loaded solutions. This is in direct relation with the different possible combinations of loading and solution concentration, and for 0,2 loading in 30 wt% MEA solution only Weiland et al. [37] was found to have experimental results as shown in Table 7.3-2. The measured heat capacity in this study coincides quite well with Weiland et al.

Table 7.3-2 Measured heat capacity and literature data for α=0,2 in 30 wt% MEA solution

	Cp, [kJ/(kg*K)]	
Temp [Cº]	**Weiland et al., 1997 [37]**	**This study**
25	3,570	
30		
35		3,60
40		
45		3,63
50		
55		3,67
60		
65		3,70

The measured heat capacity is based on 40 measurements, from which 1 is considered an outliers. The scanning sessions was performed according to mentioned experimental procedure in chapter 6. Two different amounts of MEA was used, 106,914 g and 160,771 g, and 5 scanning sessions was performed on each amount consisting of 4 measurements in each temperature interval. The individual Cp measurements can be seen in Figure 7.3-1, and it is noticed that there is a systematic difference in measured Cp between low and high filling level at the average temperatures of 35, 45 and 55 ºC. This is also apparent in Table 7.3-4. The overall standard deviation in the measurement data, as calculated by equation (7.1-3), was found to be 0,60 %. The standard deviations within each temperature interval is listed in Table 7.3-3.

Table 7.3-3 Heat capacity standard deviation from average value

Temperature interval [ºC]	**Standard deviation [%]**
70-60	0,47
60-50	0,75
50-40	0,70
40-30	0,49

The calculated heat capacities obtained in both low and high filling level show good consistency with low standard deviations. It is however noticed that the measurements performed on the low filling level, at the average temperature of 65 ºC, achieved a higher standard deviation from average value than the rest of the scanning intervals. The heat capacities and standard deviations found for low and high filling level is shown in Table 7.3-4. There is, as mentioned earlier, apparent from Table 7.3-4 that the obtained heat capctities at low filling level is systematic lower than at high filling level. These differences is however not considered significant, and subsequently both filling levels are used to obtain the heat capacities in the manor described in chapter 6.

Table 7.3-4 Comparison between Cp found at low and high filling level for loading at α=0,2

	Low filling level (106,914 g)		High filling level (160,771 g)	
Temp [ºC]	**Measured Cp [kJ/(kg*K)]**	**Standard deviation [%]**	**Measured Cp [kJ/(kg*K)]**	**Standard deviation [%]**
35	3,58	0,15	3,62	0,14
45	3,61	0,25	3,66	0,21
55	3,65	0,19	3,70	0,21
65	3,69	0,46	3,71	0,28

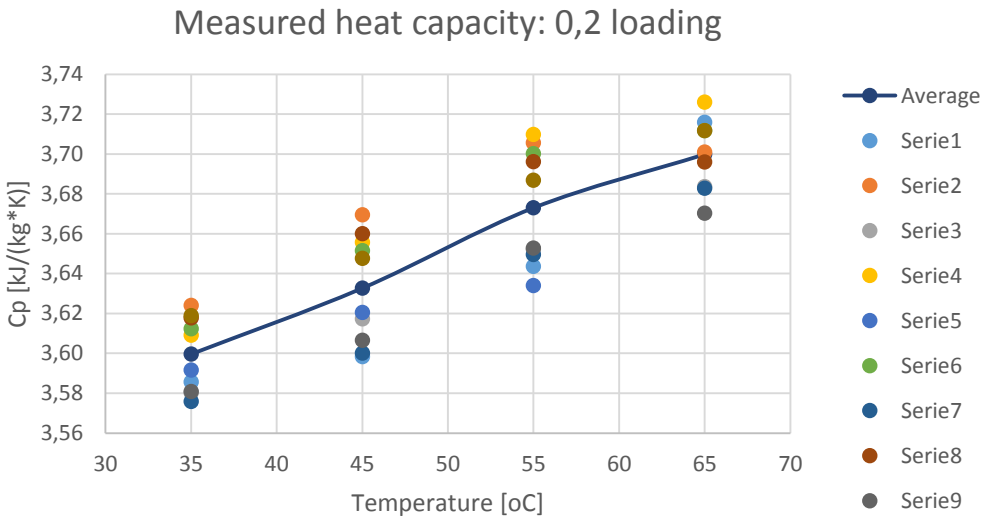

Figure 7.3-1 Heat capacity measurements by CPA202 reaction calorimeter for 30 wt% MEA solution wit 0,2 loading

7.3.2 0,4 CO_2 loading

The scarcity of literature data makes it difficult to validate the measurements of loaded solutions in this study. Just as with Cp data for solution with 0,2 loading, there was only found one study which had experimentally measured the cp for 30 wt% MEA solution at a loading of 0,4. This is given in Table 7.3-5, and just as with 0,2 loading the obtained heat capacities seems to coincide with the heat capacity found by Weiland et al. [37].

Table 7.3-5 Measured heat capacity and literature data for α=0,4 in 30 wt% MEA solution

	Cp, [kJ/(kg*K)]	
Temp [C°]	**Weiland et al., 1997 [37]**	**This study**
25	3,418	
30		
35		3,42
40		
45		3,45
50		
55		3,49
60		
65		3,51

The measured heat capacity is based on 40 measurements, from which 1 is considered an outliers. The scanning sessions was performed according to mentioned experimental procedure in chapter 6. Two different amounts of MEA was used, 107,021g and 160,534 g, and 5 scanning sessions was performed on each amount consisting of 4 measurements in each temperature interval. The individual Cp measurements can be seen in Figure 7.3-2. The overall standard deviation in the measurement data, as calculated by equation (7.1-3), was found to be 0,74 %. The standard deviations within each temperature interval is listed in Table 7.3-6.

Table 7.3-6 Heat capacity standard deviation from average value

Temperature interval [°C]	**Standard deviation [%]**
70-60	0,80
60-50	0,69
50-40	0,73
40-30	0,74

All heat capacities and standard deviations found at low and high filling level is shown in Table 7.3-7. The calculated heat capacities obtained at low filling level show a systematic lower heat capacity than at high filling level, as shown in Table 7.3-7. The variation in measurement data is low for the scanning sessions at both filling levels, and the obtained heat capacities are based on results from both filling levels in accordance with the experimental method described in chapter 6.

Table 7.3-7 Comparison between Cp found at low and high filling level for loading at α=0,4

	Low filling level (107,021 g)		High filling level (160,534 g)	
Temp [ºC]	**Measured Cp [kJ/(kg*K)]**	**Standard deviation [%]**	**Measured Cp [kJ/(kg*K)]**	**Standard deviation [%]**
35	3,39	0,39	3,44	0,35
45	3,43	0,42	3,48	0,20
55	3,47	0,54	3,51	0,20
65	3,49	0,72	3,53	0,26

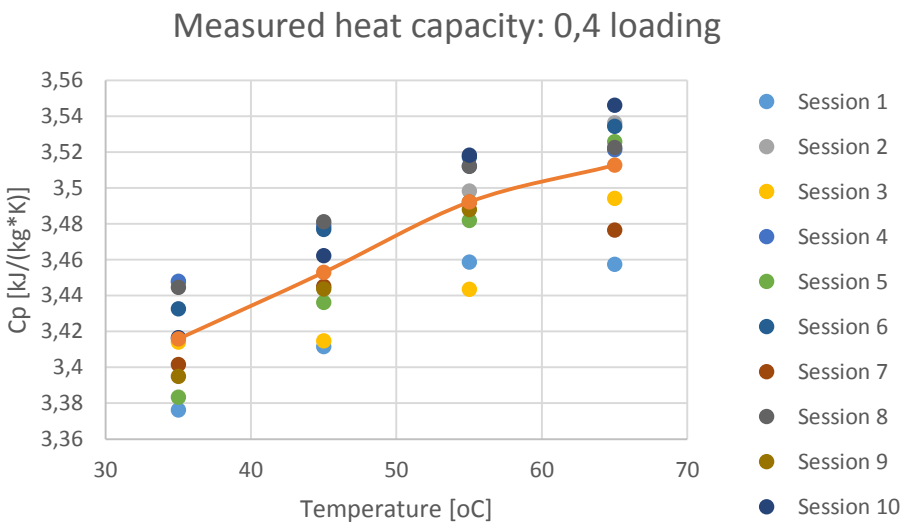

Figure 7.3-2 Heat capacity measurements by CPA202 reaction calorimeter for 30 wt% MEA solution wit 0,4 loading

7.4 N-Methyldiethanolamine, ≥99%

The measured heat capacities for pure MDEA is shown in Table 7.4-1 along with available literature data. The is some differences within the literature data, but the consistency is higher than for MEA. The obtained values for Cp in this study has a good match with experimental data from Chiu et al. [26], although the obtained Cp at 25 °C, when compared to the literature data, seems to be too low. Figure 7.4-1 show a comparison with literature data, and from this it can be seen that the fit with experimental data from Lee, Chiu et al. and Hepler et al. is good.

Table 7.4-1 Measured heat capacity and literature data for N-Methyldiethanolamine, ≥99%

	Cp, [kJ/(kg*K)]				
Temp [C°]	**Estimated values**	**Lee, 1994 [27]**	**Chiu et al., 1999 [26]**	**Hepler et al. 1997 [29]**	**This study**
20	2,308[a]				
25	2,103[b]			2,273	
30	2,279[c]	2,274	2,22		
35	2,305[c]	2,303	2,24		2,21
40	2,330[c]	2,333	2,27		
45	2,355[c]	2,363	2,30		2,33
50	2,381[b]	2,392	2,33	2,365	
55	2,406[c]	2,422	2,36		2,43
60	2,431[c]	2,452	2,39		
65	2,457[c]	2,482	2,41		2,48
70	2,482[c]	2,511	2,44		
75	2,507[c]	2,541	2,47	2,502	
80	2,533[c]	2,571	2,50		

[a] Chueh and Swanson, 1973 [30], [b] Missenard, 1965 [31], [c] Hepler, 1997 [29]

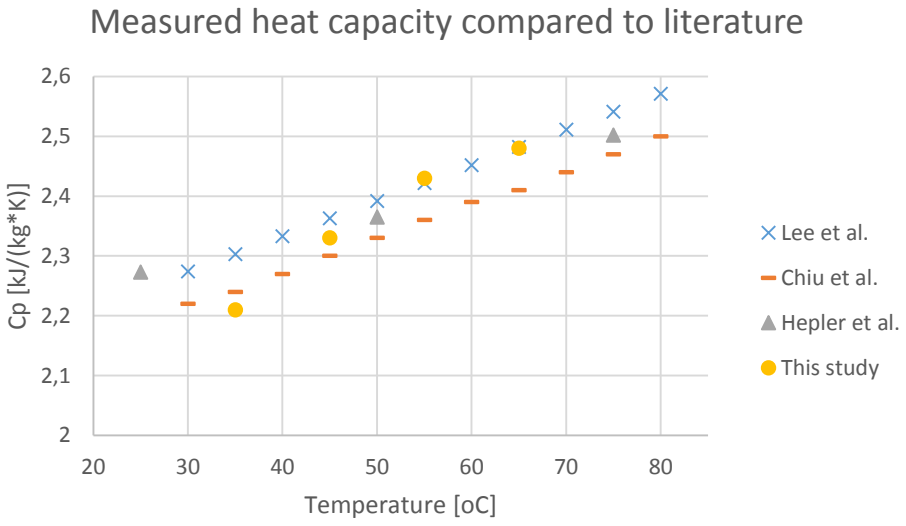

Figure 7.4-1 Measured heat capcity compared to literature for pure MDEA

Vapor pressure of pure MDEA is negligible in the temperature range used in this study. The vapor pressure of pure MDEA at 80 °C is <1,5 Pa according to data from INEOS [49]. The phase change effect

is therefor negligible for pure MDEA under the temperature scanning conditions used in this study. The latent heat of vaporization for MDEA used in this study was found by INEOS [50] to be 55340 J/mol.

The temperature dependent density was found using the prediction equation developed by Cheng et al. [32]:

$$\rho_{MDEA} = 1056.8 - 0.7407T - 0.00053T^2 \quad (7.4-1)$$

Where T is the temperature in degrees Celsius. The accuracy of the calculated density was validated with experimental data from Rebolledo-Libreros et al. [51] and Li et al. [52].

The measured heat capacity is based on 28 measurements, from which 2 are considered outliers. The scanning sessions was performed according to mentioned experimental procedure in chapter 6. Two different amounts of MEA was used, 108,302 g and 166,862 g. 4 scanning sessions was performed at low filling level and 3 sessions at high filling level. The reduction in scanning sessions was done due to time constrictions for this study. The individual Cp measurements can be seen in Figure 7.4-2. The overall standard deviation in the measurement data, as calculated by equation (7.1-3), was found to be 0,53 %. The standard deviations within each temperature interval is listed in Table 7.4-2.

Table 7.4-2 Heat capacity standard deviation from average value

Temperature interval [ºC]	Standard deviation [%]
70-60	0,65
60-50	0,60
50-40	0,39
40-30	0,47

Table 7.4-3 show the obtained heat capacities and the standard deviation in each temperature interval. It is noticed that the variation in measurement data (standard deviation) at low filling level is higher than at high filling level. As seen in Table 7.4-3, there is some deviation between heat capacities at low and high filling level. These deviations are however not systematic, and both filling levels are used to obtain the heat capacities in the manor described in chapter 6.

Table 7.4-3 Comparison between Cp found at low and high filling level for MDEA

	Low filling level (108,302 g)		High filling level (166,862 g)	
Temp [ºC]	Measured Cp [kJ/(kg*K)]	Standard deviation [%]	Measured Cp [kJ/(kg*K)]	Standard deviation [%]
35	2,24	1,51	2,19	0,28
45	2,32	1,17	2,34	0,17
55	2,40	1,27	2,46	0,25
65	2,45	1,26	2,52	0,57

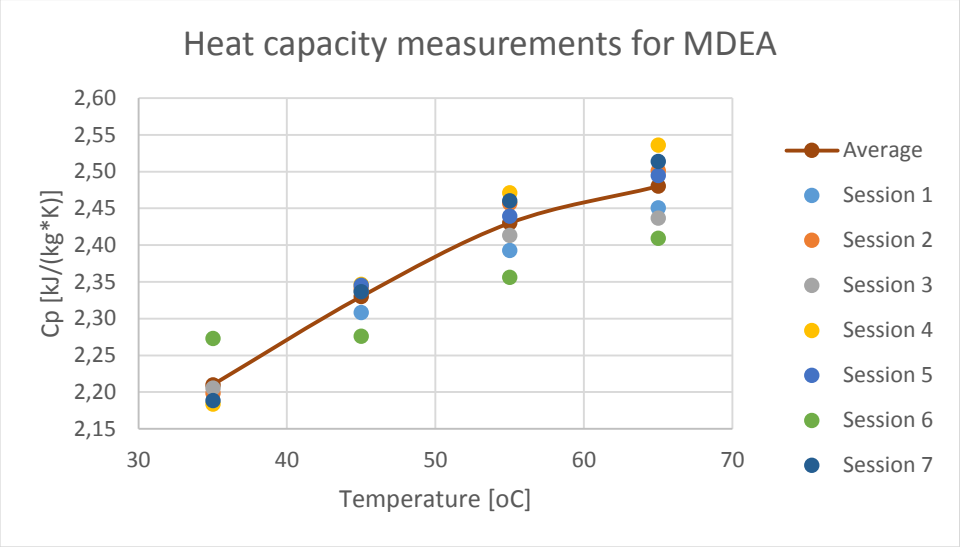

Figure 7.4-2 Heat capacity measurements for MDEA with CPA202 Reaction Calorimeter

7.5 30 wt% MDEA aqueous solution

The literature data for heat capacity of 30 wt% MDEA aqueous solution are scarce, as shown in Table 7.5-1, where literature data is listed among with the obtained heat capacities in this study. There exist a number of sources with experimental data for MDEA solutions, but only Weiland et al. [37] was found to have performed Cp measurement on 30 wt% aqueous MDEA solution. It can be seen by comparing data from Hayden et al. and Chiu et al. for 23 wt% and 50 wt% solution respectively that there is significant differences in measured heat capacity. It is difficult to assess the accuracy of the heat capacities obtained in this study due to the literature data scarcity, but it seems to be somewhat in the expected region. A visual comparison against literature data in given in Figure 7.5-1.

Table 7.5-1 Measured heat capacties and literature data for 30 wt% MDEA solution

	Cp, [kJ/(kg*K)]					
Temp [C°]	**Weiland et al., 1997 [37]**	**Hayden et al., 1993 [53]**	**Chiu et al., 1999 [39]**	**Hayden et al., 1993 [53]**	**Chiu et al., 1999 [39]**	**This study**
		x_1= 0,0432 23 wt%	**x_1= 0,0432 23 wt%**	**x_1= 0,1313 50 wt%**	**x_1= 0,1313 50 wt%**	**x_1=0,0647 30 wt %**
20						
25	3,787					
30			3,81		3,40	
35			3,82		3,43	3,75
40			3,83		3,46	
45			3,84		3,49	3,77
50		3,773	3,85	3,428	3,51	
55			3,86		3,54	3,81
60			3,87		3,57	
65			3,88		3,60	3,83
70			3,89		3,62	
75		3,794	3,90	3,527	3,65	

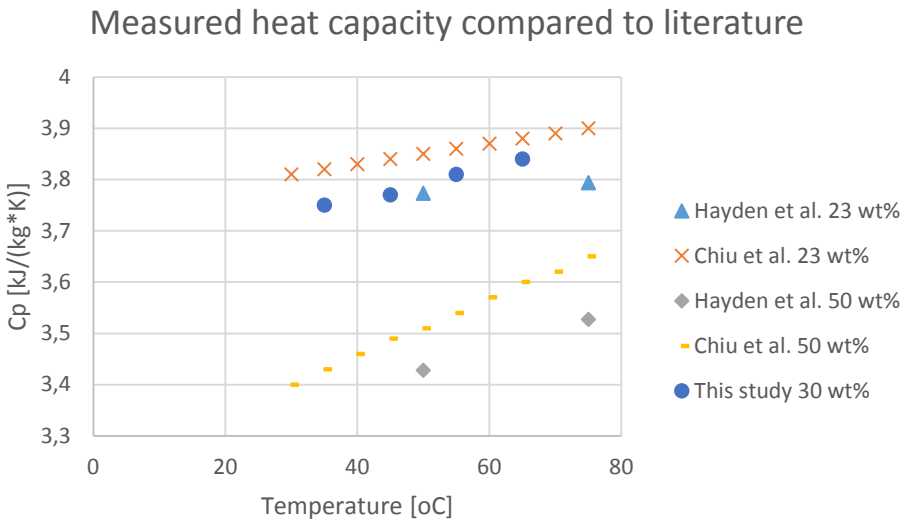

Figure 7.5-1 Measured heat capcity for 30 wt% MDEA compared to literature data

The measured heat capacity is based on 24 measurements, from which none are considered outliers. The scanning sessions was performed according to mentioned experimental procedure in chapter 6, with two different amounts of MEA, namely 107,476 g and 164,030 g. 3 scanning sessions was performed at both filling levels. As mentioned earlier the reduction in amount of measurements are due to time constrictions for this study. The individual Cp measurements can be seen in Figure 7.4-2. The overall standard deviation in the measurement data, as calculated by equation (7.1-3), was found to be 1,14 %. The standard deviations within each temperature interval is listed in Table 7.4-2.

Table 7.5-2 Heat capacity standard deviation from average value

Temperature interval [ºC]	**Standard deviation [%]**
70-60	1,05
60-50	1,02
50-40	1,18
40-30	1,32

Table 7.4-3 show the obtained heat capacities and the standard deviation in each temperature interval. In contrast with the results for pure MDEA, it is noticed that the variation in measurement data (standard deviation) at low filling level is lower than at high filling level. The heat capacities obtained in each respective filling level is consistent with each other, and subsequently both filling levels are used to obtain the heat capacities in the manor described in chapter 6.

Table 7.5-3 Comparison between Cp found at low and high filling level for 30 wt% MDEA solution

	Low filling level (107,476 g)		**High filling level (164,030 g)**	
Temp [ºC]	**Measured Cp [kJ/(kg*K)]**	**Standard deviation [%]**	**Measured Cp [kJ/(kg*K)]**	**Standard deviation [%]**
35	3,77	0,51	3,73	1,65
45	3,78	0,30	3,77	1,63
55	3,80	0,38	3,81	1,39
65	3,84	0,25	3,83	1,46

Vapor pressures for 30 wt% MDEA solution was calculated with Antoine equation (7.1-2) based on parameters found from Wu et al. [42] based on experimental data from Xu et al. [43]. The parameters are valid in the temperature interval used in this study, and for the concentration used. The parameters used are listed in Table 7.4-4. With these parameters, vapor pressure is given in Pa, an input temperature is in K.

Table 7.5-4 Antoine equation parameters from Wu et al. [42] for 30 wt% MDEA solution

A	**B**	**C**
24,116	4391,9	-25,729

The temperature dependent density was found using the prediction equation developed by Cheng et al. [32] and validated against the experimental data from Li et al. [52]. The model equation used is given below:

$$\rho = (1 - C)\rho_{H_2O} + C\rho_{MDEA} + C(1 - C)\left(63.6395 - 0.2651T + 199.4811\frac{C}{T^{0,2}}\right) \qquad (7.5 - 3)$$

Where T is the temperature [ºC], C is the solution weight fraction [dimensionless] and ρ is the density [kg/m^3].

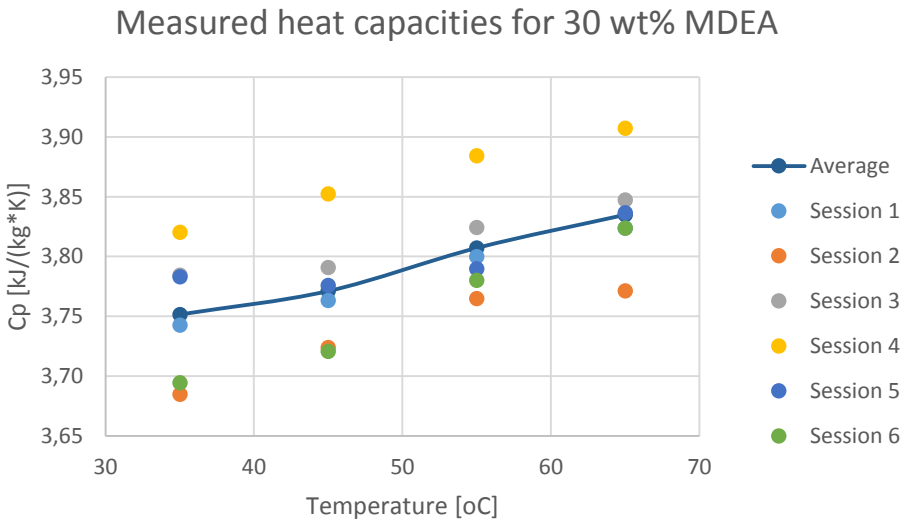

Figure 7.5-2 Measured heat capacities for 30 wt% MDEA solution

7.6 CO_2 loaded MDEA aqueous solution

Due to inconsistent measurement results for loaded 30 wt% MDEA aqueous solutions, no heat capacity was obtained. During the experimental procedure for loaded solutions, a significant reduction in reaction mass in the CPA202 Pyrex glass reactor was noticed. The deviation was verified after calculation of the measured heat capacities for 30 wt% MDEA aqueous solution at CO_2-loading of 0,2, resulting in a systematic decrease of Cp during the experimental procedure as seen in Table 7.6-1. The source of this problem was believed to be a faulty gasket in the reactor lid, resulting in a significant leakage of reaction mass. The gasket was replaced and the experiments continued. No significant changes in reaction mass was observed during the following experimental procedures. After completion of the heat capacity measurements for 30 wt% MDEA solution at 0,2 and 0,4 loading, a systematic reduction for measured heat capacity was noticed. At this point, time constrictions for the study did not allow for further fault seeking and repetition of experimental procedures. The calculated heat capacities for the respective loadings are given in Table 7.6-2.

Table 7.6-1 Measured heat capacities for 108,987 g 30 wt% MDEA solution with α=0,2

	Cp, [kJ/(kg*K)]			
Temp [°C]	**65**	**55**	**45**	**35**
Session 1	3,68	3,62	3,57	3,54
Session 2	3,47	3,31	3,20	3,17
Session 3	3,13	3,02	2,96	2,96

Table 7.6-2 Measured heat capacities for 30 wt% MDEA solution with α=0,2 and α=0,4

	Cp, [kJ/(kg*K)]							
	α = 0,2 / 109,077 g				α = 0,2 / 111,006 g			
Temp [°C]	**65**	**55**	**45**	**35**	**65**	**55**	**45**	**35**
Session 1	3,66	3,62	3,59	3,57	3,21	2,98	2,89	2,84
Session 2	3,61	3,57	3,55	3,52	2,89	2,81	2,75	2,72
Session 3	3,58	3,52	3,51	3,48	2,88	2,76	2,64	2,59
Session 4	3,53	3,47	3,43	3,42	2,68	2,59	2,55	2,53
Session 5	3,49	3,43	3,39	3,39	2,63	2,51	2,44	2,43

The reduction in measured heat capacity between each temperature scanning session was higher before the replacement of the faulty gasket, as seen in Table 7.6-1. This confirms the suspicion that significant leakage was present, and reduced by changing the gasket. However, the reduction in measured heat capacity, as seen in Table 7.6-2, are still so significant that the no reliable heat capacities can be obtained from the measurement data. The heat capacities shown in Table 7.6-2 are obtained for low filling level at both loading. The measurement for high filling level show similar trend, with systematic reduction of measured heat capacity for each consecutive scanning session.

Figure 7.6-1 show a comparison between measured reactor pressure for 30 wt% MDEA solution with 0,2 loading. Run 1 is the Cp experiment performed before gasket was changed, as shown in Table 7.6-1, and Run 2 is the Cp experiment performed after gasket was changed, as shown in Table 7.6-2. As can be seen from the figure, the change of gasket significantly reduced the pressure loss. While pressure loss can arise from a small leakage from which gas slowly leaks through, a significant reduction in measured heat flow can only arise from significant loss of liquid reaction mass, which indicate a significant leakage. This assumption is validated by Figure 7.7-1, where reduction in reactor pressure is not accompanied by reduction in measured heat flow. This experiment was successful with a low standard deviation of 0,54%, showing good consistency in measurement data. Figure 7.6-2 show a comparison between measured heat flow in Run 1 and Run 2. As seen in the figure, the reduction in measured heat flow between the first three consecutive temperature scanning sessions in Run 1 is significantly reduced after gasket is changed in Run 2. However, there is still a reduction present for Run 2, which results in the obtained Cp shown for 109,077 g in Table 7.6-2.

It is believed that the reason for the continued leakage is due to the new gasket, made of soft Teflon, deforming during experimental procedure because of relatively high temperature and overtightening of the lid, resulting in ineffective sealing. This deformation will be reduced when the new gasket has obtained final form, perfectly fitting the lid. Another hypothesis is that a second source of leakage is present. For future experiments, a pressure test of the reactor vessel is recommended so that leakages can be detected.

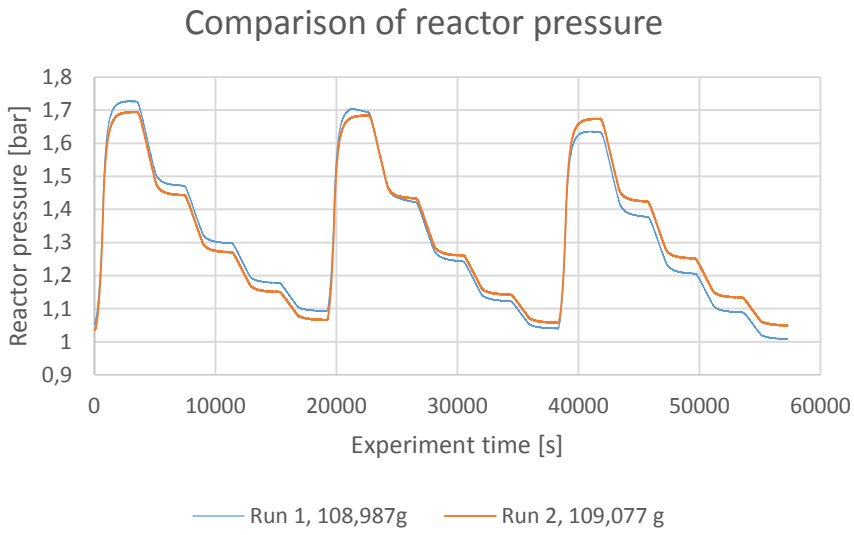

Figure 7.6-1 Comparison of measured reactor pressure between scanning experiment before (Run 1)and after (Run 2) change of faulty gasket

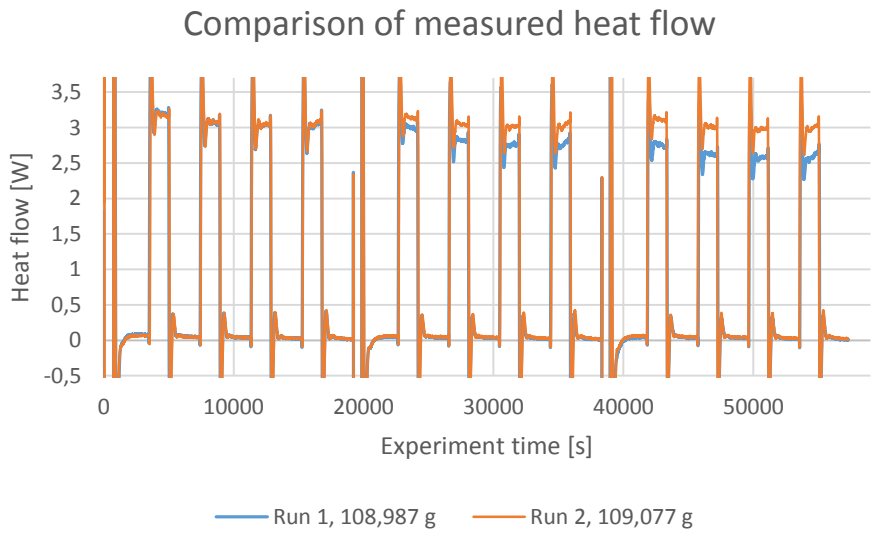

Figure 7.6-2 Comparison of measured heat flow between scanning experiment before (Run 1) and after (Run 2) change of faulty gasket

The heat capacities shown in Table 7.6-1 and 7.6-2 have been calculated according to the experimental method described in chapter 6. Vapor pressure for CO_2 at 0,2 and 0,4 loading in 30 wt% MDEA solution was found by interpolating experimental values from Shen et al. [54], assuming linear relationship between each measuring point. No density data was found for the solution concentration and loading used in this study. Therefore the density was approximated using density prediction for 30 wt% MDEA from Cheng et al. and adding density of pure carbon dioxide multiplied with mole fraction of carbon dioxide in given solution. This result in a small error source, but similar approach for MEA solution show good consistency with density for loaded solution in literature.

7.7 Discussion on observed abnormalities during this study

Pressure loss

During the entirety of this study, a small insignificant leakage from the reactor vessel has been noticed. The pressure measurements performed by the CPA202 Reaction Calorimeter during experimental procedure has shown a systematic reduction of reactor pressure as seen in Figure 7.7-1, for pure MEA at low filling level. The reactor vessel itself have not been specifically tested for leakages during the calibration and validation procedures. However, during the calibration of reactor volume the system, including the reactor vessel, was pressurized and measured with a highly sensitive digital pressure gauge as described in chapter 4.3. During this procedure, no significant leakages was noticed as multiple stable readings was obtained. This leads to the conclusion that a leakage must have occurred during the experimental part of this study, and increased towards the end of this study. It is believed that the leakage responsible for the pressure loss seen in Figure 7.7-1 come from one or more of the connections in the reactor lid, or from the stirrer which goes through the reactor lid. This pressure loss have not noticeably affected the heat capacity measurements during this study, and therefor the source of leakage have not been searched for. It is assumed that its affect is below the standard deviation, or random noise level, of the apparatus and experimental procedure, and from Figure 7.7-1 one can see that the reason for th pressure loss does not significantly affect the measured heat flow.

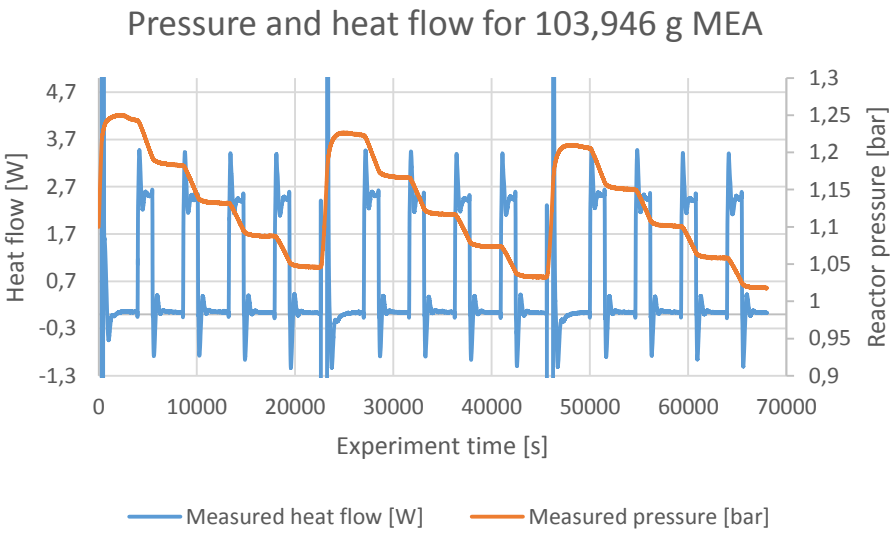

Figure 7.7-1 Measured heat flow and pressure for successful scanning experiment with pure MEA (first 3 sessions)

Frozen reaction mass and loss of contact with MSC202 dosing syringe

While performing calibration of the two MSC202 dosing syringes, the dosing syringes repeatedly turned offline and initiated inactive mode. In this mode the ChemiCall V2 software can not control the dosing syringes as they can only be operated manually. After several attempts of correcting this error, ChemiSens service staff was contacted. As a result of their "in house" testing, it was discovered that the problem was due to a faulty wire/connection between the MSC202 Dosing Syringes and the VRC202 Dosing controller unit. This lead to a loss of signal, which in turn triggered the dosing syringes to go into inactive mode as a safety protocol. A new wire connecting the two was shipped from ChemiSens, and the problem ceased.

During the initial trial runs with H_2O, a significant abnormality was observed. The reaction mass had been frozen solid overnight, as shown in Figure 7.7-2. ChemiSens service staff was contacted and the problem was believed to be a temporarily loss of signal between the reactor vessel and the ChemiCall V2 software resulting in initiation of emergency cooling as an automatic safety protocol. During this protocol, the Peltier element cools down the reaction mass to a temperature below 0 °C, at which reaction mass froze. It is believed that this happened two times during the experimental scanning procedures with water, although it was only observed one time. The scanning experiments affected by this have not been used in Cp measurements. From the discussion with ChemiSens it was concluded that further service and troubleshooting would be necessary if the problem persisted. The source of the problem was not found or corrected, as the issue did not persist.

Figure 7.7-2 Picture of frozen reaction mass (H_2O) after a unsuccessful scanning experiment

8 Conclusions

This master thesis divided into three consecutive stages. The first stage was to calibrate and validate the CPA202 Reaction Calorimeter in order to reduce future measurement errors and to achieve a sufficient degree of knowledge about the system in order to develop and perform successful heat capacity measurement experiments. The second stage was to develop an experimental procedure in which heat capacity could be measured with the highest degree of accuracy possible under the time constraints of this study. The third and final stage was to perform heat capacity measurements of alkanolamines and their loaded and unloaded solutions. The alkanolamines used was MEA and MDEA. In the following chapters, the conclusions for this study are be presented.

8.1 Calibration and validation of CPA202 Reaction Calorimeter

Before heat capacity experiments was initiated, calibration and validation of the apparatus was performed. The exact volume of the Pyrex glass reactor was found to be 258,86 ± 0,14 ml by the use of a reference volume and a connected pressurized system. The accuracy of the two MSC202 Dosing Syringes belonging to the CPA202 apparatus was assessed. Pump1 was found to have an average accuracy of 98,38%, and Pump2 of 98,37%, between preset dosing volume and actual dosing volume. On a general basis both pumps deliver less than the preset value, and it is recommended to subtract 0,14 ± 0,0205 ml from the preset value. Bot pumps have an high dosing consistency, with a standard deviation from average value of 0,31%.

The CPA202 reaction Calorimeter has two flowmeters for continuous injection of CO_2 into the reactor. The relationship between flow meter capacity and actual CO_2 flow rate was for both flowmeters found to be linear, and the relationship is described in equation (8.1-1) for Linout_A and (8.1-2) for Linout_B, both valid for 6 bar inlet pressure.

$$CO_2\ flow\ rate\left[\frac{mL}{min}\right] = 26.26 * X\ [V] - 24.669 \quad (8.1-1)$$

$$CO_2\ flow\ rate\left[\frac{mL}{min}\right] = 26.257 * X[V] - 26.78 \quad (8.1-2)$$

The inlet pressure is adjusted with a manual valve, and a change of ± 2 bar inlet pressure results in a change of CO_2 flow rate of ± 1,15 % accordingly. It is recommended to use flowmeters at capacities higher than 3V (30 %), as flowrate uncertainty drastically increase at lower capacities.

The heat flow measurements performed by the CPA202 was found to have an accuracy of >98,75% when validated against the internal validation heater.

8.2 Experimental method for heat capacity measurements with CPA202 Reaction Calorimeter

As part of the master thesis, a procedure for accurate heat capacity experiments on the CPA202 Reaction Calorimeter was developed. The procedure has its basis in recommended methods from ChemiSens, and have successfully achieved high accuracy as demonstrated by the results in the validation experiment with ethanol as listed in Table 8.2-1. Here the measured specific heat capacities had an average deviation from literature data of 1,47% [23].

Table 8.2-1 Validation: Specific heat capacity for ethanol compared to literature data

	Cp, [kJ/(kg*K)]		
Temp [C°]	**Sun et al., 1988 [23]**	**This study**	**Deviation from Sun et al.**
35	2,52	2,51	1,66 %
45	2,62	2,62	0,12 %
55	2,73	2,75	2,49 %
65	2,84	2,86	1,63 %

The developed procedure uses two or more filling levels in order to reduce the effect of wetted glass area and other unmonitored heat flows, and phase transition effects (ΔH_{vap}) are subtracted from measured heat flows. In order to correct for the intrinsic heat capacity of the reactor vessel and inserts, and unmonitored heat losses through the Pyrex glass wall of the reactor, a series of correction factors ($HC_{Reactor+inserts,\Delta T}$) was obtained through a reference liquid, H_2O, and data fitting to experimental heat capacities from Osborne et al. The calculation approach is shown in equation 8.2-1, and its constituents can be found in chapter 6. The conditions recommended is listed in Table 8.2-2.

$$\frac{\int Total\ power\ dt - \Delta H_{vap}}{\Delta T} - HC_{Reactor+inserts,\Delta T} = m_{liquid} * C_p \qquad (8.2-1)$$

Table 8.2-2 Conditions for heat capacity experiments

Condition	**Setting**
Stirrer speed	100 RPM
Filling level	105 ml – 165 ml
Number of filling levels used	>2 (ΔV_{liq} should exceed 50 ml)
Temperature scanning interval	$\Delta T < 10$ °C
Scanning speed	0,5 – 0,3 °C/min (downwards)
Operation mode	Isothermal
Heat flow integrated	Total Power

The CPA202 Reaction Calorimeter is sensitive to changes in filling level and differences in physical properties such as thermal conductivity and viscosity. It is therefore recommended that correction factors are obtained with the use of liquid with similar properties to the liquid studied. To achieve a good description of how the correction factor changes with wetted wall height, 2 or more filling levels should be used as basis in accordance with the approach described in chapter 5.4.

8.3 Heat capacity measurements for loaded and unloaded solutions of MEA and MDEA

As discussed in the introduction, physical data such as heat capacity is important for process control and planning. The necessity for heat capacity data on loaded and un-loaded solutions of new alkanolamines such as MEA and MDEA is apparent when confronted with the scarce literature data available. During this study a reaction calorimeter from ChemiSens (CPA202) has been used to measure the heat capacities for mentioned alkanolamines and their respective loaded and unloaded solutions. The solution concentration used in this study was 30 wt% aqueous solution with a loading of 0,2 and 0,4. It was chosen based on experiences from earlier work in the Environmental Engineering and Reactor Technology group [48] and the use of similar concentrations for carbon capture in the industry. A method for experimental procedure for heat capacity measurement with the mentioned calorimeter was developed, and heat capacities was successfully obtained with a high degree of accuracy of $\leq \pm 1.95$ % as shown with the ethanol validation.

The heat capacities obtained in this study is listed in Table 8-1. The overall standard deviation for the total data set for all experiments was 0,66 % from average value. This indicate a low variation in the data set and as such, stable readings from the apparatus can be expected in future experiments. Heat capacities was not obtained for loaded MDEA solutions due to a combination of leakage in the system and time constrictions for this study. The capability of accurate heat capacity experiments with the CPA202 Reaction Calorimeter have been assessed during this study, and the conclusion is that the apparatus can be utilized for future works with an acceptable degree of accuracy.

Table 8.3-1 Obtained heat capacities for MEA, MDEA and un-loaded and loaded solutions of the respective alkanolamines

Cp, [kJ/(kg*K)]								
	Monoethanolamine				**N-Methyldiethanolamine**			
Temp [C°]	**≥ 99%**	**30 wt%**	**30 wt% α=0,2**	**30 wt% α=0,4**	**≥ 99%**	**30 wt%**	**30 wt% α=0,2**	**30 wt% α=0,4**
35	2,84	3,89	3,60	3,42	2,21	3,75		
45	2,91	3,93	3,63	3,45	2,33	3,77	*Not obtained due to system leakage*	
55	2,98	3,96	3,67	3,49	2,43	3,81		
65	3,01	3,98	3,69	3,51	2,48	3,83		
SD	0,54 %	0,41 %	0,60 %	0,74 %	0,53 %	1,14 %		

9 References

1. Nilsson, H. and U. Hess, *Introduction of a calibration-free reaction calorimeter that combines the benefits of DSCS and reaction calorimeters.* Journal of Thermal Analysis and Calorimetry, 2008. **93**(1): p. 219-224.
2. Landau, R., *Expanding the role of reaction calorimetry.* Thermochimica acta, 1996. **289**(2): p. 101-126.
3. Kierzkowska-Pawlak, H., *Enthalpies of absorption and solubility of CO2 in aqueous solutions of methyldiethanolamine.* Separation Science and Technology, 2007. **42**(12): p. 2723-2737.
4. Kohl, A.L.a.R., F.C., *Gas purification.* Gulf publishing: Houston, 1997. **5th edition**.
5. Lavoisier, A. and P. De Laplace, *Two essays about heat (Zwei Abhandlungen über die Wärme) 1780 and 1784*, in *Ostwald's Klassiker der Exakten Wissenschafen*. 1892, W. Engelmann Leipzig. p. 28.
6. Townsend, D., *Hazard evaluation of self-accelerating reactions.* Chemical Engineering Progress, 1977. **73**(9): p. 80-81.
7. Gill, P., S. Sauerbrunn, and M. Reading, *Modulated differential scanning calorimetry.* Journal of Thermal Analysis and Calorimetry, 1993. **40**(3): p. 931-939.
8. Diedrichs, A. and J. Gmehling, *Measurement of heat capacities of ionic liquids by differential scanning calorimetry.* Fluid Phase Equilibria, 2006. **244**(1): p. 68-77.
9. Guldbæk Karlsen, L. and J. Villadsen, *Isothermal reaction calorimeters—I. A literature review.* Chemical Engineering Science, 1987. **42**(5): p. 1153-1164.
10. Osborne, N.S., H.F. Stimson, and D.C. Ginnings, *Measurements of Heat Capacity and Heat of Vaporization of Water in the Range of 0° to 100° C*. 1939: US Department of Commerce, National Bureau of Standards.
11. Zábranský, M., V. Růžička Jr, and V. Majer, *Heat Capacities of Organic Compounds in the Liquid State I. C1 to C18 1-Alkanols.* Journal of Physical and Chemical Reference Data, 1990. **19**(3): p. 719-762.
12. Chen, Y.-J. and M.-H. Li, *Heat Capacity of Aqueous Mixtures of Monoethanolamine with 2-Amino-2-methyl-l-propanol.* Journal of Chemical & Engineering Data, 2001. **46**(1): p. 102-106.
13. ChemiSens, *User manual CPA202 system hardware.* 2011(ChemiSense document Z202-010): p. 59.
14. Widell, R. and H.T. Karlsson, *Autocatalytic behaviour in esterification between anhydrides and alcohols.* Thermochimica Acta, 2006. **447**(1): p. 57-63.
15. Khan, A., *A liquid water model: Density variation from supercooled to superheated states, prediction of H-bonds, and temperature limits.* The Journal of Physical Chemistry B, 2000. **104**(47): p. 11268-11274.
16. GmbH, M.I.D., *Digital mass flow controller Instruction manual.* 2006. **Y-1951579A**.
17. Nilsson, H., *CPA202 Dynamic test.* ChemiCall Experiment Report, 2005.
18. ChemiSens, *Determination of heat capacity.* 2007. **ChemiSens document Z600-010 (2007-05-28)**.
19. Wagner, W. and A. Pruß, *The IAPWS formulation 1995 for the thermodynamic properties of ordinary water substance for general and scientific use.* Journal of Physical and Chemical Reference Data, 2002. **31**(2): p. 387-535.
20. ChemiSens, *User Manual ChemiCall V2.* ChemiSens document Z202-011.
21. Kretschmer, C.B. and R. Wiebe, *Liquid-Vapor Equilibrium of Ethanol--Toluene Solutions.* Journal of the American Chemical Society, 1949. **71**(5): p. 1793-1797.
22. Ortega, J., *Densities and refractive indices of pure alcohols as a function of temperature.* Journal of Chemical and Engineering Data, 1982. **27**(3): p. 312-317.
23. Sun, T., et al., *Acoustic and Thermodynamic Properties of Ethanol from 273.15 to 333.1 5 K and up to 280 MPa.* Physics and Chemistry of Liquids an International Journal, 1988. **18**(2): p. 107-116.
24. Lide, D.R., *Handbook of organic solvents*. 1994: CRC Press.
25. Riddick, J.A., W.B. Bunger, and T.K. Sakano, *Organic solvents: physical properties and methods of purification.* 1986.

26. Chiu, L.-F., H.-F. Liu, and M.-H. Li, *Heat capacity of alkanolamines by differential scanning calorimetry*. Journal of Chemical & Engineering Data, 1999. **44**(3): p. 631-636.
27. Lee, L., *Thermodynamic models for natural gas sweetening fluids.* Annual report to the Gas Research Institute, University of Oklahoma: Norman, OK, 1994.
28. Pagé, M., J.-Y. Huot, and C. Jolicoeur, *A comprehensive thermodynamic investigation of water-ethanolamine mixtures at 10, 25, and 40 C.* Canadian journal of chemistry, 1993. **71**(7): p. 1064-1072.
29. Hepler, L., et al., *Molar heat capacities of alkanolamines from 299.1 to 397.8 K Group additivity and molecular connectivity analyses.* Journal of the Chemical Society, Faraday Transactions, 1997. **93**(9): p. 1747-1750.
30. Chueh, C.F.S., A.C., *Estimation of Liquid Heat Capacity.* Chem. Eng. Prog., 1973. **69, 83-85**(Can. J. Chem. Eng. 1973, 51): p. 596-600.
31. Missenard, F.A., C. R. Acad. Sci., 1965. **260**: p. 521.
32. Cheng, S., A. Meisen, and A. Chakma, *Predict amine solution properties accurately.* Hydrocarbon processing, 1996. **75**(2).
33. Mandal, B.P., M. Kundu, and S.S. Bandyopadhyay, *Density and viscosity of aqueous solutions of (N-methyldiethanolamine+ monoethanolamine),(N-methyldiethanolamine+ diethanolamine),(2-amino-2-methyl-1-propanol+ monoethanolamine), and (2-amino-2-methyl-1-propanol+ diethanolamine).* Journal of Chemical & Engineering Data, 2003. **48**(3): p. 703-707.
34. Kapteina, S., et al., *Vapor pressures and vaporization enthalpies of a series of ethanolamines.* Journal of Chemical & Engineering Data, 2005. **50**(2): p. 398-402.
35. Matthews, J., J. Sumner, and E. Moelwyn-Hughes, *The vapour pressures of certain liquids.* Transactions of the Faraday Society, 1950. **46**: p. 797-803.
36. Information, N.C.f.B., PubChem Compound database. **CID=700**.
37. Weiland, R.H., J.C. Dingman, and D.B. Cronin, *Heat capacity of aqueous monoethanolamine, diethanolamine, N-methyldiethanolamine, and N-methyldiethanolamine-based blends with carbon dioxide.* Journal of Chemical & Engineering Data, 1997. **42**(5): p. 1004-1006.
38. Abdulkadir, A., et al., *Heat of Absorption and Specific Heat of Carbon Dioxide in Aqueous Solutions of Monoethanolamine, 3-piperidinemethanol and Their Blends.* Energy Procedia, 2014. **63**: p. 2070-2081.
39. Chiu, L.-F. and M.-H. Li, *Heat capacity of alkanolamine aqueous solutions.* Journal of Chemical & Engineering Data, 1999. **44**(6): p. 1396-1401.
40. Hilliard, M.D., *A predictive thermodynamic model for an aqueous blend of potassium carbonate, piperazine, and monoethanolamine for carbon dioxide capture from flue gas.* 2008.
41. Amundsen, T.G., *CO2 absorption in alkaline solution.* 2008.
42. Wu, S.-H., et al., *Vapor pressures of aqueous blended-amine solutions containing (TEA/AMP/MDEA) + (DEA/MEA/PZ) at temperatures (303.15–343.15) K.* Experimental Thermal and Fluid Science, 2013. **48**(0): p. 1-7.
43. Xu, S., et al., *Vapor pressure measurements of aqueous N-methyldiethanolamine solutions.* Fluid phase equilibria, 1991. **67**: p. 197-201.
44. Han, J., et al., *Density of Water (1)+ Monoethanolamine (2)+ CO2 (3) from (298.15 to 413.15) K and Surface Tension of Water (1)+ Monoethanolamine (2) from (303.15 to 333.15) K.* Journal of Chemical & Engineering Data, 2012. **57**(4): p. 1095-1103.
45. Weiland, R.H., et al., *Density and viscosity of some partially carbonated aqueous alkanolamine solutions and their blends.* Journal of Chemical & Engineering Data, 1998. **43**(3): p. 378-382.
46. Richard M. Stepheson, S.M., *Handbook of the thermodynamics of organic compounds* 1987.
47. Jou, F.Y., A.E. Mather, and F.D. Otto, *The solubility of CO2 in a 30 mass percent monoethanolamine solution.* The Canadian Journal of Chemical Engineering, 1995. **73**(1): p. 140-147.
48. Ma'mun, S., et al., *Solubility of carbon dioxide in 30 mass% monoethanolamine and 50 mass% methyldiethanolamine solutions.* Journal of Chemical & Engineering Data, 2005. **50**(2): p. 630-634.
49. Oxide, I., *GAS/SPEC MDEA.*
50. INEOS, *GAS/SPEC MDEA Specialty Amine.*

51. Rebolledo-Libreros, M.E. and A. Trejo, *Density and Viscosity of Aqueous Blends of Three Alkanolamines: N-Methyldiethanolamine, Diethanolamine, and 2-Amino-2-methyl-1-propanol in the Range of (303 to 343) K.* Journal of Chemical & Engineering Data, 2006. **51**(2): p. 702-707.
52. Li, M.-H. and Y.-C. Lie, *Densities and viscosities of solutions of monoethanolamine+ N-methyldiethanolamine+ water and monoethanolamine+ 2-amino-2-methyl-1-propanol+ water.* Journal of Chemical and Engineering Data, 1994. **39**(3): p. 444-447.
53. Hayden, T.A., T.G. Smith, and A.E. Mather, *Heat capacity of aqueous methyldiethanolamine solutions.* Journal of Chemical and Engineering Data, 1983. **28**(2): p. 196-197.
54. Shen, K.P. and M.H. Li, *Solubility of carbon dioxide in aqueous mixtures of monoethanolamine with methyldiethanolamine.* Journal of chemical and Engineering Data, 1992. **37**(1): p. 96-100.

Appendix A: Calibration and validation data

Measurement data for continuous addition assessment

	Measured THF	t1	t2	Inlet_temp	Delta T	Added vol	Calculated Cp
1	-723,47	2,00	1046,00	19,10	30,90	7,50	3,13
2	-2104,51	672,00	1976,00	19,10	30,90	20,08	3,40
3	-2047,63	3118,00	4420,00	19,10	30,90	20,08	3,31
4	-1833,64	72,00	1088,00	18,40	26,60	20,08	3,44
5	-1870,57	1088,00	2342,00	18,40	26,60	20,08	3,51
6	-668,12	4324,00	5848,00	22,10	27,90	7,58	3,16
7	-684,85	8532,00	10170,00	22,10	27,90	7,58	3,24
8	-696,69	12832,00	14472,00	22,10	27,90	7,58	3,30
9	-694,77	17224,00	18908,00	22,10	27,90	7,58	3,29
10	-697,88	21978,00	23482,00	22,10	27,90	7,58	3,31
11	-709,66	26372,00	28078,00	22,10	27,90	7,58	3,36
12	-710,38	3562,00	5120,00	22,10	17,90	10,00	4,01
13	-711,45	7982,00	9618,00	22,10	17,90	10,08	3,99
14	-685,73	12480,00	14116,00	22,10	17,90	10,08	3,84
15	-675,86	17132,00	18768,00	22,10	17,90	10,08	3,79
16	-646,92	21748,00	23442,00	22,10	17,90	10,00	3,66

Heat capacity measurement of distilled deionized water

Experiment 1			**Mass**	**100,12**	
Område	**THF [J]**	**t1 [s]**	**t2 [s]**	**T1 [oC]**	**T2 [oC]**
70-60	8145,23317	3140	5720	70,114	60,126
60-50	8040,81318	5710	9720	60,126	50,136
50-40	8047,64246	9720	13620	50,136	40,149
40-30	8135,3413	13620	17430	40,149	30,163
70-60	8122,39673	21640	24810	70,12	60,129
60-50	8034,76019	24810	28350	60,129	50,138
50-40	8032,87227	28350	32000	50,138	40,15
40-30	8108,74527	32000	35000	40,15	30,167
70-60	8158,39672	38940	42330	70,119	60,129
60-50	8059,39591	42330	45800	60,129	50,138
50-40	8028,82541	45800	49350	50,138	40,149
40-30	8134,53768	49350	53000	40,149	30,162

Experiment 2			Mass	151,34	
Område	THF [J]	t1 [s]	t2 [s]	T1 [oC]	T2 [oC]
70-60	10571,38141	4260	7820	70,12	60,1321
60-50	10460,48886	7820	11500	60,1321	50,14224
50-40	10468,54886	11500	15290	50,14224	40,15456
40-30	10636,30959	15290	18850	40,15456	30,16761
70-60	10559,59088	22730	26230	70,1243	60,13458
60-50	10474,32464	26230	29990	60,13458	50,14343
50-40	10499,88723	29990	33730	50,14343	40,15604
40-30	10645,29019	33730	37270	40,15604	30,16967
70-60	10553,3843	41160	44800	70,12445	60,13427
60-50	10454,68992	44800	48490	60,13427	50,14326
50-40	10475,70476	48490	52330	50,14326	40,1561
40-30	10647,16687	25330	56000	40,1561	30,16699

Experiment 3			Mass	125,04	
Område	THF [J]	t1 [s]	t2 [s]	T1 [oC]	T2 [oC]
70-60	9261,39447	3710	7120	70,11753	60,1276
60-50	9162,57594	7120	10520	60,1276	50,13656
50-40	9134,63456	10520	14170	50,13656	40,14818
40-30	9274,71294	14170	17740	40,14818	30,15982
70-60	9228,00368	21050	24330	70,12361	60,13154
60-50	9158,29997	24330	27850	60,13154	50,13939
50-40	9142,3287	27850	31510	50,13939	40,15086
40-30	9280,01317	31510	35000	40,15086	30,1625
70-60	9236,63989	38310	41720	70,12249	60,1317
60-50	9143,74677	41720	45130	60,1317	50,13908
50-40	9141,29712	45130	48790	50,13908	40,15117
40-30	9281,12947	48790	52210	40,15117	30,16292

Experiment 4 (Isothermal)				Mass	100,69
Område	THF [J]	t1 [s]	t2 [s]	T1 [oC]	T2 [oC]
70 - 60	8045,194390	1058	3990	69,99952	59,99998
60 - 50	8060,912340	3990	6866	59,99998	49,99989
50 - 40	8048,408940	6866	9856	49,99989	40,00025
40 - 30	8089,436620	9856	12790	40,00025	30,00046
30 - 40	-8271,791130	12790	15848	30,00046	40,00019

40 - 50	-8225,017730	15848	18712	40,00019	49,99994
50 - 60	-8254,171460	18712	21658	49,99994	60,00005
60 - 70	-8410,229100	21658	24612	60,00005	70,00011
70 - 60	8143,269410	24612	27478	70,00011	60,00023
60 - 50	8083,671380	27478	30434	60,00023	49,99989
50 - 40	8065,177130	30434	33446	49,99989	39,99966
40 - 30	8091,106510	33446	36402	39,99966	29,9999
30 - 40	-8286,833560	36402	39370	29,9999	40,00007
40 - 50	-8243,211340	39370	42314	40,00007	49,99954
50 - 60	-8261,508990	42314	45246	49,99954	60,00013
60 - 70	-8418,573690	45246	48158	60,00013	69,99989
70 - 60	8160,025880	48158	51078	69,99989	59,99997
60 - 50	8077,084870	51078	54034	59,99997	50,00075
50 - 40	8065,049170	54034	57002	50,00075	40,00008
40 - 30	8103,153040	57002	60000	40,00008	29,99998
30 - 40	-8272,258510	60000	62970	29,99998	40,00027
40 - 50	-8244,238470	62970	65870	40,00027	50
50 - 60	-8252,110270	65870	58780	50	59,9998
60 - 70	-8414,136950	58780	71554	59,9998	70,00025

Experiment 5 (Isothermal)				**Mass**	**159,99**
Område	**THF [J]**	**t1 [s]**	**t2 [s]**	**T1 [oC]**	**T2 [oC]**
70 - 60	10989,205000	2412	5358	69,99977	59,99982
60 - 50	10996,720630	5358	8378	59,99982	50,00023
50 - 40	10983,230510	8378	11456	50,00023	40,00034
40 - 30	11041,829650	11456	14552	40,00034	30,0004
30 - 40	-11265,720170	14552	17724	30,0004	40,0001
40 - 50	-11229,689120	17724	20708	40,0001	50,00056
50 - 60	-11234,882850	20708	23766	50,00056	59,99953
60 - 70	-11318,118040	23766	26730	59,99953	70,00019
70 - 60	11130,600470	26730	29712	70,00019	59,99952
60 - 50	10988,661540	29712	32600	59,99952	50,00014
50 - 40	10980,922240	32600	35754	50,00014	39,99984
40 - 30	11074,428690	35754	38982	39,99984	30,00004
30 - 40	-11282,863790	38982	42136	30,00004	39,99984
40 - 50	-11264,073960	42136	45120	39,99984	49,99968
50 - 60	-11258,204800	45120	48140	49,99968	60,00021
60 - 70	-11361,951180	48140	51046	60,00021	70,00005

70 - 60	11109,701850	51046	54086	70,00005	59,99995
60 - 50	11020,696020	54086	57088	59,99995	50,00014
50 - 40	11009,365100	57088	60242	50,00014	39,99998
40 - 30	11083,409040	60242	63338	39,99998	29,99985
30 - 40	-11259,026920	63338	66320	29,99985	40,00009
40 - 50	-11262,556190	66320	69474	40,00009	49,99972
50 - 60	-11263,217640	69474	72380	49,99972	59,99996
60 - 70	-11339,910490	72380	75212	59,99996	69,99964

Experiment 6 (Isothermal)				**Mass**	**107,88**
Område	**THF [J]**	**t1 [s]**	**t2 [s]**	**T1 [oC]**	**T2 [oC]**
70-60	8482,298700	678	3460	69,999880	60,000520
60-70	-8692,685640	3460	6290	60,000520	70,000080
70-60	8518,344030	6290	9168	70,000080	60,000210
60-70	-8693,519240	9168	11902	60,000210	69,999470
70-60	8531,721980	11902	14756	69,999470	59,999570
60-70	-8674,761580	14756	17516	59,999570	69,999610
60-50	8367,028260	19260	22020	60,000390	49,999930
50-60	-8561,983920	22020	24850	49,999930	60,000280
60-50	8442,812180	24850	27632	60,000280	49,999730
50-60	-8598,776970	27632	30440	49,999730	60,000040
60-50	8438,801680	30440	33388	60,000040	50,000150
50-60	-8575,977770	33388	36004	50,000150	59,999940
50-40	8355,991940	37868	40698	49,999890	39,999910
40-50	-8572,945790	40698	43480	39,999910	50,000090
50-40	8441,816070	43480	46334	50,000090	40,000010
40-50	-8579,881070	46334	49164	40,000010	50,000180
50-40	8438,878650	49164	52042	50,000180	40,000110
40-50	-8593,334350	52042	54682	40,000110	50,000220
40-30	8402,501420	56570	59518	40,000250	30,000100
30-40	-8643,994080	59518	62394	30,000100	40,000070

Experiment 7 (Isothermal)				**Mass**	**157,91**
Område	**THF [J]**	**t1 [s]**	**t2 [s]**	**T1 [oC]**	**T2 [oC]**
70-60	10900,159810	1300	4140	69,999940	59,999970
60-70	-11127,784730	4140	7100	59,999970	70,000030
70-60	10974,780450	7100	9984	70,000030	60,000160
60-70	-11157,576050	9984	12914	60,000160	69,999950

70-60	10972,035080	12914	15814	69,999950	60,000180
60-70	-11142,039260	15814	18684	60,000180	70,000130
60-50	10824,563490	20514	23414	60,000190	49,999790
50-60	-11032,312640	23414	26314	49,999790	59,999860
60-50	10889,692850	26314	29186	59,999860	49,999840
50-60	-11044,744860	29186	32114	49,999840	59,999750
60-50	10900,617980	32114	35058	59,999750	50,000020
50-60	-11076,259440	35058	37930	50,000020	60,000290
50-40	10769,100920	39878	42938	50,000090	40,000350
40-50	-11106,836990	42938	45838	40,000350	50,000360
50-40	10876,984640	45838	48900	50,000360	40,000040
40-50	-11089,901060	48900	51872	40,000040	50,000220
50-40	10875,821800	51872	54918	50,000220	39,999600
40-50	-11091,253700	54918	57716	39,999600	49,999330
40-30	10869,073320	59796	62944	40,000100	29,999640
30-40	-11161,914660	62944	66152	29,999640	40,000170
40-30	10948,654890	66152	69316	40,000170	30,000280
30-40	-11155,540530	69316	72332	30,000280	39,999810
40-30	10953,950250	72332	75526	39,999810	29,999950
30-40	-11195,440390	75526	78484	29,999950	39,999840

Experiment 8 (Isothermal)				**Mass**	**157,91**
Område	**THF [J]**	**t1 [s]**	**t2 [s]**	**T1 [oC]**	**T2 [oC]**
70-60	10918,940250	1300	4194	69,999800	59,999620
60-70	-11155,850980	4194	7116	59,999620	70,000120
70-60	10977,447290	7116	10024	70,000120	60,000540
60-70	-11148,482030	10024	12904	60,000540	69,999910
70-60	11025,326690	12904	15826	69,999910	59,999510
60-70	-11140,202950	15826	18600	59,999510	70,002000
60-50	10816,136830	20484	23406	59,999990	49,999870
50-60	-11066,352730	23406	26340	49,999870	60,000920
60-50	10901,940580	26340	29222	60,000920	49,999980
50-60	-11062,918360	29222	32170	49,999980	60,000350
60-50	10906,722600	32170	35038	60,000350	49,999630
50-60	-11049,220640	35038	37918	49,999630	60,000000
50-40	10810,321760	39858	42940	49,999370	40,000200
40-50	-11090,581170	42940	45836	40,000200	49,999360
50-40	10917,327140	45836	48904	49,999360	39,999680
40-50	-11092,478300	48904	51812	39,999680	49,999990
50-40	10913,628230	51812	54814	49,999990	40,000530

40-50	-11095,515140	54814	57736	40,000530	50,000120
40-30	10918,413930	59648	62852	40,000130	29,999940
30-40	-11158,541920	62852	65908	29,999940	39,999740
40-30	10977,877280	65908	69046	39,999740	29,999860
30-40	-11186,278060	69046	72114	29,999860	40,000150
40-30	10963,447230	72114	75346	40,000150	29,999580
30-40	-11190,202680	75346	78294	29,999580	39,999690

Experiment 9 (Isothermal) **Mass** **163,77**

Område	THF [J]	TP [J]	t1 [s]	t2 [s]	T1 [oC]	T2 [oC]
70-60	11149,997640		3622	7958	70,000000	60,000290
60-70	-11448,511830	-8058,322950	7958	12230	60,000290	69,999750
70-60	11288,288390	7880,839840	12230	16502	69,999750	59,999680
60-70	-11448,257460	-8066,327220	16502	20888	59,999680	70,000110
70-60	11287,073870	7884,112280	20888	25152	70,000110	59,999950
60-70	-11491,134770		25152	29442	59,999950	70,000130
60-50	11069,863800		33180	37410	60,000130	49,999900
50-60	-11356,427060	-7949,897910	37410	41714	49,999900	59,999500
60-50	11189,124050	7786,519180	41714	46018	59,999500	50,000010
50-60	-11340,328850	-7947,904900	46018	50308	50,000010	60,000520
60-50	11255,897300	7840,195570	50308	54586	60,000520	49,999620
50-60	-11324,225340	-7938,370340	54586	58864	49,999620	60,000000
50-40	11091,922540		62542	66818	49,999800	39,999720
40-50	-11361,574270	-7974,466350	66818	71122	39,999720	49,999850
50-40	11209,955010	7795,166660	71122	75386	49,999850	39,999930
40-50	-11356,507100	-7949,294800	75386	79742	39,999930	49,999610
50-40	11214,477230	7815,992350	79742	84020	49,999610	39,999740
40-50	-11366,735490	-7983,976800	84020	88310	39,999740	49,999960
40-30	11145,347690		91988	96344	40,000330	29,999810
30-40	-11429,391710	-8051,689310	96344	100752	29,999810	40,000130
40-30	11262,471700	7856,079800	100752	105146	40,000130	29,999980
30-40	-11424,734530	-8020,113630	105146	109490	29,999980	39,999680
40-30	11288,326030	7882,261260	109490	113898	39,999680	30,000080
30-40	-11444,338100	-8061,484700	113898	118202	30,000080	40,000060

Experiment 10 (Isothermal) **Mass** **106,79**

Område	THF [J]	t1 [s]	t2 [s]	T1 [oC]	T2 [oC]
70-60	8316,259910	3640	7808	69,999590	60,000210
60-70	-8645,760570	7808	11850	60,000210	69,999630

70-60	8484,156190	11850	16000	69,999630	60,000220
60-70	-8614,892300	16000	20000	60,000220	70,000270
70-60	8470,762640	20000	24190	70,000270	59,999890
60-70	-8605,557460	24190	28160	59,999890	70,000530
60-50	8243,834930	31694	35842	59,999670	49,999980
50-60	-8460,723430	35842	39920	49,999980	59,999510
60-50	8410,835450	39920	44072	59,999510	50,000230
50-60	-8487,458380	44072	48088	50,000230	59,999790
60-50	8378,707150	48088	52268	59,999790	50,000590
50-60	-8534,795280	52268	56266	50,000590	59,999930
50-40	8191,116790	59668	63866	49,999930	39,999860
40-50	-8507,510430	63866	67882	39,999860	49,999830
50-40	8367,679870	67882	72054	49,999830	40,000240
40-50	-8520,618780	72054	76080	40,000240	50,000140
50-40	8347,434050	76080	80232	50,000140	39,999860
40-50	-8526,016630	80232	84240	39,999860	50,000200
40-30	8285,824640	87812	92174	39,999630	30,000060
30-40	-8583,138220	92174	96472	30,000060	40,000200
40-30	8405,080880	96472	100788	40,000200	30,000260
30-40	-8569,350930	100788	105086	30,000260	39,999700
40-30	8421,600560	105086	109430	39,999700	30,000210
30-40	-8556,611810	109430	13554	30,000210	39,999270

Experiment 11 (Isothermal)				**Mass**	**175,65**
Område	**THF [J]**	**T1 [oC]**	**T2 [oC]**	**Avg. T [oC]**	**Delta T [oC]**
70-60	11879,628110	69,999870	59,999550	64,99971	10,000320
60-70	-12015,954420	59,999550	70,000250	64,9999	-10,000700
70-60	11875,544800	70,000250	60,000210	65,00023	10,000040
60-70	-11992,417480	60,000210	69,999660	64,999935	-9,999450
70-60	11878,792220	69,999660	60,000010	64,999835	9,999650
60-70	-12013,595530	60,000010	69,999510	64,99976	-9,999500
60-50	11772,809390	60,000110	49,999870	54,99999	10,000240
50-60	-11904,016410	49,999870	59,999800	54,999835	-9,999930
60-50	11809,983330	59,999800	49,999930	54,999865	9,999870
50-60	-11926,690610	49,999930	60,000020	54,999975	-10,000090
60-50	11790,368290	60,000020	50,000070	55,000045	9,999950
50-60	-11927,430040	50,000070	59,999920	54,999995	-9,999850
50-40	11743,324860	49,999290	39,999480	44,999385	9,999810
40-50	-11978,075570	39,999480	49,999900	44,99969	-10,000420

50-40	11791,117980	49,999900	40,000180	45,00004	9,999720
40-50	-11952,500300	40,000180	50,000150	45,000165	-9,999970
50-40	11826,736700	50,000150	40,000090	45,00012	10,000060
40-50	-11944,351110	40,000090	49,999980	45,000035	-9,999890
40-30	11866,742680	39,999840	29,999650	34,999745	10,000190
30-40	-12017,024560	29,999650	39,999640	34,999645	-9,999990
40-30	11878,986790	39,999640	30,000000	34,99982	9,999640
30-40	-12047,457110	30,000000	40,000090	35,000045	-10,000090
40-30	11866,500990	40,000090	30,000360	35,000225	9,999730
30-40	-12060,975470	30,000360	40,000290	35,000325	-9,999930

Experiment 12 (Isothermal)			**Mass**	**121,7**
Område	**THF [J]**	**T1 [oC]**	**T2 [oC]**	**Avg. T [oC]**
70-60	9364,688370	69,999900	60,000360	65,00013
60-70	-9449,676440	60,000360	69,999810	65,000085
70-60	9333,724860	69,999810	59,999960	64,999885
60-70	-9464,218840	59,999960	70,000410	65,000185
70-60	9340,187330	70,000410	60,000230	65,00032
60-70	-9471,730510	60,000230	70,000230	65,00023
60-50	9269,076040	60,000220	49,999990	55,000105
50-60	-9311,456060	49,999990	59,999710	54,99985
60-50	9346,552300	59,999710	50,000240	54,999975
50-60	-9315,618190	50,000240	60,000810	55,000525
60-50	9305,546800	60,000810	49,999900	55,000355
50-60	-9334,800220	49,999900	59,999810	54,999855
50-40	9263,072040	49,999440	40,000090	44,999765
40-50	-9373,272610	40,000090	50,000430	45,00026
50-40	9305,432530	50,000430	39,999800	45,000115
40-50	-9383,322270	39,999800	50,000140	44,99997
50-40	9327,554330	50,000140	39,999840	44,99999
40-50	-9359,973010	39,999840	49,999967	44,9999035
40-30	9380,468060	39,999960	29,999590	34,999775
30-40	-9423,615970	29,999590	39,999960	34,999775
40-30	9386,675250	39,999960	29,999600	34,99978
30-40	-9465,581460	29,999600	39,999680	34,99964
40-30	9380,151060	39,999680	30,000060	34,99987
30-40	-9440,757970	30,000060	40,000060	35,00006

Experiment 13 (Isothermal)			Mass	158,04
Område	**THF [J]**	**T1 [oC]**	**T2 [oC]**	**Avg. T [oC]**
70-60	11132,376890	70,000280	59,999820	65,00005
60-70	-11197,841950	59,999820	70,000050	64,999935
70-60	11195,585040	70,000050	59,999390	64,99972
60-70	-11204,071200	59,999390	69,999470	64,99943
70-60	11159,304440	69,999470	60,000090	64,99978
60-70	-11233,515280	60,000090	69,999840	64,999965
60-50	11048,254420	60,000010	50,000330	55,00017
50-60	-11111,297240	50,000330	59,999900	55,000115
60-50	11111,382800	59,999900	50,000650	55,000275
50-60	-11132,742110	50,000650	59,999920	55,000285
60-50	11103,247790	59,999920	50,000210	55,000065
50-60	-11137,742780	50,000210	59,999430	54,99982
50-40	11194,189400	50,000400	40,000260	45,00033
40-50	-11178,358870	40,000260	49,999640	44,99995
50-40	11097,554980	49,999640	40,000280	44,99996
40-50	-11146,775620	40,000280	49,999940	45,00011
50-40	11125,871280	49,999940	39,999690	44,999815
40-50	-11166,184350	39,999690	49,999360	44,999525
40-30	11185,759570	40,000460	30,000050	35,000255
30-40	-11237,097420	30,000050	39,999700	34,999875
40-30	11187,645240	39,999700	30,000290	34,999995
30-40	-11277,643540	30,000290	39,999930	35,00011
40-30	11166,209980	39,999930	29,999760	34,999845
30-40				

Wetted wall height for experiment 6-13

Experiment 6			Experiment 10		
107,88	**THF/K [J/K]**	**WWH [cm]**	**106,79**	**THF/K [J/K]**	**WWH [cm]**
65	857,494945	2,8030874	**65**	851,933174	2,75755926
55	848,047228	2,7793149	**55**	841,791606	2,73402695
45	848,561812	2,75862866	**45**	842,434284	2,71354972
35			**35**	848,106183	2,69640052

Experiment 7			Experiment 11		
157,91	**THF/K [J/K]**	**WWH [cm]**	**175,65**	**THF/K [J/K]**	**WWH [cm]**
65	1102,98867	4,99136881	**65**	1192,97069	5,77681503
55	1095,0112	4,95448353	**55**	1184,60785	5,73578597
45	1096,06096	4,92238688	**45**	1186,64728	5,7000835
35	1104,24119	4,89550669	**35**	1195,22629	5,67018353

Experiment 8			Experiment 12		
157,91	**THF/K [J/K]**	**WWH [cm]**	**121,7**	**THF/K [J/K]**	**WWH [cm]**
65	1104,4624	4,99136881	**65**	938,218005	3,38824384
55	1095,53822	4,95448353	**55**	929,839602	3,35981617
45	1097,95234	4,92238688	**45**	932,488992	3,33507913
35	1106,06507	4,89550669	**35**	940,595387	3,31436244

Experiment 9			Experiment 13		
163,77	**THF/K [J/K]**	**WWH [cm]**	**158,04**	**THF/K [J/K]**	**WWH [cm]**
65	1135,3018	5,25082286	**65**	1117,10825	4,99716889
55	1126,65211	5,21256877	**55**	1109,68898	4,96025301
45	1127,8593	5,17928103	**45**	1114,41869	4,92812973
35	1134,65996	5,15140333	**35**	1121,73043	4,90122725

Calculated reactor constants

		Måling 10		**Måling 12**
		106,79		121,7
Område	**WWH**	**HC_reactor**	**WWH**	**HC_reactor**
70-60			3,38824384	424,856181
60-70	2,75755926	415,14748	3,38824384	433,363865
70-60	2,75755926	398,986951	3,38824384	421,73082
60-70	2,75755926	412,006351	3,38824384	434,723761
70-60	2,75755926	397,565586	3,38824384	422,346326
60-70	2,75755926	411,022247	3,38824384	435,517417
Snitt	**2,75755926**	**406,945723**	**3,38824384**	**428,756395**
60-50			3,35981617	416,440303
50-60	2,73402695	397,852116	3,35981617	420,725618
60-50	2,73402695	392,88407	3,35981617	423,711011
50-60	2,73402695	400,523195	3,35981617	420,515133
60-50	2,73402695	389,677699	3,35981617	419,47647
50-60	2,73402695	405,275834	3,35981617	422,494733
Snitt	**2,73402695**	**397,242583**	**3,35981617**	**420,560545**
50-40			3,33507913	416,792876
40-50	2,71354972	403,375016	3,33507913	427,720954
50-40	2,71354972	389,423673	3,33507913	420,910223
40-50	2,71354972	404,691812	3,33507913	428,725886
50-40	2,71354972	387,34149	3,33507913	423,153008
40-50	2,71354972	405,194139	3,33507913	426,410953
Snitt	**2,71354972**	**398,005226**	**3,33507913**	**423,952317**
40-30			3,31436244	428,935837
30-40	2,69640052	411,444349	3,31436244	433,250468
40-30	2,69640052	393,655659	3,31436244	429,557471

30-40	2,69640052	410,125575	3,31436244	437,474291
40-30	2,69640052	395,345503	3,31436244	428,974438
30-40	2,69640052	408,884083	3,31436244	434,999509
Snitt	**2,69640052**	**403,891034**	**3,31436244**	**432,198669**

		Måling 8		**Måling 13**
		157,91		158,04
Område	**WWH**	**HC_reactor**	**WWH**	**HC_reactor**
70-60	4,991368806	429,245948	4,99716889	450,011886
60-70	4,991368806	452,900949	4,99716889	456,583808
70-60	4,991368806	435,162317	4,99716889	456,310053
60-70	4,991368806	452,28989	4,99716889	457,2235
70-60	4,991368806	439,860181	4,99716889	452,824868
60-70	4,991368806	451,114918	4,99716889	460,204903
Snitt	**4,991368806**	**443,429034**	**4,99716889**	**455,526503**
60-50	4,954483526	420,159901	4,96025301	442,873649
50-60	4,954483526	445,07839	4,96025301	449,190344
60-50	4,954483526	428,650878	4,96025301	449,234425
50-60	4,954483526	444,81013	4,96025301	451,368291
60-50	4,954483526	429,153002	4,96025301	448,369834
50-60	4,954483526	443,440409	4,96025301	451,873959
Snitt	**4,954483526**	**435,215452**	**4,96025301**	**448,818417**
50-40	4,922386876	420,528789	4,92812973	458,263839
40-50	4,922386876	448,558165	4,92812973	456,76571
50-40	4,922386876	431,174569	4,92812973	448,687038
40-50	4,922386876	448,620411	4,92812973	453,575996
50-40	4,922386876	430,828661	4,92812973	451,419893
40-50	4,922386876	449,003919	4,92812973	455,515819
Snitt	**4,922386876**	**438,119086**	**4,92812973**	**454,038049**
40-30	4,895506694	431,670129	4,90122725	457,833005
30-40	4,895506694	455,725971	4,90122725	463,051943
40-30	4,895506694	437,650367	4,90122725	458,133393
30-40	4,895506694	458,444853	4,90122725	467,107824
40-30	4,895506694	436,131735	4,90122725	455,904911
30-40	4,895506694	458,857436		
Snitt	**4,895506694**	**446,413415**	**4,90122725**	**460,406215**

		Måling 9		Måling 11
		163,77		175,65
Område	**WWH**	**HC_reactor**	**WWH**	**HC_reactor**
70-60			5,77681503	451,327712
60-70	5,25082286	457,850629	5,77681503	464,9143
70-60	5,25082286	441,758649	5,77681503	450,952608
60-70	5,25082286	457,714286	5,77681503	462,710511
70-60	5,25082286	441,627053	5,77681503	451,323626
60-70	5,25082286	462,030522	5,77681503	464,822431
Snitt	**5,25082286**	**452,196228**	**5,77681503**	**457,675198**
60-50			5,73578597	441,832447
50-60	5,21256877	449,809872	5,73578597	454,989707
60-50	5,21256877	433,091199	5,73578597	445,593414
50-60	5,21256877	448,096886	5,73578597	457,238075
60-50	5,21256877	439,610311	5,73578597	443,622459
50-60	5,21256877	446,501324	5,73578597	457,340621
Snitt	**5,21256877**	**443,421918**	**5,73578597**	**450,102787**
50-40			5,7000835	439,770632
40-50	5,17928103	451,108356	5,7000835	463,173123
50-40	5,17928103	435,970153	5,7000835	444,560642
40-50	5,17928103	450,652719	5,7000835	460,669459
50-40	5,17928103	436,427982	5,7000835	448,082423
40-50	5,17928103	451,614248	5,7000835	459,864088
Snitt	**5,17928103**	**445,154692**	**5,7000835**	**452,686728**
40-30			5,67018353	452,482834
30-40	5,15140333	458,301824	5,67018353	467,534762
40-30	5,15140333	441,629494	5,67018353	453,772535
30-40	5,15140333	457,906925	5,67018353	470,565977
40-30	5,15140333	444,27695	5,67018353	452,513233
30-40	5,15140333	459,835308	5,67018353	471,937092
Snitt	**5,15140333**	**452,3901**	**5,67018353**	**461,467739**

Calibration of pumps

TEST PUMP 1

	Dry weight beaker	ChemiCall (ml)	Wet ewight beaker	Weight water	Temperature	Flowrate
1	31,5	10,08	41,39	9,89	21,6	5
2	31,49	10,08	41,4	9,91	21,2	5
3	31,5	10,08	41,38	9,88	21	5
4	31,51	10,08	41,39	9,88	21	5
5	31,5	10,08	41,41	9,91	21,1	5

6	31,5	10,08	41,41	9,91	21,2	5
1	31,5	5,04	36,397	4,897	21,3	2,5
2	31,472	5,04	36,412	4,94	21,1	2,5
3	31,471	5,04	36,407	4,936	21,1	2,5
4	31,473	5,04	36,425	4,952	21,3	2,5
5	20,671	5,04	25,61	4,939	21,4	2,5
6	31,472	5,04	36,399	4,927	21	2,5
7	20,674	5,04	25,609	4,935	21	2,5
8	31,471	5,04	36,412	4,941	21,1	2,5
9	20,672	5,04	25,615	4,943	21	2,5

TEST PUMP 2 Temp reservoir: 20,1 Temp rom: 22,2-22,6

	Dry weight beaker	ChemiCall (ml)	Wet ewight beaker	Weight water	Temperature	Flowrate
1	31,472	5,084	36,402	4,93	22,3	5
2	31,473	5,083	36,365	4,892	22,1	5
3	20,675	5,084	25,609	4,934	22,1	5
4	31,476	5,083	36,364	4,888	21,9	5
5	20,678	5,083	25,6	4,922	22	5
6	20,674	5,083	25,612	4,938	22,1	5
7	31,471	5,083	36,402	4,931	22,1	5
8	20,674	5,083	25,567	4,893	22,1	5
9	31,472	5,083	36,4	4,928	22,1	5
1	81,443	10,083	91,309	9,866	22,1	5
2	81,442	10,083	91,402	9,96	22,2	5
3	81,443	10,083	91,345	9,902	22,1	5
4	81,419	10,083	91,442	10,023	22,7	5
5	81,442	10,083	91,301	9,859	22,2	5

Calibration of flowmeters

Linout_A

pressure_A 1,02 bar
CO2 faktor 0,74

% Capacity	Volt	CPAflow	Measured flow	CO2 flow	Measured flow 2	CO2 flow 2
0 %	0	0	0	0	0	0
5 %	0,5	0,0008	37,5	27,75	34	25,16
10 %	1	0,0016	73,5	54,39	70,5	52,17
15 %	1,5	0,0025	109,5	81,03	106,5	78,81
20 %	2	0,0033	145	107,3	142,5	105,45

25 %	2,5	0,0041	181	133,94	178,5	132,09
30 %	3	0,0049	217	160,58	214,5	158,73
35 %	3,5	0,0058	252,5	186,85	250,5	185,37
40 %	4	0,0066	288,5	213,49	286	211,64
45 %	4,5	0,0074	323,5	239,39	321,5	237,91
50 %	5	0,0082	359	265,66	357	264,18
55 %	5,5	0,0091	394,5	291,93	392,5	290,45
60 %	6	0,0099	429,5	317,83	428	316,72
65 %	6,5	0,0107	465	344,1	464	343,36
70 %	7	0,0115	500	370	499	369,26
75 %	7,5	0,0124	535	395,9	534	395,16
80 %	8	0,0132	570	421,8	569	421,06
85 %	8,5	0,014	605,5	448,07	604,5	447,33
90 %	9	0,0148	640	473,6	639,5	473,23
95 %	9,5	0,0157	675,5	499,87	675	499,5
100 %	10	0,0165	711	526,14	710,5	525,77

200 mL/min

capacity	**Measured flow 3**	**CO2 flow 3**
0	0	0
0,05	37,5	27,75
0,1	73,75	54,575
0,15	109,6	81,104
0,2	145	107,3
0,25	179,5	132,83

Linout_B

pressure_B -0,11 bar
CO2 faktor 0,74

% Capacity	**Volt**	**CPAflow**	**Measured flow**	**CO2 flow**	**Measured flow 2**	**CO2 flow 2**
0 %	0	0	0	0	0	0
5 %	0,5	0,0008	31,5	23,31	31,5	23,31
10 %	1	0,0016	67,5	49,95	68	50,32
15 %	1,5	0,0025	103,5	76,59	104	76,96
20 %	2	0,0033	139,5	103,23	140	103,6
25 %	2,5	0,0041	176	130,24	176	130,24
30 %	3	0,0049	212	156,88	212	156,88
35 %	3,5	0,0058	248	183,52	248	183,52
40 %	4	0,0066	283,5	209,79	283,5	209,79
45 %	4,5	0,0074	319	236,06	319,5	236,43
50 %	5	0,0082	354,5	262,33	355	262,7
55 %	5,5	0,0091	390,5	288,97	390	288,6

60 %	6	0,0099	425,5	314,87	426	315,24
65 %	6,5	0,0107	461	341,14	461,5	341,51
70 %	7	0,0115	496,5	367,41	496,5	367,41
75 %	7,5	0,0124	531,5	393,31	531,5	393,31
80 %	8	0,0132	567,5	419,95	567	419,58
85 %	8,5	0,014	602	445,48	602	445,48
90 %	9	0,0148	637,5	471,75	637,5	471,75
95 %	9,5	0,0157	673	498,02	672,5	497,65
100 %	10	0,0165	708,5	524,29	708	523,92

	200 mL/min	
capacity	**Measured flow 3**	**CO2 flow 3**
0	0	0
0,05	36,5	27,01
0,1	72,8	53,872
0,15	108,8	80,512
0,2	144,2	106,708
0,25	178,5	132,09

Calibration of reactor volume

Verifisering av SS-sylinder 1000 mL volum

Veiing 1

Tørrvekt	3147,26 g
Romtemperatur	21,9 °C
Destillert vann temperatur	22,6 °C
Våtvekt	4147,62 g
Vekt vannmengde	1000,36 g
ρ_{H2O} ved 22 °C	0.9978 g/cm^3
ρ_{H2O} ved 24 °C	0.9973 g/cm^3
ρ_{H2O} ved 22,6 °C (interpolert)	0,99765 g/cm^3
Tankvolum	1002,7164 cm^3

Veiing 2

Tørrvekt	3147,25 g
Romtemperatur	22,1 °C
Destillert vann temperatur	22,6 °C
Våtvekt	4147,65 g
Vekt vannmengde	1000,40 cm^3
ρ_{H2O} ved 22,6 °C (interpolert)	0,99765 g/cm^3
Tankvolum	1002,7565 cm^3

Veiing 3

Tørrvekt	3147,19 g
Romtemperatur	21,9 ^{o}C
Destillert vann temperatur	22,7 ^{o}C
Våtvekt	4147,54 g
Vekt vannmengde	1000,35 g
ρ_{H2O} ved 22,7 ^{o}C (interpolert)	0,997625 g/cm^3
Tankvolum	1002,7315 cm^3

Veiing 4

Tørrvekt	3147,16 g
Romtemperatur	21,9 ^{o}C
Destillert vann temperatur	22,8 ^{o}C
Våtvekt	4147,50 g
Vekt vannmengde	1000,34 g
ρ_{H2O} ved 22,8 ^{o}C (interpolert)	0,9976 g/cm^3
Tankvolum	1002,7465 cm^3

Veiing 5

Tørrvekt	3147,16 g
Romtemperatur	21.9 ^{o}C
Destillert vann temperatur	23,9 ^{o}C
Våtvekt	4147,20 g
Vekt vannmengde	1000,04 g
ρ_{H2O} ved 23,9 ^{o}C (interpolert)	0,997325 g/cm^3
Tankvolum	1002,7222 cm^3

Veiing 6

Tørrvekt	3147,16 g
Romtemperatur	21.9 ^{o}C
Destillert vann temperatur	22,4 ^{o}C
Våtvekt	4147,58 g
Vekt vannmengde	1000,42 g
ρ_{H2O} ved 23,9 ^{o}C (interpolert)	0,99770g/cm^3
Tankvolum	1002,7263 cm^3

Test of operation mode effect

Isoperibolic

	t1	t2	T1	T2	delta t	RPM
1	1800,0000	4808,0000	30,0000	50,1280	3008,0000	400,0000
2	4808,0000	8190,0000	50,1280	30,1560	3382,0000	400,0000
3	14040,0000	16750,0000	30,1690	50,1280	2710,0000	400,0000
4	16750,0000	19929,0000	50,1280	30,1560	3179,0000	400,0000
5	19929,0000	22519,0000	30,1560	50,1410	2590,0000	600,0000
6	22519,0000	25399,0000	50,1410	30,1690	2880,0000	600,0000
7	8190,0000	10930,0000	30,1560	50,1400	2740,0000	600,0000
8	10930,0000	14040,0000	50,1400	30,1690	3110,0000	600,0000

Isothermal

	t1	t2	T1	T2	delta t	RPM
1	25399,0000	27659,0000	30,1690	49,9990	2260,0000	400,0000
2	27659,0000	30229,0000	49,9990	29,9990	2570,0000	400,0000
3	34849,0000	37139,0000	30,0000	49,9990	2290,0000	400,0000
4	37139,0000	39649,0000	49,9990	30,0000	2510,0000	400,0000
5	39649,0000	41740,0000	30,0000	50,0000	2091,0000	600,0000
6	41740,0000	44155,0000	50,0000	30,0000	2415,0000	600,0000
7	30229,0000	32329,0000	29,9990	50,0000	2100,0000	600,0000
8	32329,0000	34849,0000	50,0000	30,0000	2520,0000	600,0000

Heat flow validation with calibration heater

Validation heater

Ved 6 W

		THF	V. heater	TP	t1	t1
50 °C	**1**	6101,25396	6027,17722	6097,75406	1638	4346
	2	6133,96476	6092,43428	6130,23756	5688	8442
	3	6423,31093	6379,5268	6430,21024	10126	12810
	4	6773,92736	6729,68828	6780,28098	14494	17178
	5	7370,45975	7337,52758	7372,7227	18840	21706
	6	7631,63068	7558,19913	7619,19355	23390	26302
	7	7584,81046	7517,33908	7590,45068	28032	30968
40 °C	**1**	6179,95766	6077,18894	6181,5593	954	3602
	2	7205,79946	7074,22711	7212,31622	5160	8022
	3	7446,68215	7335,22023	7448,82786	9618	12460
	4	7612,65622	7488,10292	7611,87559	14096	17056
	5	7812,84833	7697,70847	7823,27093	18627	21670
	6	8050,03797	7930,33567	8061,82924	23442	26342

Scanning speed test

Scan speed	Interval	THF [J]	T1 [oC]	T2 [oC]
0,5	**70-60**	10092,348100	70,000600	59,999530
	60-70	-10174,961330	59,999530	69,999860
	70-60	10057,629500	69,999860	60,000350
	60-70	-10190,693640	60,000350	69,999470
	70-60	10059,265550	69,999470	60,000020
	60-70	-10215,153370	60,000020	70,000390
	70-60	10054,230820	70,000390	60,000280
	60-70	-10232,210200	60,000280	70,000380
	70-60	10084,282790	70,000380	59,999100
	60-70	-10154,647270	59,999100	69,999860
0,3	**70-60**	10117,000500	69,999860	60,000010
	60-70	-10167,193230	60,000010	70,000190
	70-60	10119,114960	70,000190	59,999300
	60-70	-10187,676510	59,999300	69,999550
	70-60	10081,226870	69,999550	59,999880
	60-70	-10202,914700	59,999880	69,999850
	70-60	10081,933920	69,999850	59,999770
	60-70	-10184,911180	59,999770	69,999390
	70-60	10153,385390	69,999390	60,000080
	60-70	-10174,674470	60,000080	69,999820
0,5	**70-60**	10048,714030	70,00134	60,000240
	60-70	-10106,993960	60,000240	70,000310
	70-60	10036,781780	70,000310	60,000480
	60-70	-10057,221410	60,000480	69,999970
	70-60	9970,703250	69,999970	59,999910
	60-70	-10042,110540	59,999910	70,000580
	70-60	10000,858400	70,000580	60,000380
	60-70	-10075,207020	60,000380	70,000210
	70-60	9971,666520	70,000210	59,999790
	60-70	-10023,616750	59,999790	70,000010
0,3	**70-60**	10079,809810	70,000010	59,999830
	60-70	-10009,792100	59,999830	70,000000
	70-60	10079,538980	70,000000	59,999550
	60-70	-10045,460130	59,999550	69,999850
	70-60	10080,546710	69,999850	59,999900
	60-70	-10029,180750	59,999900	70,000340
	70-60	10050,783550	70,000340	59,999280
	60-70	-10062,963600	59,999280	69,999790

	70-60	10050,345560	69,999790	60,000010
	60-70	-10076,572510	60,000010	69,999380
0,2	**70-60**	10057,307860	69,999380	59,999570
	60-70	-10063,975890	59,99957	70,000680
	70-60	10071,377130	70,00068	59,999520
	60-70	-10130,821320	59,99952	69,999590
	70-60	10081,527500	69,99959	59,999550
	60-70	-10067,122390	59,99955	70,000140
	70-60	10100,652310	70,00014	60,000010
	60-70	-10078,772810	60,00001	70,000280
	70-60	10116,123750	70,00028	59,999690
	60-70	-10098,318970	59,99969	70,000170

Reactor volume calibration

	P_evakuert	P_system1	P_system2	P_system3	V_system1	V_system2	V_system3	V_reactor
Måling 1		5,435	5,418	4,364	0,001	0,001	0,001	242,862
Måling 2	0,024	5,458	5,450	4,332	0,001	0,001	0,001	258,509
Måling 3	0,026	5,210	5,202	4,134	0,001	0,001	0,001	258,823
Måling 4	0,025	5,102	5,093	4,047	0,001	0,001	0,001	258,917
Måling 5	0,019	5,161	5,153	4,095	0,001	0,001	0,001	258,789
Måling 6	0,026	5,208	5,201	4,133	0,001	0,001	0,001	258,905
Måling 7	0,024	6,524	6,514	5,177	0,001	0,001	0,001	258,808
Måling 8	0,024	6,513	6,503	5,168	0,001	0,001	0,001	258,965

Heat capacity measurements on water for correction factor

104,85

T [oC]	TP [J]	T1 [oC]	T2 [oC]	THF/K [J/K]	Vol [cm^3]	WWH [cm]	ΔHvap [J]
70-60	5065,74709	69,99909	59,99961	504,12809	106,937631	2,6764	24,7283322
60-50	4994,52092	59,99954	49,99999	497,749694	106,373459	2,6533	17,2479647
50-40	4981,44239	49,99999	39,99978	496,966596	105,882531	2,6332	11,6720657
40 30	5037,05375	39,9999	29,99964	502,928613	105,471391	2,6164	7,63685535
70-60	5041,97487	70,00034	59,99966	501,690539	106,937631	2,6764	24,7283322
60-50	4959,40925	59,99962	49,99991	494,230461	106,373459	2,6533	17,2479647
50-40	4950,63764	49,99991	40,00002	493,90199	105,882531	2,6332	11,6720657
40 30	5002,77621	40,00002	30,00042	499,533917	105,471391	2,6164	7,63685535

160,17

T [oC]	TP [J]	T1 [oC]	T2 [oC]	THF/K [J/K]	Vol [cm^3]	WWH [cm]	ΔHvap [J]
70-60	7753,02933	70,00036	60,00013	773,727403	163,361722	5,0913	15,5773387
60-50	7675,70054	59,99974	49,99949	766,458668	162,499873	5,0539	10,922244
50-40	7648,29513	49,99949	39,99973	764,105382	161,749914	5,0214	7,42469702
40 30	7718,31618	39,99973	30,00034	771,391068	161,121841	4,9941	4,87605061
70-60	7756,08058	69,99981	59,99967	774,039488	163,361722	5,0913	15,5773387
60-50	7656,18068	60,00018	49,9996	764,481504	162,499873	5,0539	10,922244
50-40	7679,4394	49,9996	40,0001	767,239832	161,749914	5,0214	7,42469702
40 30	7742,00521	40,0001	30,0007	773,759341	161,121841	4,9941	4,87605061

Heat capacity measurements on ethanol for validation of correction factor

82,849

T [oC]	TP [J]	T1 [oC]	T2 [oC]	THF/K [J/K]	Vol [cm^3]	WWH [cm]	ΔHvap [J]
70-60	3081,57228	70,00017	59,99999	303,021912	112,124780	2,8888	51,2986146
60-50	2906,93556	60,00037	50,00081	287,048009	110,480064	2,8215	36,5817747
50-40	2783,3464	50,00081	39,99987	275,775068	108,882902	2,7561	25,3364906
40 30	2735,34635	39,99987	30,00031	271,847909	107,331261	2,6925	16,986878
70-60	3117,95963	70,00033	60,00029	306,664875	112,124780	2,8888	51,2986146
60-50	2919,45899	59,99986	50,00012	288,295217	110,480064	2,8215	36,5817747
50-40	2799,45534	50,00012	40,00052	277,422982	108,882902	2,7561	25,3364906
40 30	2761,76387	40,00052	29,99968	274,454645	107,331261	2,6925	16,986878

126,6

T [oC]	TP [J]	T1 [oC]	T2 [oC]	THF/K [J/K]	Vol [cm^3]	WWH [cm]	ΔHvap [J]
70-60	4706,23142	69,99972	59,99967	467,553228	171,335769	5,4375	30,6757597
60-50	4489,43133	59,99997	50	446,719366	168,822510	5,2107	22,2510749
50-40	4306,25653	50	40,00009	429,06368	166,381916	5,1108	15,6583446
40 30	4205,1024	40,00009	29,99958	419,423261	164,010882	5,0137	10,6558825
70-60	4746,4402	69,99949	60,00016	471,608042	171,335769	5,3137	30,6757597
60-50	4501,96766	60,00006	50,00022	447,978826	168,822510	5,2107	22,2510749
50-40	4324,86984	50,00022	40,00017	430,918995	166,381916	5,1108	15,6583446
40 30	4227,20045	40,00017	29,99959	421,630002	164,010882	5,0137	10,6558825

Appendix B: Heat capacity measurement data

Heat capacity measurements on Monoethanolamine

103,9

T [oC]	TP [J]	T1 [oC]	T2 [oC]	TP /K [J/K]	Vol [cm^3]	WWH [cm]	ΔHvap [J]
70-60	3751,04544	70,00049	60,00019	374,901705	106,396906	2,6543	1,91592062
60-50	3647,37262	60,00019	50,00116	364,678661	105,461321	2,6159	0,93974402
50-40	3548,15826	50,00116	39,99974	354,714891	104,542046	2,5783	0,50565417
40 30	3547,32076	39,99974	30,00009	354,719174	103,63866	2,5413	0,25317038
70-60	3761,39802	69,99935	60,00005	376,002	106,396906	2,6543	1,64122105
60-50	3643,80544	60,00005	50,00137	364,334662	105,461321	2,6159	0,93974402
50-40	3558,3747	50,00137	40,00014	355,743148	104,542046	2,5783	0,50565417
40 30	3567,47409	40,00014	29,99965	356,704613	103,63866	2,5413	0,25317038
70-60	3764,496	70,00075	59,99974	376,247477	106,396906	2,6543	1,64122105
60-50	3651,88712	59,99974	50,00058	365,125408	105,461321	2,6159	0,93974402
50-40	3562,26292	50,00058	40,00022	356,162905	104,542046	2,5783	0,50565417
40 30	3562,28876	40,00022	29,9999	356,192161	103,63866	2,5413	0,25317038
70-60	3779,51376	69,9991	60,00017	377,827681	106,396906	2,6543	1,64122105
60-50	3644,0206	60,00017	50,00093	364,335775	105,461321	2,6159	0,93974402
50-40	3563,66892	50,00093	40,00005	356,284974	104,542046	2,5783	0,50565417
40 30	3566,38335	40,00005	30,00007	356,613731	103,63866	2,5413	0,25317038
70-60	3778,61751	70,00005	60,00013	377,700651	106,396906	2,6543	1,64122105
60-50	3677,33187	60,00013	49,99782	367,554308	105,461321	2,6159	0,93974402
50-40	3583,78041	49,99782	39,99921	358,37729	104,542046	2,5783	0,50565417
40 30	3573,11712	39,99921	29,9991	357,282465	103,63866	2,5413	0,25317038

155,4

T [oC]	TP [J]	T1 [oC]	T2 [oC]	TP /K [J/K]	Vol [cm^3]	WWH [cm]	ΔHvap [J]
70-60	5665,55207	69,99983	60,00039	566,47935	159,11223	4,9069	1,07579559
60-50	5597,04829	60,00039	49,99941	559,587911	157,713101	4,8461	0,62078515
50-40	5487,53442	49,99941	40,00029	548,76808	156,338363	4,7865	0,33653575
40 30	5431,99857	40,00029	29,99989	543,161159	154,987385	4,7278	0,16971487
70-60	5714,58102	70,00011	59,99982	571,333954	159,11223	4,9069	1,07579559
60-50	5591,34983	59,99982	49,99952	559,056133	157,713101	4,8461	0,62078515
50-40	5484,63219	49,99952	39,99967	548,437792	156,338363	4,7865	0,33653575
40 30	5426,12872	39,99967	29,99992	542,609466	154,987385	4,7278	0,16971487
70-60	5686,45579	70,00085	59,99947	568,459552	159,11223	4,9069	1,07579559
60-50	5568,23489	59,99947	49,99946	556,760854	157,713101	4,8461	0,62078515
50-40	5478,99587	49,99946	40,00034	547,91415	156,338363	4,7865	0,33653575
40 30	5402,07388	40,00034	29,99999	540,171511	154,987385	4,7278	0,16971487

70-60	5689,72996	70,00048	60,00057	568,870536	159,11223	4,9069	1,07579559
60-50							1,58350821
50-40	5475,06623	49,99955	40,00003	547,499249	156,338363	4,7865	0,33653575
40 30	5416,40355	40,00003	30,00035	541,640716	154,987385	4,7278	0,16971487
70-60	5696,48734	69,99948	59,99974	569,555963	159,11223	4,9069	1,07579559
60-50	5563,7761	59,99974	50,00078	556,373394	157,713101	4,8461	0,62078515
50-40	5442,66082	50,00078	40,00008	544,194335	156,338363	4,7865	0,33653575
40 30	5415,604	40,00008	29,99996	541,53693	154,987385	4,7278	0,16971487

Heat capacity measurements on 30 wt% aqueous Monoethanolamine

108,4

T [oC]	**TP [J]**	**T1 [oC]**	**T2 [oC]**	**TP /K [J/K]**	**Vol [cm^3]**	**WWH [cm]**	**ΔHvap [J]**
70-60	4949,69509	70,00021	59,9998	492,715389	109,425494	2,7783	22,3391826
60-50	4869,2081	59,9998	49,99966	485,357141	108,812438	2,7532	15,5687363
50-40	4837,43952	49,99966	39,9999	482,702623	108,252274	2,7302	10,5291394
40 30	4860,83914	39,9999	29,9996	485,380646	107,735273	2,7091	6,88706136
70-60	4977,10881	69,99995	59,99988	495,473494	109,425494	2,7783	22,3391826
60-50	4899,6998	59,99988	50,00018	488,427759	108,812438	2,7532	15,5687363
50-40	4862,76661	50,00018	39,99968	485,199487	108,252274	2,7302	10,5291394
40 30	4858,59993	39,99968	30,00003	485,188268	107,735273	2,7091	6,88706136
70-60	4930,57873	70,00085	59,99969	490,767026	109,425494	2,7783	22,3391826
60-50	4847,27735	59,99969	50,00011	483,191155	108,812438	2,7532	15,5687363
50-40	4844,26085	50,00011	40,00003	483,369304	108,252274	2,7302	10,5291394
40 30	4872,65569	40,00003	30,00014	486,582215	107,735273	2,7091	6,88706136
70-60	4979,26366	70,00007	60,00046	495,711781	109,425494	2,7783	22,3391826
60-50	4867,13369	60,00046	50,00005	485,136605	108,812438	2,7532	15,5687363
50-40	4832,94897	50,00005	39,99984	482,231856	108,252274	2,7302	10,5291394
40 30	4884,60053	39,99984	29,99999	487,778664	107,735273	2,7091	6,88706136
70-60	4983,53373	69,99946	59,99972	496,132354	109,425494	2,7783	22,3391826
60-50	4888,89337	59,99972	50,00009	487,350495	108,812438	2,7532	15,5687363
50-40	4841,66411	50,00009	39,99956	483,087893	108,252274	2,7302	10,5291394
40 30	4844,86624	39,99956	29,99975	483,80711	107,735273	2,7091	6,88706136

160,6

T [oC]	**TP [J]**	**T1 [oC]**	**T2 [oC]**	**TP /K [J/K]**	**Vol [cm^3]**	**WWH [cm]**	**ΔHvap [J]**
70-60	7411,2035	69,99973	60,00013	739,699894	162,054575	5,0346	14,5004352
60-50	7289,86349	60,00013	49,99963	727,934109	161,146665	4,9952	10,1584377
50-40	7241,46362	49,99963	39,99996	723,479989	160,317086	4,9592	6,90247953
40 30	7264,52792	39,99996	30,00018	726,015339	159,551429	4,9259	4,53425644
70-60	7425,15577	69,99963	59,99998	741,091472	162,054575	5,0346	14,5004352

60-50							
	7315,88999	59,99998	49,9998	730,560005	161,146665	4,9952	10,1584377
50-40							
	7240,29682	49,9998	40,00014	723,364028	160,317086	4,9592	6,90247953
40 30							
	7252,10972	40,00014	30,00027	724,766968	159,551429	4,9259	4,53425644
70-60	7420,46288	70,0003	60,00042	740,605132	162,054575	5,0346	14,5004352
60-50	7301,79501	60,00042	50,00018	729,146158	161,146665	4,9952	10,1584377
50-40	7226,54549	50,00018	40,00001	721,952028	160,317086	4,9592	6,90247953
40 30	7232,33467	40,00001	30,00021	722,794497	159,551429	4,9259	4,53425644
70-60	7443,53829	69,99974	59,99962	742,894871	162,054575	5,0346	14,5004352
60-50	7321,6733	59,99962	49,99967	731,155142	161,146665	4,9952	10,1584377
50-40	7267,83951	49,99967	39,99963	726,090799	160,317086	4,9592	6,90247953
40 30	7277,73702	39,99963	29,9995	727,310821	159,551429	4,9259	4,53425644
70-60	7446,37567	69,99997	59,9998	743,17489	162,054575	5,0346	14,5004352
60-50	7326,00301	59,9998	49,99996	731,596163	161,146665	4,9952	10,1584377
50-40	7251,11151	49,99996	39,99978	724,407864	160,317086	4,9592	6,90247953
40 30	7260,03488	39,99978	29,99998	725,564574	159,551429	4,9259	4,53425644

Heat capacity measurements on 30 wt% aqueous Monoethanolamine with 0,2 loading

106,914

T [oC]	**TP [J]**	**T1 [oC]**	**T2 [oC]**	**TP /K [J/K]**	**Vol [cm^3]**	**WWH [cm]**	**ΔHvap [J]**
70-60	4627,08569	70,00006	60,00048	460,508649	105,782131	2,6291	22,1926147
60-50	4478,73531	60,00048	50,0001	446,313078	105,157864	2,6035	15,4349337
50-40	4422,19829	50,0001	39,99978	441,162974	104,566483	2,5793	10,4273806
40 30	4463,57197	39,99978	29,99965	445,669704	104,005318	2,5563	6,8169968
70-60	4592,80463	70,00004	60,00011	457,064401	105,782131	2,6291	22,1926147
60-50	4487,77148	60,00011	49,99991	447,22471	105,157864	2,6035	15,4349337
50-40	4442,36674	49,99991	39,99979	443,188618	104,566483	2,5793	10,4273806
40 30	4457,52547	39,99979	30,00001	445,080639	104,005318	2,5563	6,8169968
70-60	4541,91468	69,99978	60,00019	451,990738	105,782131	2,6291	22,1926147
60-50	4468,36253	60,00019	50,00011	445,289197	105,157864	2,6035	15,4349337
50-40	4445,99707	50,00011	39,99956	443,532575	104,566483	2,5793	10,4273806
40 30	4469,75556	39,99956	30,00005	446,315726	104,005318	2,5563	6,8169968
70-60	4591,903	70,00007	59,99996	456,966012	105,782131	2,6291	22,1926147
60-50	4484,76451	59,99996	50,00028	446,94726	105,157864	2,6035	15,4349337
50-40	4424,11971	50,00028	39,99972	441,344518	104,566483	2,5793	10,4273806
40 30	4452,76233	39,99972	30,00046	444,627436	104,005318	2,5563	6,8169968
70-60	4578,60064	70,00009	59,99983	455,628956	105,782131	2,6291	22,1926147
60-50	4488,31628	59,99983	49,99989	447,290818	105,157864	2,6035	15,4349337
50-40	4430,38105	49,99989	40,00057	442,025425	104,566483	2,5793	10,4273806
40 30	4458,54858	40,00057	30,00009	445,151791	104,005318	2,5563	6,8169968

160,771

T [oC]	TP [J]	T1 [oC]	T2 [oC]	TP /K [J/K]	Vol [cm^3]	WWH [cm]	ΔHvap [J]
70-60	6968,00233	69,99997	60,00007	695,35769	159,068962	4,9050	14,4949611
60-50	6894,3725	60,00007	50,00018	688,431387	158,130225	4,8642	10,1343595
50-40	6838,54105	50,00018	39,99998	683,152421	157,240942	4,8256	6,88020837
40 30	6833,02669	39,99998	29,99958	682,823479	156,397095	4,7890	4,51877406
70-60	7008,21644	69,99986	60	699,381939	159,068962	4,9050	14,4949611
60-50	6901,65893	60	49,99957	689,122825	158,130225	4,8642	10,1343595
50-40	6815,44562	49,99957	40,00057	680,924634	157,240942	4,8256	6,88020837
40 30	6809,02504	40,00057	30,00025	680,428853	156,397095	4,7890	4,51877406
70-60	6985,39859	69,99993	60,00003	697,097334	159,068962	4,9050	14,4949611
60-50	6885,52602	60,00003	50,00028	687,556355	158,130225	4,8642	10,1343595
50-40	6809,48918	50,00028	40,00004	680,244571	157,240942	4,8256	6,88020837
40 30	6814,04321	40,00004	29,99974	680,932016	156,397095	4,7890	4,51877406
70-60	6959,36551	69,99928	60,00026	694,555121	159,068962	4,9050	14,4949611
60-50	6879,42884	60,00026	50,00002	686,912962	158,130225	4,8642	10,1343595
50-40	6823,0582	50,00002	39,99993	681,611665	157,240942	4,8256	6,88020837
40 30	6822,64135	39,99993	29,99999	681,816348	156,397095	4,7890	4,51877406
70-60	6984,80956	69,99938	60,00006	697,078861	159,068962	4,9050	14,4949611
60-50	6864,35879	60,00006	50,00005	685,421758	158,130225	4,8642	10,1343595
50-40	6803,17602	50,00005	40,00026	679,643854	157,240942	4,8256	6,88020837
40 30	6825,09408	40,00026	29,99958	682,011154	156,397095	4,7890	4,51877406

Heat capacity measurements on 30 wt% aqueous Monoethanolamine with 0,4 loading

107,021

T [oC]	TP [J]	T1 [oC]	T2 [oC]	TP/K [J/K]	Vol [cm^3]	WWH [cm]	ΔHvap [J]
70-60	4378,55868	70,00039	59,99974	435,572351	109,271518	2,7720	22,5520505
60-50	4306,64524	59,99974	49,99959	429,128884	108,579722	2,7436	15,2920264
50-40	4248,01948	49,99959	40,00028	423,814141	107,944623	2,7176	10,1705002
40 30	4266,45699	40,00028	29,99987	425,969826	107,370421	2,6941	6,58407913
70-60	4417,44204	69,99977	60,00035	439,514491	109,271518	2,7720	22,5520505
60-50	4290,56027	60,00035	50,00007	427,514854	108,579722	2,7436	15,2920264
50-40	4251,73829	50,00007	40,00004	424,155507	107,944623	2,7176	10,1705002
40 30	4306,90442	40,00004	29,99967	430,016123	107,370421	2,6941	6,58407913
70-60	4451,53853	70,00014	59,9999	442,888019	109,271518	2,7720	22,5520505
60-50	4331,32349	59,9999	50,00006	431,610052	108,579722	2,7436	15,2920264
50-40	4274,51537	50,00006	40,00046	426,451545	107,944623	2,7176	10,1705002
40 30	4274,20353	40,00046	29,99983	426,735061	107,370421	2,6941	6,58407913
70-60	4398,66772	69,99975	59,99999	437,62207	109,271518	2,7720	22,5520505
60-50	4342,32483	59,99999	50,00009	432,707607	108,579722	2,7436	15,2920264
50-40	4284,09456	50,00009	40,00012	427,393688	107,944623	2,7176	10,1705002
40 30	4293,4758	40,00012	29,9999	428,679741	107,370421	2,6941	6,58407913
70-60							
60-50	4337,83446	59,9997	50,00022	432,276722	108,579722	2,7436	15,2920264
50-40	4282,69867	50,00022	40,00004	427,245127	107,944623	2,7176	10,1705002

40 30	4286,51965	40,00004	29,99966	427,977294	107,370421	2,6941	6,58407913

160,534

T [oC]	TP [J]	T1 [oC]	T2 [oC]	TP /K [J/K]	Vol [cm^3]	WWH [cm]	ΔHvap [J]
70-60	6728,7531	69,99962	60,00001	671,467005	163,909829	5,1151	14,3449211
60-50	6585,38914	60,00001	49,99996	657,556871	162,872119	5,0701	9,78755623
50-40	6558,00284	49,99996	39,99986	655,139109	161,919456	5,0287	6,5462327
40 30	6574,88099	39,99986	29,99972	657,052987	161,05814	4,9913	4,25913065
70-60	6704,67591	69,99965	60,00016	669,067221	163,909829	5,1151	14,3449211
60-50	6607,82251	60,00016	49,99999	659,792279	162,872119	5,0701	9,78755623
50-40	6555,84121	49,99999	40,00008	654,935392	161,919456	5,0287	6,5462327
40 30	6575,38653	40,00008	30,00008	657,11274	161,05814	4,9913	4,25913065
70-60	6725,82584	69,99965	59,99984	671,160844	163,909829	5,1151	14,3449211
60-50	6615,13026	59,99984	50,00041	660,571923	162,872119	5,0701	9,78755623
50-40	6553,64864	50,00041	39,99973	654,665723	161,919456	5,0287	6,5462327
40 30	6550,79305	39,99973	29,99991	654,665176	161,05814	4,9913	4,25913065
70-60	6706,60689	69,9994	59,99979	669,252298	163,909829	5,1151	14,3449211
60-50	6607,13975	59,99979	49,99986	659,739838	162,872119	5,0701	9,78755623
50-40	6559,7621	49,99986	40,00044	655,359598	161,919456	5,0287	6,5462327
40 30	6570,53035	40,00044	29,99959	656,571313	161,05814	4,9913	4,25913065
70-60	6744,98608	70,00018	59,99997	673,049982	163,909829	5,1151	14,3449211
60-50	6617,22911	59,99997	50,00007	660,750763	162,872119	5,0701	9,78755623
50-40	6529,73507	50,00007	40	652,314318	161,919456	5,0287	6,5462327
40 30	6525,03711	40	29,99988	652,069973	161,05814	4,9913	4,25913065

Heat capacity measurements on N-methyldiethanolamine

108,302

T [oC]	TP [J]	T1 [oC]	T2 [oC]	THF/K [J/K]	Vol [cm^3]	WWH [cm]	ΔHvap [J]
70-60	3283,4564	70,00029	59,99991	328,333163	107,611644	2,7040	64,4547241
60-50	3191,9001	59,99991	49,99951	319,177243	106,75846	2,6691	57,8091078
50-40	3104,77268	49,99951	40,00004	310,493724	105,929678	2,6351	57,3595373
40 30	3019,42494	40,00004	30,00003	301,942192	105,124481	2,6021	63,0966595
70-60	3253,82547	70,00066	59,9999	325,35782	107,611644	2,7040	64,4547241
60-50	3129,45355	59,9999	50,00071	312,970706	106,75846	2,6691	57,8091078
50-40	3038,90916	50,00071	40,00018	303,874811	105,929678	2,6351	57,3595373
40 30	3092,75392	40,00018	29,99971	309,260857	105,124481	2,6021	63,0966595
70-60	3298,43224	69,99982	59,99981	329,842894	107,611644	2,7040	64,4547241
60-50	3169,25575	59,99981	49,99991	316,928744	106,75846	2,6691	57,8091078
50-40	3073,47523	49,99991	40,00041	307,362891	105,929678	2,6351	57,3595373
40 30	3204,00572	40,00041	29,99967	320,376864	105,124481	2,6021	63,0966595
70-60	3346,24656	70,00041	59,99989	334,607256	107,611644	2,7040	64,4547241
60-50	3219,58394	59,99989	50,00039	321,974493	106,75846	2,6691	57,8091078
50-40	3113,70946	50,00039	39,99997	311,357869	105,929678	2,6351	57,3595373
40 30	3244,28365	39,99997	30,0002	324,435827	105,124481	2,6021	63,0966595

166,862

T [oC]	TP [J]	T1 [oC]	T2 [oC]	THF/K [J/K]	Vol [cm^3]	WWH [cm]	ΔHvap [J]
70-60	5264,47469	70,00012	60,00024	526,453786	165,798362	5,1971	103,324313
60-50	5077,21489	60,00024	49,99976	507,69712	164,483851	5,1401	95,3752836
50-40	4872,31884	49,99976	40,00023	487,254785	163,20694	5,0846	95,741223
40 30	4669,2394	40,00023	30,00021	466,923006	161,966364	5,0308	102,580954
70-60	5227,58355	69,99997	60,00019	522,769856	165,798362	5,1971	103,324313
60-50	5058,38335	60,00019	50,00051	505,854522	164,483851	5,1401	95,3752836
50-40	4856,23528	50,00051	39,99975	485,586623	163,20694	5,0846	95,741223
40 30	4677,11968	39,99975	29,99997	467,722258	161,966364	5,0308	102,580954
70-60	5206,60767	70,00038	60,00051	520,667536	165,798362	5,1971	103,324313
60-50	5053,15	60,00051	50,00012	505,295293	164,483851	5,1401	95,3752836
50-40	4864,32025	50,00012	39,99993	486,422783	163,20694	5,0846	95,741223
40 30	4694,45386	39,99993	29,9992	469,411119	161,966364	5,0308	102,580954

Heat capacity measurements on 30 wt% aqueous N-methyldiethanolamine

107,476

T [oC]	TP [J]	T1 [oC]	T2 [oC]	THF/K [J/K]	Vol [cm^3]	WWH [cm]	ΔHvap [J]
70-60	4799,5719	69,99934	59,99967	477,596248	107,08899	2,6826	23,76703115
60-50	4702,29735	59,99967	49,99945	468,568387	106,382316	2,6537	16,51039769
50-40	4657,42055	49,99945	39,9999	464,648675	105,7283	2,6269	11,14288777
40 30	4705,44604	39,9999	29,99985	469,813886	105,122499	2,6021	7,283692046
70-60	4787,80837	69,99972	60,00029	476,43129	107,08899	2,6826	23,76703115
60-50	4665,30869	60,00029	49,99986	464,85984	106,382316	2,6537	16,51039769
50-40	4641,59197	49,99986	39,99974	463,039352	105,7283	2,6269	11,14288777
40 30	4703,81925	39,99974	30,00022	469,6761	105,122499	2,6021	7,283692046
70-60	4774,75036	70,00044	59,99972	475,064128	107,08899	2,6826	23,76703115
60-50	4675,94009	59,99972	50,00018	465,964404	106,382316	2,6537	16,51039769
50-40	4628,17198	50,00018	39,99982	461,686289	105,7283	2,6269	11,14288777
40 30	4660,58668	39,99982	29,99963	465,321458	105,122499	2,6021	7,283692046

164,03

T [oC]	TP [J]	T1 [oC]	T2 [oC]	THF/K [J/K]	Vol [cm^3]	WWH [cm]	ΔHvap [J]
70-60	7440,79171	69,99943	59,99992	742,618105	163,439345	4,9903	14,9745432
60-50	7321,54313	59,99992	50,00017	731,125512	162,360818	4,9461	10,470789
50-40	7271,18434	50,00017	39,99995	726,391549	161,362658	4,9052	7,109047646
40 30	7286,32728	39,99995	29,99986	728,158942	160,438084	4,8674	4,672322464
70-60	7303,93431	69,99927	59,99966	728,924405	163,439345	4,9903	14,9745432
60-50	7150,05856	59,99966	50,00047	714,016612	162,360818	4,9461	10,470789
50-40	7054,85955	50,00047	40,00076	704,795489	161,362658	4,9052	7,109047646
40 30	7080,26329	40,00076	29,99986	707,495422	160,438084	4,8674	4,672322464
70-60	7218,32961	70,00005	60,00009	720,338388	163,439345	4,9903	14,9745432
60-50	7125,47423	60,00009	50,00042	711,523824	162,360818	4,9461	10,470789

50-40	7060,22731	50,00042	40,00044	705,313237	161,362658	4,9052	7,109047646
40 30	7064,12195	40,00044	29,99994	705,909667	160,438084	4,8674	4,672322464

Heat capacity measurements on 30 wt% aqueous N-methyldiethanolamine with 0,2 loading

109,077

T [oC]	TP [J]	T1 [oC]	T2 [oC]	THF/K [J/K]	Vol [cm^3]	WWH [cm]	ΔHvap [J]
70-60	4665,24343	70,00005	59,99972	464,167822	108,681618	2,7478	23,4120311
60-50	4550,80506	59,99972	49,99996	453,465327	107,964451	2,7185	16,2606215
50-40	4508,43699	49,99996	40,00021	449,757974	107,300724	2,6913	10,9696878
40 30	4544,60786	40,00021	30,00004	453,736432	106,685928	2,6661	7,1664063
70-60	4617,92075	69,99991	60,00044	459,475224	108,681618	2,7478	23,4120311
60-50	4495,286	60,00044	50,00023	447,893132	107,964451	2,7185	16,2606215
50-40	4471,26114	50,00023	40,0006	446,045649	107,300724	2,6913	10,9696878
40 30	4493,99641	40,0006	29,99993	448,652941	106,685928	2,6661	7,1664063
70-60	4577,93072	70,00008	60,00016	455,455513	108,681618	2,7478	23,4120311
60-50	4440,23006	60,00016	50,00042	442,408446	107,964451	2,7185	16,2606215
50-40	4425,73351	50,00042	39,99991	441,453868	107,300724	2,6913	10,9696878
40 30	4447,42566	39,99991	30,00031	444,043687	106,685928	2,6661	7,1664063
70-60	4529,24801	69,99964	60,00023	450,610184	108,681618	2,7478	23,4120311
60-50	4390,02985	60,00023	50,00029	437,379547	107,964451	2,7185	16,2606215
50-40	4337,79243	50,00029	39,99996	432,667996	107,300724	2,6913	10,9696878
40 30	4383,9097	39,99996	30,00014	437,682208	106,685928	2,6661	7,1664063
70-60	4484,47613	70,00007	60,00022	446,113102	108,681618	2,7478	23,4120311
60-50	4347,73069	60,00022	50,00067	433,166499	107,964451	2,7185	16,2606215
50-40	4292,64412	50,00067	40,00007	428,141755	107,300724	2,6913	10,9696878
40 30	4341,61904	40,00007	29,9995	433,420558	106,685928	2,6661	7,1664063

166,102

T [oC]	TP [J]	T1 [oC]	T2 [oC]	THF/K [J/K]	Vol [cm^3]	WWH [cm]	ΔHvap [J]
70-60	7193,66569	70,00007	59,99956	717,87129	165,499913	5,1842	14,5866746
60-50	6995,24156	59,99956	49,99982	698,522285	164,407814	5,1368	10,20033
50-40	6914,5422	49,99982	40,00002	690,775618	163,397094	5,0929	6,92417734
40 30	6912,41289	40,00002	29,99996	690,782221	162,460885	5,0522	4,54922879
70-60	6974,00689	70,00032	60,00018	695,932278	165,499913	5,1842	14,5866746
60-50	6869,81213	60,00018	50,00021	685,963238	164,407814	5,1368	10,20033
50-40	6796,07543	50,00021	39,99986	678,891364	163,397094	5,0929	6,92417734
40 30	6797,3637	39,99986	30,00046	679,322206	162,460885	5,0522	4,54922879
70-60	6898,74127	69,99955	60,00004	688,449194	165,499913	5,1842	14,5866746
60-50	6765,59199	60,00004	49,99985	675,526331	164,407814	5,1368	10,20033
50-40	6711,294	49,99985	39,99952	670,414859	163,397094	5,0929	6,92417734
40 30	6720,65048	39,99952	30,00024	671,658485	162,460885	5,0522	4,54922879

Heat capacity measurements on 30 wt% aqueous N-methyldiethanolamine with 0,2 loading

111,006

T [oC]	TP [J]	T1 [oC]	T2 [oC]	THF/K [J/K]	Vol [cm^3]	WWH [cm]	ΔHvap [J]
70-60	4253,47162	70,00063	59,99984	422,903824	110,606279	2,8266	24,0992874
60-50	3920,98964	59,99984	49,99993	390,447468	109,876394	2,7968	16,5501006
50-40	3819,47296	49,99993	39,99993	380,85059	109,200897	2,7691	10,9670646
40 30	3810,08675	39,99993	29,99976	380,301949	108,575199	2,7435	7,00261312
70-60	3900,80655	70,00006	60,00014	387,673828	110,606279	2,8266	24,0992874
60-50	3737,59857	60,00014	49,99976	372,090707	109,876394	2,7968	16,5501006
50-40	3658,28825	49,99976	40,00002	364,741602	109,200897	2,7691	10,9670646
40 30	3686,38169	40,00002	29,99961	367,922823	108,575199	2,7435	7,00261312
70-60	3884,20686	70,00042	60,0003	386,006125	110,606279	2,8266	24,0992874
60-50	3676,38983	60,0003	50,00018	365,979581	109,876394	2,7968	16,5501006
50-40	3536,21367	50,00018	39,99997	352,517258	109,200897	2,7691	10,9670646
40 30	3534,39121	39,99997	29,99997	352,73886	108,575199	2,7435	7,00261312
70-60	3666,15769	69,99988	60,00029	364,220773	110,606279	2,8266	24,0992874
60-50	3487,0034	60,00029	50,00021	347,042554	109,876394	2,7968	16,5501006
50-40	3431,88679	50,00021	39,99967	342,073501	109,200897	2,7691	10,9670646
40 30	3469,45959	39,99967	29,99969	346,24639	108,575199	2,7435	7,00261312
70-60	3604,41632	69,99936	59,99913	358,023469	110,606279	2,8266	24,0992874
60-50	3404,80093	59,99913	49,99978	338,847108	109,876394	2,7968	16,5501006
50-40	3317,14782	49,99978	40,00007	330,627664	109,200897	2,7691	10,9670646
40 30	3356,0488	40,00007	29,99976	334,894237	108,575199	2,7435	7,00261312

111,006

T [oC]	TP [J]	T1 [oC]	T2 [oC]	THF/K [J/K]	Vol [cm^3]	WWH [cm]	ΔHvap [J]
70-60	7246,99899	69,9994	59,99978	722,840024	110,606279	2,8266	18,8734296
60-50	7081,37167	59,99978	49,99985	706,922873	109,876394	2,7968	12,1924264
50-40	6976,21017	49,99985	40,00067	696,899626	109,200897	2,7691	7,7853647
40 30	6970,55735	40,00067	30,00054	696,454899	108,575199	2,7435	5,91782058
70-60	7167,32237	70,00009	60,00005	714,842035	110,606279	2,8266	18,8734296
60-50	7001,59602	60,00005	49,99994	698,932671	109,876394	2,7968	12,1924264
50-40	6918,55713	49,99994	40,00007	691,086161	109,200897	2,7691	7,7853647
40 30	6894,38003	40,00007	29,99973	688,822801	108,575199	2,7435	5,91782058
70-60	7077,39563	69,99989	60,00007	705,864926	110,606279	2,8266	18,8734296
60-50	6893,71172	60,00007	50,00033	688,169822	109,876394	2,7968	12,1924264
50-40	6812,93549	50,00033	39,99994	680,488473	109,200897	2,7691	7,7853647
40 30	6803,06088	39,99994	30,00042	679,746934	108,575199	2,7435	5,91782058
70-60	6960,74058	69,9999	60,00031	694,215178	110,606279	2,8266	18,8734296
60-50	6796,9199	60,00031	50,00001	678,452394	109,876394	2,7968	12,1924264
50-40	6711,61977	50,00001	39,99998	670,381429	109,200897	2,7691	7,7853647
40 30	6692,53785	39,99998	30	668,66334	108,575199	2,7435	5,91782058
70-60	6892,09479	69,99977	59,99982	687,325573	110,606279	2,8266	18,8734296
60-50	6722,9014	59,99982	49,99967	671,060831	109,876394	2,7968	12,1924264
50-40	6648,00718	49,99967	40,00023	664,059369	109,200897	2,7691	7,7853647
40 30	6660,87315	40,00023	30,00044	665,509509	108,575199	2,7435	5,91782058